UNIVERSITY OF OSLO
Department of Geosciences, MetOs section

Elemental carbon in Svalbard snow from local sources and its impact on surface albedo

Master thesis in Geosciences

Borgar Aamaas

1st June 2009

UNIS

Tutors: Frode Stordal (UiO)
Carl Egede Bøggild (UNIS)
Terje Berntsen (UiO)
Kim Holmén (UNIS)

This work is published digitally through DUO – Digitale Utgivelser ved UiO
http://www.duo.uio.no
It is also catalogued in BIBSYS (http://www.bibsys.no/english)

Cover picture: A snow pit excavated at Longyearbyen Airport. The dark layers in the snow indicate very high elemental carbon (EC) concentrations.

Contents

List of Figures

List of Tables

Samandrag på norsk

Svalbard, ei øygruppe i Arktis, vert påverka både av langtransportert og lokal forureining. I denne oppgåva har konsentrasjonar av elementært karbon (EC) i snøen og effekten det har på albedo blitt undersøkt. Eit overslag av den lokale EC-forureininga på snøen har for første gong blitt gjort. Dette vart utført ved å ta snøprøver frå langs utgåande profilar frå Longyearbyen, Ny-Ålesund og Svea i 2008. Nokre av desse prøvene vart tatt i upåverka område. Desse prøvene vart smelta og filtrert på UNIS. Sjølve EC-analysen blei gjort ved ITM i Stockholm. Sidan denne metoden både er dyr og tidkrevjande vart ein alternativ metode undersøkt. Snøstratigrafien vart undersøkt ved kvart målepunkt. Dette kunne då bli samanlikna med vêrdata for å datere snølaga. Modellkøyringar av den kjemiske transportmodellen Oslo CTM2 vart sett opp mot EC-prøvene tatt i snøen. Dei lokale EC-kjeldene på Svalbard vart talfesta og samanlikna med det fjerntransporterte EC. Til slutt vart ein mogeleg relasjon mellom EC-konsentrasjon og isotopparameteren $\delta^{18}O$ undersøkt.

Ein studie av Forsström et al. (manuskript innlevert) har funne EC-konsentrasjonen på Svalbard til å vere $4.1\,\mu g/l$. Her vart EC-konsentrasjonen rundt Ny-Ålesund målt til å vere på linje med bakgrunnsnivået ($6.58\,\mu g/l$). Oslo CTM2-modellen gjev data som stemmer bra overeins med dette og gav ein EC-konsentrasjon for vinteren 2007/08 på $5.35\,\mu g/l$. Svært høge EC-konsentrasjonar vart observert rundt Longyearbyen og Svea. I desse områda var misfarga snø lett synleg på satellittbilete. Område utsett for kolstøv frå kolhaugar var spesielt påverka. EC-konsentrasjonen rundt Svalbard Lufthamn og sentrum av Longyearbyen var over $1000\,\mu g/l$. Longyearbyen og Svea skil seg frå Ny-Ålesund grunna kolstøvet og storleiken på tettstadene. Prosessar i snøen vil generelt auke EC-konsentrasjonen etter at snøen har lagt seg. Sublimering og smelting av snø kan doble den opphavlege EC-konsentrasjonen.

Albedoreduksjonen i nysnø grunna bakgrunnsnivået av EC vart modellert til å vere 0.0011 på Svalbard. Dette er basert på den direkte albedoeffekten av EC i snø, der sekundære effektar ikkje er inkludert. Den lokale forureininga frå Longyearbyen tilsvarar $2.2\,\%$ av langtransportforureininga, mens Svea bidrar med $5.4\,\%$. Dette er konservative overslag, og større overslag vert indikert. I sum er den lokale effekten $11.2\,\%$ av den totale, men kan vere så stor som $20\,\%$. EC i snø har sekundære klimaeffektar. Den viktigaste er at snømetamorfose og snøkornvekst går fortare med EC. Dessutan vert EC-partiklane liggande att i snøen ved smelting, og med det vert EC oppkonsentrert, spesielt i overflatelaget. På Longyearbreen auka EC konsentrasjonen i snøoverflatelaget med ein faktor 18 frå april til august. Det reduserer albedoen med 0.08. Forureininga frå Svalbard er ubetydeleg sett for heile Arktis under eitt, der mesteparten av Arktis er urørt natur.

EC har vore i fokus sidan det reduserer snøalbedo mykje meir effektivt enn støv. Likevel er støvkonsentrasjonane mykje høgare enn EC-konsentrasjonane. Dette skuldast kraftige vindar, tørt klima og lause sedimentære bergartar som gir naturleg lokalt svært store støvkjelder på Svalbard. Albedoeffekten av støv i snø vart grovt rekna til å vere ein faktor 8 større enn det EC i snø gjev.

Abstract

Svalbard, a remote archipelago in the Arctic, is affected by both long-range and local pollution. In this thesis, the elemental carbon (EC) concentrations in the snow pack and its effect upon surface albedo have been investigated. The impact of local EC sources for the snow pack have for the first time been estimated. That was done by gathering snow samples from the snow pack along transects around Longyearbyen, Ny-Ålesund, and Svea in 2008. Some of these samples were taken in pristine areas. These samples were melted and filtered at UNIS. The final EC analysis was done at ITM in Stockholm. Since this analysis is both expensive and time demanding, an alternative method was investigated. Simple snow stratigraphy investigations were done in every snow pit. This was compared to weather data in order to date the snow layers. Model runs from the Oslo CTM2 chemical transport model were compared with the EC measurements. The local EC emissions in Svalbard were estimated and compared to the long-range transported EC. Finally, a possible relation between EC concentration and the isotope parameter $\delta^{18}O$ was investigated.

A study by Forsström et al. *(Submitted) has found the average EC concentration on Svalbard to be* $4.1\ \mu g/l$*. Here, the EC concentration around Ny-Ålesund was found to be in line with the background concentration (*$6.58\ \mu g/l$*). The Oslo CTM2 model fits well with these result, and an EC concentration of* $5.35\ \mu g/l$ *was modeled for the winter 2007/08. Highly elevated EC concentrations were observed around Longyearbyen and Svea. In those areas, darkened snow was clearly visible from satellite images. Areas influenced by coal dust from open coal piles were the most affected. The EC concentration around Svalbard Airport and the centre of Longyearbyen was above* $1000\ \mu g/l$*. Longyearbyen and Svea differ from Ny-Ålesund due to available coal dust and the size of the settlements. Post-depositional processes in the snow pack will, in general, increase the EC concentration. Sublimation and melting of snow can double the initial EC concentration.*

The albedo reduction in new snow from the background EC was modeled to be 0.011 *on Svalbard. This is based on the direct albedo effect of EC in snow, where secondary effects are not included. The local pollution from Longyearbyen was estimated to have an albedo effect of* $2.2\,\%$ *and from Svea of* $5.4\,\%$ *relative to the long-range pollution. These estimates are at the low end of the scale, and some higher estimates are given. In total, the local effect is conservatively set to* $11.2\,\%$ *of the total, but may be as large as* $20\,\%$ *of the total effect. EC in snow has secondary climate effects. Most importantly, snow metamorphism and snow grain growth are accelerated by the presence of EC. Further, the EC particles are staying in the snow during melting, and the EC concentration is especially elevated in the snow surface. On Longyearbreen, an increase by a factor of* 18 *was measured in the surface snow from April to August. That reduces the albedo by about* 0.08*. The pollution from Svalbard is insignificant compared to the vastness of the entire Arctic and its wilderness with few or no local EC sources.*

EC has been the focus since its impact on snow albedo for a specific contamination burden is much higher than for dust. However, dust concentrations are generally much higher than EC concentrations. Due to windy conditions, dry climate, and soft sedimentary rocks, the local non-anthropogenic source of dust is very high in Svalbard. The albedo effect of dust in snow is found to be crudely a factor 8 *of the effect of EC in snow.*

Chapter 1

Introduction

1.1 The significance of light absorbing particles in snow

The Arctic (see Figure 1.1) is covered by snow and ice during most of the year. In January, about $49\,\%$ of the land surface on the Northern Hemisphere is snow covered (Lemke *et al.*, 2007). These surfaces have a relatively high albedo compared to other areas in the world. It has been known for centuries that impurities can darken (Visted & Stigum, 1971; Dahl, 1998), and, hence, lower the albedo of snow significantly. The most effective light absorbing particle at reducing snow albedo is soot. Soot is produced by incomplete combustion processes of fossil fuel, biofuel, or biomass. Thus, the sources are both anthropogenic and natural (e.g. from forest fires). This impurity is about 50 times more effective than dust and 200 times more effective than volcanic ash in reducing snow albedo (Warren, 1984). Warren & Wiscombe (1980) were the first to quantity a relation between soot concentrations and reduction in snow albedo by modeling.

Strongly light absorbing particles affect the radiation balance both on highly reflective surfaces, such as on snow and ice surfaces, and in the atmosphere. The radiative forcing of soot, often called black carbon (BC), in the atmosphere is set to $0.34 \pm 0.25\,W/m^2$ and $0.10 \pm 0.10\,W/m^2$ for the surface albedo effect in the latest Intergovernmental Panel on Climate Change (IPCC) assessment (Forster *et al.*, 2007). The forcing from perturbations in the albedo comes mainly from BC on snow and ice surfaces.

1.2 How to measure light absorbing particles in snow?

There is no perfect measurement technique of soot or light absorbing carbonaceous particles. One technique, the optical method, observes changes in the light attenuation of filters with different amounts of particles (Clarke, 1981). This will measure everything that absorbs radiation, not just soot. These particles are called black carbon (BC). In the thermo-optical method, the sample is heated to volatilize the carbon (Birch & Cary, 1996). This proxy measures elemental carbon (EC). Both definitions of light absorbing carbonaceous particles are operationally and are only proxies. As they are measured differently, BC and EC concentrations will differ for the same snow sample. Since the method utilized in this project is the thermo-optical, soot will be referred to as EC in this thesis. In the historical background given in Section 2.3, the generalized term soot will be used as an exception.

Figure 1.1: A map of the Arctic. There is no unique definition of the Arctic; however, we could state that all land and ocean areas north of the polar circle ($66^o33'N$) are within the Arctic. The circle on the map indicates the polar circle. Svalbard is the archipelago situated between mainland Norway, the Arctic Ocean, and Greenland. The sea ice extent is from August 2007. The map is provided by Erika Aamaas using data from the Norwegian Mapping Authority.

1.3 Motivation, objective, and structure of this thesis

Although the radiative perturbations of EC has been well known since 1980 (Warren & Wiscombe, 1980), few measurements have been taken in the Arctic. Only two studies have measured the background level of EC in Svalbard (Clarke & Noone, 1985; Forsström *et al.*, Submitted). When measuring in pristine areas, e.g. in Svalbard, there is a risk that contamination from local sources will bias the measurements. For instance, the wide range of air measurements at the Zeppelin station are sensitive to local pollution from the nearby village of Ny-Ålesund. A field campaign showed that local pollution affected the Zeppelin station $6.4\,\%$ of the time (Beine *et al.*, 1996). Little effort has been put into establishing EC concentrations around local sources found in pristine areas. Two exceptions are the study by Grenfell *et al.* (2002) at the SHEBA experiment in the Arctic Ocean and a study at the Vostok Station on the Antarctic Plateau (Grenfell *et al.*, 1994).

The objective of this master thesis is to quantify the effect of EC concentrations in snow from the local sources in Svalbard. Then, we can estimate the impact of locally produced and long-range transported EC in Svalbard snow. Further, the resulting perturbations in surface albedo have been calculated. Variations in EC concentrations throughout the winter are also investigated.

This objective was solved by taking snow samples along radial transects around the settlements of Longyearbyen, Ny-Ålesund, and Svea, including areas believed to be pristine during the winter of 2007/08. These samples were melted and filtered, and the EC concentration was determined by analysis of the filter. These measurements were compared to data from the Oslo CTM2 chemical transport model.

A general overview of theory and background relating to EC in snow is given in Chapter 2. In Chapter 3, the methods used are shown. The results from these measurements are analyzed in Chapter 4. To set these measurements into a wider context, perspectives and processes important for this data are given in Chapter 5. The findings are discussed in Chapter 6 with a final conclusion in Chapter 7.

Chapter 2

Background and definitions

2.1 The cryosphere

The cryosphere is an important component of the climate system. $10\,\%$ of the land surface is permanently ice covered, and an annual mean of $7\,\%$ of the oceans are ice covered (Lemke *et al.*, 2007). Further, an area of $4.52 \cdot 10^7\,km^2$ of land on the Northern Hemisphere is snow covered in January, which is a coverage of about $49\,\%$. In August, $1.9 \cdot 10^6\,km^2$ is covered by snow. Hence, large areas are covered by snow. As a result, it is vital to be able to estimate the albedo of these snow covered areas to understand the climate system precisely. Perturbations in the albedo caused by contaminants in the snow are, also, of importance regarding the cryosphere. First, a historic overview will be given of how the knowledge of the light absorbing particles in snow was used.

2.2 Ash on snow

Ash has historically been used by farmers to hurry the snow melt on their fields. As described by a vicar from Rana in Northern Norway in 1834, farmers covered the snow pack with sand in April (Visted & Stigum, 1971). He tells (in Norwegian):

> ...sprer sanden med sin skuffel over sneen paa det sted hvor ageren ligger under. Dette middel er meget virksomt, ti de paa den hvide sne brekkede solstraaler samler sig paa sanden, deen oppvarmes og æder sig gjennem sneen som tæres hastig bort.

In Bondal, a mountain village in Southern Norway, the farmers were digging for dirt to cover the snowy fields, as well as applying ash on the snow surface (Dahl, 1998). This ash was called ”åt” or ”åte” as it ate itself through the snow. Consequently, the harvest of barley could be done about a week or two earlier than otherwise (Øystein Bondal, personal communication). An old saying states that a day of work in the spring could give an extra week in the fall. The cultivation of grains is very limited due to the harsh climate in such mountain villages, and, thus, this use of the ash was a necessity in order for the farmers to feed their families. An experiment set in Hjartdal, which is in the same municipality as Bondal, during the snow melt of 2009 validated this historic fact (see Figure 2.2). The melting of the snow pack was shortened by $4\,days$, which in average resulted in an increase of melt by about $38\,\%$. The snow melting period was short that particular year due to sunny skies and daily maximum temperatures of at least $10\,^\circ C$. For a longer melt period, the effect is expected to be larger. Thus, a week or two earlier snow melt is realistic. Further, the effect was larger in a sun exposed plot than in a more sheltered plot.

(a) March 31st (b) April 4th

(c) April 8th (d) April 9th

Figure 2.1: (a), (b), (c), and (d): Ash was applied to the snow pack in Hjartdal early in the melt season. The snow depth was $53\,cm$ when the ash was distributed evenly over the snow on March 31st 2009. The contaminated area was completely melted within $9\,days$, while the surrounding snow pack melted in $13\,days$. A second patch of ash that was more exposed to sunshine also hastened the snow melt by $4\,days$, from 9 to $5\,days$ in total. Photos by Bjørg Aamaas and Thorbjørn Aamaas.

2.3 How did we get here?

As seen in Section 2.2, the knowledge of light absorbing particles in the snow pack and the way they influence the radiation properties of the snow have existed for a long time. In a study by Elgmork *et al.* (1985), grey bands were found in the snow pack in Southern Norway. They accredited these bands from airborne pollution events. Previous studies stated that those impurities in the snow could reduce the albedo of the snow (Dunkle & Bevans, 1956; Giddings & LaChapelle, 1961); however, Giddings and LaChapelle concluded that this effect is probably negligible. Warren & Wiscombe (1980) were the first to quantify a relation between soot concentrations and snow albedos. Such highly absorbing carbonaceous particles were further investigated in the 80s (Warren, 1984; Clarke & Noone, 1985). As part of this interest, the first soot measurements in Svalbard snow were done by Clarke & Noone (1985). Warren & Wiscombe (1985) were probably the first to suggest global climate effects due to anthropogenic contaminants in the snow.

There was, then, less attention to the field until new studies modeled the climate forcing of soot more accurately. These studies focused first on soot in the atmosphere as a radiative perturbation (Haywood *et al.*, 1997; Myhre *et al.*, 1998; Jacobson, 2001; Sato *et al.*, 2003). Further, this sparked renewed interest in the radiative effect of soot in snow and ice (Hansen & Sato, 2001). Hansen & Nazarenko (2004) studied snow darkening from soot using a global climate model. Jacobson (2004) improved this by including a radiative transfer solution that relied on local soot deposition. It is now clear that this climate forcing for soot in snow has a potential important perturbation in the climate system (Hansen & Nazarenko, 2004; Flanner *et al.*, 2007). In addition to model studies, measurements of soot in the atmosphere (e.g. Sharma *et al.* (2004)), in snow (e.g. Forsström *et al.* (Submitted)), and glacier ice cores (e.g. McConnell *et al.* (2007)) have been done. In the latest IPCC assessment, the radiative forcing of soot in snow is set to $0.1 \pm 0.1\, W/m^2$ (Forster *et al.*, 2007). Flanner *et al.* (2007) have indicated a lower estimate of $0.054\, W/m^2$ with an uncertainty range from 0.007 to $0.13\, W/m^2$. Thus, the uncertainties are still large. Soot also has secondary effects on the snow. Flanner *et al.* (2007) observed that soot accelerate snow grain growth and, hence, the reduction of snow albedo. These feedbacks lead to a high "efficacy," a change in global mean temperature per unit of radiative forcing (Hansen & Nazarenko, 2004; Flanner *et al.*, 2007). During the spring snow melt, Flanner *et al.* (2007) modeled the maximum zonally averaged forcing to be almost $1.5\, W/m^2$ in the Arctic. Quinn *et al.* (2008) calculated a seasonally averaged forcing of soot in snow specifically for the Arctic that estimated a temperature response of about $0.5\,^{\circ}C$.

This master thesis is a part of this upswing. New and more data, modeling, and thoroughly interpretation is needed to understand the climate effect of soot. Measurements of EC concentrations in Svalbard and the study of local anthropogenic sources in the High Arctic is a part of this. To understand the importance of EC in the snow covered Arctic, we must first know the optical properties of snow.

2.4 The optics of snow

2.4.1 Theory of scattering and absorption

When radiation enters a snow grain, three outcomes are possible. The photons can either be absorbed, scattered, or transmitted by the grain. Similarly, photons will either be absorbed or scattered by a semi-infinite snow pack (Bohren, 1987). The ratio between the scattered outgoing radiation and all incoming radiation is called albedo. The total albedo is an integration of the spectral albedo over a range of wavelengths. As most of the incoming radiation reaching the Earth's surface is solar, the

total albedo is effectively given by the range in wavelength between 0.3 and $5\,\mu m$. Warren (1982) reviewed various definitions of albedo in a clear way. Thus, the albedo is a dimensionless number between 0 and 1, or given as a percentage between $0\,\%$ and $100\,\%$. 0 is a result of total absorption, while all radiation is reflected at 1.

For scattering by individual snow grains, the extinction cross section (σ_{ext}), single-scatter albedo ($\overline{\omega}$), and asymmetry factor (g) are the three decisive parameters (Wiscombe & Warren, 1980). These are affected by the dimensionless size parameter $x = 2 \cdot \pi \cdot r/\lambda$ and the complex refractive index $m(\lambda)$. r is the mean snow grain radius, λ the wavelength, and $m(\lambda) = m_{re}(\lambda) - im_{im}(\lambda)$. The mean optical snow grain radius is not only affected by the actual snow grain size, but also the grain shape and sintering between the grains. While the real index of refraction for ice is almost constant with varying wavelengths, the imaginary index of refraction varies significantly. The value is less than 10^{-8} in the visible and increases to about 10^{-1} at $3\,\mu m$. See Figure 1 in Wiscombe & Warren (1980) for details. In the following discussion, the individual snow grains are assumed to scatter like spheres in each other's far field. The extinction cross section is given by $\sigma_{ext} = \pi \cdot r^2 \cdot Q_{ext}$, where Q_{ext} is the dimensionless extinction efficiency. The quantity is only needed when the ground below the snow pack is optically seen; thus, the snow pack is not optically semi-infinite. In this study, this parameter can be neglected due to mostly opaque snow packs (see Section 4.2). The single-scatter albedo is a ratio of scattering cross section (σ_{sca}) over extinction cross section: $\overline{\omega} = \frac{\sigma_{sca}}{\sigma_{ext}}$. This parameter is a dimensionless value in the range $0 \leq \overline{\omega} \leq 1$. At 1, everything is scattered, as opposed to complete absorption for $\overline{\omega} = 0$. The asymmetry factor, g, is the mean value of $cos\Theta$, where Θ is the scattering angle. g varies within $-1 \leq g \leq 1$. $g = 0$ gives isotropic scattering, while completely forward-directed scattering is when $g = 1$. Snow is scattering strongly in the forward direction since photons tend to be refracted through ice particles, rather than be reflected by the snow particle surface (Flanner, 2007). Wiscombe & Warren (1980) explain how these parameters vary as a function of wavelength in great detail. The extinction efficiency, Q_{ext}, is only weakly sensitive to wavelength. The extinction efficiency will decrease slightly with increasing snow grain radius. The asymmetry parameter, g, is somewhat more sensitive to wavelength, varying between 0.88 and 1. The forward scattering is the least pronounced in the visible. The single-scattering coalbedo, defined as $1 - \overline{\omega}$, is sensitive to both wavelength and snow grain size. Increasing grain size results in increasing single-scattering coalbedo. The coalbedo is at its lowest in the visible at about 10^{-5} and increases steadily to about 0.1 or 0.5 at $\lambda = 1.5\,\mu m$.

From the parameters above, exact equations can model the radiative properties of snow. However, they are so advanced that they have to be solved with approximations. Bohren (1987) avoided this by using approximate equations that can be solved exact. If we consider the snow pack as a continuous scattering-absorbing medium, laterally infinite, and bounded by parallel planes, we can calculate the albedo R from multiple scattering as:

$$R = (\sqrt{1 - \overline{\omega} \cdot g} - \sqrt{1 - \overline{\omega}})/(\sqrt{1 - \overline{\omega} \cdot g} + \sqrt{1 - \overline{\omega}})$$

By using this equation, the spectral albedo of snow can be modeled rather accurately. Examples of measured spectral albedos over a snow surface for a range of wavelengths are given in Figure 2.2(a). The spectral albedo is the highest in the visible and is, for new snow, above 0.9. As the wavelength increases, the spectral albedo, generally, decreases to less than 0.1 at $1.5\,\mu m$. In the infrared, the spectral albedo is mostly very low with a few minor spikes. The spectrally integrated albedo for the 350-$1800\,nm$ spectrum for the clean snow in Figure 2.2(a) is 0.91. Altogether, the spectral albedo of snow surfaces is very sensitive to the wavelength. As Bohren (1987) cleverly states, "snow is the whitest natural substance on our planet; it is also the blackest." This observation is mainly due to the

fact that the absorption in ice varies greatly between the visible and infrared part of the spectrum. Ice is a weak absorber in the visible spectrum. If small amounts of light absorbing impurities are present, this can alter the visible albedo. That will be discussed in Section 2.5.1.

The albedo is also sensitive to external parameters that might affect the snow grain or radiation properties. The four most important physical parameters are the snow grain size (r), solar zenith angle (Θ_0), cloud cover, and snow pack thickness (Wiscombe & Warren, 1980). An increase in snow grain size leads to an increase in absorption and forward scattering. The albedo reduction is primarily caused by a decrease in the single-scatter albedo $\overline{\omega}$ for $\lambda < 2.5\,\mu m$. The sensitivity is largest in the near infrared. The variability in the snow grain size was the decisive factor at wavelengths longer than $1000\,nm$ for the albedo spectrums shown in Figure 2.2(a). The grain size was typically $1\,mm$ for the clean snow, 1-2 mm for dust contaminated snow, while a firnspiegel with snow grains of 2-4 mm in size was observed for the EC contaminated snow. Thus, the spectral albedo for $> 1000\,nm$ was decreasing with increasing grain size.

The albedo will increase with increasing zenith angle. In the visible, the effect is only a few percent, but the sensitivity is larger in the near infrared. A cloud cover will convert direct radiation into diffuse radiation. That will affect the effective zenith angle, and for purely diffusive radiation, it is $\Theta_0 = 50\,^\circ$. Further, clouds will alter the spectral composition of radiation reaching the snow surface. The visible wavelengths will get relatively richer, leading to an increase in the spectrally integrated albedo. This effect outwins any effects from a changing effective zenith angle.

Albedo sensitivity due to snow pack thickness is here discussed. As snow and ice layers are finite in depth, radiation might penetrate through these layers. Thus, the surface below will affect the albedo. Since radiation penetrates snow much easier in the visible than in the near infrared, this will mainly affect the visible albedo. Wiscombe & Warren (1980) found that the albedo would effectively follow that of a semi-infinite snow pack for $20\,cm$ of fluffy new snow, $20\,cm$ of fine-grained old snow, or $50\,cm$ of old melting snow. The average snow depth in the work here was $67\,cm$ and the snow pits were rarely shallower than $20\,cm$. Hence, we can assume the semi-infinite approach to be valid. Thus, the albedo can be seen as an integration of the scattering in the upper part of the snow pack. These values were calculated for pure snow. Flanner & Zender (2005) modeled that about 20 to $45\,\%$ of the solar absorption occurs at more than $2\,cm$ beneath the surface. The solar zenith angle is, in general, high in Svalbard, and, hence, this percentage is somewhat smaller.

The majority of the radiation reaching the surface of the Earth is in the visible and near infrared part of the spectrum where the spectral albedo is high. Hence, snow has a high spectrally integrated albedo. Albedos over snow surfaces in late winter and spring are typically 75 to $90\,\%$, while it drops to about $60\,\%$ when snowmelt begins (Warren, 1982). This stands in contrast to other surfaces found on the Earth. For example, dry tundra was measured to have an albedo of $17.3\,\%$ and wet tundra $12.4\,\%$ in Barrow, Alaska, under clear sky conditions (Grenfell & Perovich, 2004). A similar variability is observed between snow-covered and bare ground surfaces in Ny-Ålesund (see Figure 2.2(b)).

2.4.2 Snow grain size

As explained in Section 2.4.1, the effective snow grain size determines the albedo. In addition, this parameter is important for the depth profile of absorption (Flanner & Zender, 2005). Snow metamorphism will typically lead to an effective grain growth, and, thus, lowering of the albedo. There are five primary processes affecting the evolution of grain size (Flanner & Zender, 2006). First, vapour density gradients are caused by difference in curvature of particles as given by Kelvin's Law. The equilibrium vapour pressure is

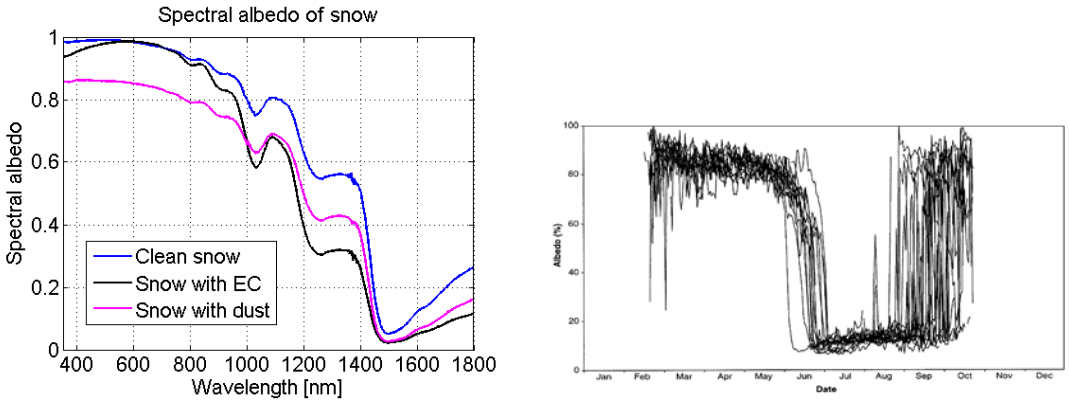

(a) Albedo spectrums of snow

(b) Albedo in Ny-Ålesund

Figure 2.2: (a): A typical albedo spectrum of snow with different physical properties and concentrations of contaminants. The three lines indicate albedo rendered by clean snow, snow heavily contaminated by EC, and snow highly contaminated by Aeolian sediments. The clean snow site is on Tellbreen, far from any pollution sources. Snow near the end moraine of Tellbreen is classified as the dusty snow, as sand grains were easily observed in the snow. Longyeardalen was classified as a polluted site and represents snow with EC. The albedo for the 350-1800 nm spectrum was 0.91, 0.86, 0.78 for the clean, EC contaminated and dust contaminated sites, respectively. These values were calculated with help from weighted solar spectrum fluxes given by C.A. Pedersen (personal communication). The noise around 1380 nm is caused by a water vapour absorption band in the atmosphere (Liou, 2002) that affects the measurements. (b): The daily surface albedo in Ny-Ålesund. Every line stands for a year between 1981 and 1997, and, altogether, they show the range in the natural variability. Since there is no sunlight in winter, there is, also, no albedo data. The figure is adapted from Winther *et al.* (2002).

$$p_s(r,T) = p_{eq} \cdot \left(\frac{2 \cdot \gamma}{R_v \cdot T \cdot \rho_i \cdot r}\right)$$

where p_{eq} is the saturation vapour pressure over a plane surface, γ the surface tension of ice against air, R_v the specific gas constant for vapour, T temperature, and ρ_i the density of ice. The grains are typically not getting larger than $1\,mm$. This process, the equitemperature metamorphism, is important during the first days after a snow fall when branch dendrites are broken down. The second process is important when there is a significant temperature gradient between the ground and snow surface and is called temperature gradient metamorphism. That is typical during most of the winter in Svalbard. This will cause a vapour density gradient. Under a temperature gradient, the grain growth will (Flanner & Zender, 2006) 1) increase with increasing temperature gradient 2) increase with increasing temperature 3) increase with decreasing snow density 4) decrease with time and increasing particle size. A large temperature gradient, together with high air temperature and low snow density will, then, cause the most rapid grain growth. If the temperature gradient remains for several weeks, snow crystals several millimetres in size will develop, called depth hoar. Depth hoar crystals need a temperature gradient greater than about $0.15\,^{\circ}C$ to be formed (Jones *et al.*, 2001). Third, melt-freeze metamorphism will lead to very rapid grain growth, up to several millimetres, during melting and freezing of snow. The fourth process is wind ventilation that will transport vapour around in the surface snow. The fifth and final theory is that sintering between snow grains can affect the snow grain size.

2.4.3 Albedo feedbacks

Changes in climate, such as the extent of snow cover, are responding to externally forced perturbations. These changes are called feedbacks and can either strengthen or weaken the initial climate perturbation. Melting of snow is a highly non-linear process that will lead to such feedbacks, mostly

positive feedbacks (Flanner, 2007). The most striking positive feedback is the snow-albedo feedback (Randall *et al.*, 1994). An arbitrarily reduction in snow cover will decrease the surface albedo, leading to an increase in temperature. This gives sensitivity to the system since snow and ice surfaces have such high albedos compared to most other types of surfaces on the Earth. That will reduce the snow cover even more. The temperature increase will also promote snow grain growth, which reduces the albedo. Snow metamorphism will be thoroughly discussed in Section 5.1.2. This warming-induced grain growth is a second positive feedback. The maximum forcing of these feedbacks coincides with the onset of snow melt. These feedbacks are influenced by contaminants, as discussed in Section 2.5.1.

Radiation measurements are continuously measured in Ny-Ålesund (Ørbæk *et al.*, 1999; Winther *et al.*, 2002). Both studies show a clear decrease in albedo from winter to summer. (Ørbæk *et al.*, 1999) state that the albedo is typically above $80\,\%$ from the return of the sun in February until middle of May. A minor reduction in albedo is caused by snow metamorphism as the snow ages. As seen in Figure 2.2(b) (adapted from Winther *et al.* (2002)), a sharp and swift decline is observed during the snowmelt, which starts in early June. The albedo drops from $80\,\%$ to below $20\,\%$ within 15 to $20\,days$. Winther *et al.* (2002) found no significant trends in changes of the observed seasonal albedo variations in the period 1981-1997. Any feedbacks that will alter the date of transition between snow cover and bare ground will, thus, have large impacts on the climate system.

2.5 Light absorbing aerosols and particles

Aerosols consist of a variety of different compounds, among them light absorbing particles. Bond & Bergstrom (2006) gave a good overview of carbonaceous particles and their optical properties. This field of science is complicated by the different scientific communities defining these particles differently. That is partly due to the fact that the different groups are focused on different aspects, as well as the wide range of instrumentation used. Whether to name soot particles as black carbon (BC) or elemental carbon (EC) is a result of this variability in instruments with dissimilar measuring techniques. The light absorbing particles have been called soot, black carbon, carbon soot, and carbon black in the literature. Due to the measuring technique used in this project, these particles are, here, called elemental carbon (EC). An overview of terms related to EC is shown in the list under (as used in (Wiscombe & Warren, 1980; Jones *et al.*, 1997; Bond & Bergstrom, 2006)):

Terminology for light absorbing particles

- **Ash**: The mineral-rich powdery residue left on-site after a fire. The ash is created in a fire by mineralization, a process where organic substances are converted into inorganic substances.
- **Coal dust**: Coal is mined on Spitsbergen. Since coal is brittle of nature, coal dust is created during mining, transportation, and mechanical handling of coal. The coal has on a geological time scale been processed from vegetable matter due to high pressure and temperatures. In the process, the substance turns blacker. Combustion of coal will produce ash and soot.
- **Soot**: Black, blackish, or brown particles that are produced by incomplete combustion of fossil fuel (coal, oil, and gas), biofuel (charcoal, firewood, and dung), and biomass burning. These are formed by gas phase processes and gas-to-particles conversion. They are typically 0.05 to $0.2\,\mu m$ in size. Soot consists mainly of carbon and is a broad term for different carbon species, including weakly-absorbing, non-absorbing, as well as strongly absorbing black carbon (BC).

- **Black carbon (BC)**: Soot particles that strongly absorb radiation. They consist mainly of carbon. Black carbon is measured by a filter-based optical method and is, thus, an instrumental definition.
- **Elemental carbon (EC)**: This is pure carbon that does not volatilize below temperatures around $550\,^{\circ}C$. As for BC, this is an instrumental expression linked to the thermal-optical method.
- **Brown carbon**: Organic matter that partly absorbs light, but not as effective as BC.
- **Organic carbon (OC)**: The thermal-optical measuring technique has organic carbon as one of its parameters. This carbon has at a stage been a part of an organism. The light absorbing part of OC is called brown carbon.
- **Carbonate carbon**: This compound is a salt or an ester of carbonic acid. Carbonates are found in Svalbard soil and rocks.
- **Total carbon**: The sum of EC and OC is by the thermal-optical method, defined as total carbon (TC).
- **Light-absorbing carbon (LAC)** Operationally based definitions can be avoided if we use LAC as a general term for carbonaceous light-absorbing particles.
- **Dust**: Sediments that are made airborne and redeposited, often called Aeolian sediments. There is a range of dust particles, where clay minerals is a major component. Clay minerals include iron oxide and carbon or organic materials. The major source is deserts.

In the literature, soot concentrations have been given as either BC or EC. As these two methods measure differently, they tend to give dissimilar results. A fixed ratio between these two parameters has not been established. A study by Watson *et al.* (2005) states that the methods differ by a factor between 2 and 7. As Bond & Bergstrom (2006) point out, the strongly light-absorbing component in a carbonaceous aerosol or particle consists of a few percent, and it is difficult to separate. BC may be an overestimate of the soot content as any absorbing substance, including dust, minerals, and organic matter, will affect the readings. EC is expected to underestimate the soot level as some light-absorbing carbon, often defined as brown carbon, will not be detected as EC by the thermo-optical method (Andreae & Gelencsér, 2006). High natural variability in the snow pack adds to the complexity when comparing BC and EC concentrations. An accuracy of about $100\,\%$ is expected when all error sources are included for the work done in this thesis (Forsström *et al.*, Submitted).

Particles are called aerosols once they are suspended in the atmosphere. These aerosols are, then, transported from the emission site. The transport of EC particles in the atmosphere and inside the snow pack is mostly described with physical processes since the material is practically inert, non-volatile and insoluble (Ogren & Charlson, 1983). According to Bond & Bergstrom (2006), this substance has a high electrical and thermal conductivity due to the free movement of π-electrons. Further, the EC particles absorb radiation from a broad electromagnetic spectrum since the energy levels of these electrons are so close. In addition to be such a significant absorber, the EC particles will, also, easily warm a surrounding snow surface due to its thermal conductivity. The scattering and absorption of EC particles is mainly given by its physical form. The morphology depends by the molecular form (sp^2 and sp^3 bonds), size, shape, and state of mixing. From this and the substance's refractive index, scattering and absorption cross sections can be calculated (Bond & Bergstrom, 2006).

2.5.1 Implications for a snow pack

In Section 2.4.1, the weak absorptive properties of ice in the visible spectrum (Wiscombe & Warren, 1980) was reviewed. Small amounts of light absorbing particles will, therefore, reduce the visible albedo (Warren & Wiscombe, 1980). Since ice is highly absorptive in the infrared, the effect of light absorbing particles is minimal in that part of the spectrum. Warren & Wiscombe (1980) showed that EC is the most efficient natural absorber, while dust can also reduce the albedo at larger concentrations. EC is about 50 times more effective at reducing the albedo than dust (Warren, 1984). Both dust and EC increase the single-scattering coalbedo $(1 - \overline{\omega})$ significantly for $\lambda < 0.9\,\mu m$. That is in the same part of the spectrum as the imaginary refractive indexes are $m_{im}(EC) >> m_{im}(ice)$ and $m_{im}(dust) >> m_{im}(ice)$. EC tends to reduce the albedo in such a way that the visible albedo is almost constant with wavelength. Dust, on the other hand, reduces the spectral albedo most significantly at the lower wavelengths. This is a direct result from the constant single-scattering coalbedo $(1-\overline{\omega})$ for EC in snow in the visible spectrum, while a minimum around 0.6 to $0.7\,\mu m$ is observed for dust. That is likely due to the red iron oxide often found in dust (Warren & Wiscombe, 1980). Large quantities of dust and sand grains were observed in the dust contaminated snow given in Figure 2.2(a). That explains the reduced spectral albedo for $< 700\,nm$. The EC concentration in snow was much lower in the soot contaminated snow sample than the sand content in the dust contaminated sample. Even though EC is much more effective at reducing the visible albedo than dust, the reduced albedo effect is, then, largest for the dusty snow sample due to the extremely high dust concentration. The difference in spectral albedo between the clean and EC contaminated sample in Figure 2.2(a) is minimal in the visible wavelengths. Hence, to optically measure EC concentrations is difficult in-situ on natural snow packs. That is partly due to the high natural variability in snow albedo. The smaller the particles are, the larger the radiation effect is for a given EC or dust concentration. The effect is also larger for old, coarse grained snow than new, fine grained snow. As observed in Section 2.4.1, radiation penetrates deeper and can interact with more contaminants the coarser the snow grains are. Then, the perturbation in snow albedo due to contaminants is proportional to the grain size (Flanner *et al.*, 2007). Warren & Wiscombe (1980) argued that the depth needed for a snow pack to appear semi-infinite is thinner for snow with light absorbing particles since the particles will absorb the radiation in a greater extent than the snow itself. Then, only a fifth of the snow layer depth is needed for EC contaminated snow to appear semi-infinite for typical EC values.

The state of mixing can be divided into three using the terminology suggested by Bond & Bergstrom (2006). The EC particles could be in an external mixture with other particles and snow crystals. A volume mixture is a perfect homogenous mix on the molecular level. What is mostly observed in aerosols and in snow crystals is an encapsulated mixing. This internal mixture is a heterogeneous particle composition. A newly emitted EC particle is typically $50\,nm$ in size (Bond *et al.*, 2006). How these particles evolve in the atmosphere is described in Section 2.7. When EC particles are in the atmosphere, they tend to coagulate with each other and other particles and increase in size. An aggregate will tend to decrease the mass absorption cross section (Bond & Bergstrom, 2006). One explanation of this is that aging results in the collapsing of the particles to more compact clusters. However, if the EC particle is coated by other less absorbing particles, this mass absorption cross section will increase. The second process will be the most important, and Bond *et al.* (2006) calculated that the absorption of an aged aerosol is about $50\,\%$ greater than for a fresh aerosol. This knowledge can be transferred into the absorption and scattering properties of EC particles in the snow pack. EC particles found inside snow crystals are much more absorbing than particles found on the surface of snow crystals (Warren, 1982, 1984). Chýlek *et al.* (1983) found that an internal mixture of EC and snow is almost twice as effective as an external mixture at reducing albedo.

The introduction of contaminants to the snow pack will trigger and enhance the two feedbacks mentioned in Section 2.4.3, the snow-albedo feedback and the warming-induced grain growth feedback. In addition, Flanner *et al.* (2007) observed that heating due to contaminants in the snow pack leads to a more rapid grain growth. Another positive feedback is that EC will stay on the snow surface during the spring melt (Conway *et al.*, 1996), resulting in higher surface concentrations of EC. That will further reduce the albedo and enhance melting. In sum, these feedbacks will lead to an earlier snow melt. That will result in a prolonged time with a typical summer albedo (below $20\,\%$) instead of a typical winter albedo ($80\,\%$). These albedo values are those generally measured in Ny-Ålesund, as seen in Figure 2.2(b).

2.6 Sources

In this study, local sources within Svalbard will be distinguished from remote pollutant sources. First, an overview of long-range transported sources is given followed by more detailed information about the local sources.

2.6.1 Regional and global sources

Bond *et al.* (2004) estimated that the global annual emission of EC in 1996 was $8.0\,Tg$, with an uncertainty range of 4.3 - $22\,Tg$. The sources are burning of fossil fuel ($38\,\%$), biofuel ($20\,\%$), and open burning ($42\,\%$). All continents in the world contribute significantly to the contained combustion estimates. Here, contained combustion is a summation of fossil fuel and biofuel burning. Industrial regions in the Northern Hemisphere are heavy contributors. Asia has, clearly, the largest share, as China alone stands for $29.5\,\%$ of the global emissions. $55.7\,\%$ of the emissions come from Asia. EC from open burning is dominated by Africa ($44.3\,\%$) and Central/South America ($27.4\,\%$). In summer, forest fires are widespread in the Arctic, especially in Siberia and Canada. For a visual look at the global EC emissions in 2000, see Figure $B2$ in Dentener *et al.* (2006). The EC emissions have varied throughout the years. In the last decades, the EC emissions from fossil fuel have decreased significantly in Europe, former USSR, and USA, while it is spiking rapidly in China and India (Novakov *et al.*, 2003). This will gradually change the emission estimates and possibly the resulting EC concentrations in the Svalbard snow pack.

Since the atmospheric lifetime of EC is about 7 days (Schulz *et al.*, 2006) and the distances to Svalbard from most of the polluting regions of the world are vast, only small amounts are transported to Svalbard. The lifetime is governed by scavenging processes, such as wet and dry fallout. The deposition processes are given more attention in Section 2.7. Stohl (2006) defines the time air has been continuously north of $70\,^{\circ}N$ as the air's Arctic age. Near the surface north of $80\,^{\circ}N$, this mean Arctic age is about 1 week during winter. The major meteorological patterns are important for the transport of EC to the Arctic. This transport of pollutants into the Arctic can be divided in three different pathways (Stohl, 2006). The first is low-level transport with ascent in the Arctic, while the second does not include the ascent. Finally, there can be uplift outside the Arctic followed by descent once the air parcel is in the Arctic. Pollution from Europe can follow all three pathways in winter, but only the first and third in summer. Asian and North American pollution can also only be transported by the third path. Even though China is the largest EC emitter, very little of this EC reaches the Arctic. That is caused by the great distance and the temperature gradient, as discussed in the next paragraph. Stohl (2006) observed that EC is most likely to be transported into the Arctic from Europe and Siberia in winter and from Siberia in summer.

Some studies have investigated where polluted air entering Svalbard come from. During winter, Eneroth *et al.* (2003) observed that high CO_2 mixing ratios were observed for air coming from Europe and Siberia, while low from the Atlantic sector. Forsström *et al.* (Submitted) saw that air arriving from east of Svalbard contained more than two and half times more EC than air from southwest. From trajectory analysis, Eleftheriadis *et al.* (2009) found that air masses originate mainly from the Arctic and Russia. Sources of high EC content were modeled to mainly come from Northern and Central Russia, from the Kola Peninsula in the west to Siberia in the east. Reddy & Boucher (2007) estimated that Europe is the largest contributor of EC deposition in snow north of $60\,^{\circ}$ with a $63\,\%$ share. That is confirmed by Shindell *et al.* (2008) who found that the European emissions are the most important for EC deposition in the entire Arctic excluding Greenland.

One reason why pollution cannot reach Svalbard is that the High Arctic is somewhat isolated by the Arctic front (Law & Stohl, 2007). Air parcels and pollutants in those parcels south of this transport barrier will not be able to infiltrate the lower troposphere of the High Arctic. Any northward travelling air parcels will ascend along constant potential temperature surfaces. In winter time, this dome of cold Arctic air expands southward to include highly inhabited areas of Europe, North America, and Northern Asia. In winter, diabatic cooling can lead polluted air into the lower Arctic troposphere as modeled by Klonecki *et al.* (2003). Due to the general circulation patterns, transport of pollution is favoured from Europe and Central Asia (Bottenheim *et al.*, 2004; Stohl, 2006). A maximum in pollution in the Arctic is seen in late winter and early spring (Ström *et al.*, 2003). Due to its distinct appearance, this phenomenon has been named Arctic Haze (Shaw, 1995). These plumes can stay for several weeks due to the typical temperature inversion, little precipitation and water vapour available, and little turbulent exchange in the Arctic. Suzuki *et al.* (1996) estimated the aerosol residence time in Ny-Ålesund to vary between 26 and $78\,days$ in February and March 1995. As the Arctic Haze appears at the same time as the return of the sun in the High Arctic, carbonaceous light-absorbing particles settling on snow surfaces will give a significant perturbation to the radiation balance.

Svalbard is situated on the borderline between cold Arctic air and mild maritime air. As a result, the cyclonic activity in the areas is large (Førland *et al.*, 1997a). Hence, events can transport pollutants, e.g. EC, to Svalbard, and these events are important for the total EC transport to Svalbard. Some of these observed events will be discussed in the rest of this section. An extreme Arctic Haze event with the highest ever recorded EC concentrations at Zeppelin was observed in spring 2006 (Stohl *et al.*, 2007). A combination of abnormal high temperatures in the European Arctic and heavy agricultural fires in Eastern Europe resulting in plumes recorded in late April and early May 2006 over Svalbard. Discolouration of snow in the matter of hours was observed on a glacier near Ny-Ålesund. That particular study points to drifting snow as an important process of the discoloration as dry deposition would be too slow.

A study by Stohl *et al.* (2006) shows that boreal forest fires in North America can affect most of the Arctic in the summertime. The summer of 2004 was a very active forest fire season, especially in Alaska. Elevated concentrations of light absorbing aerosols were observed in the entire Arctic. The snow albedo dropped by about $3\,\%$ at Summit on Greenland during a passage of the largest fire plume.

2.6.2 Local sources

Most of the pollution originating locally comes from the settlements on Spitsbergen. These are Longyearbyen (population: 2100), Ny-Ålesund (25), Svea (240), Barentsburg (500), and Hornsund (10). Statistics over all registered vehicles in Svalbard are given in Table (2.1). According to this statistics, Longyearbyen has clearly the largest potential impact on EC concentration in snow. Svea comes second and Ny-Ålesund third. Barentsburg is a Russian mining town with heavy machinery

Table 2.1: Registered vehicles in Svalbard as of December 31st 2007. This information is given by Petter Braaten from Sysselmannen. All vehicles in Svalbard registered with an address outside the archipelago are here put under the statistics of Longyearbyen since most of the people and companies are located there. The actual number of vehicles in Barentsburg is much larger than what is shown here. LYR = Longyearbyen, Ny-Å = Ny-Ålesund, Bar = Barentsburg, Horn = Hornsund, Bjø = Bjørnøya

Type	LYR	Svea	Ny-Å	Bar	Horn	Bjø	**Total**
Cars	1006	144	17	-	-	-	**1167**
Snowmobiles	2600	26	54	2	5	1	**2688**
Trucks	95	10	2	-	-	-	**109**
Motorbikes	80	-	4	-	-	-	**84**
Tractors	15	3	3	-	-	-	**21**
Tracked vehicles	20	-	-	-	-	-	**20**
Trailers	93	19	5	-	-	-	**117**
Total	**3909**	**202**	**85**	**2**	**5**	**1**	**4206**

and a number of vehicles. These are somehow not included in the numbers given. The actual number of vehicles in Barentsburg is probably similar to Svea or greater. Kallenborn *et al.* (2009) estimated an annual EC emission of $79\,tons$ in 2007 for land and ocean areas within Svalbard, as well from transport routes directly linked to Svalbard. That is nearly a doubling in EC emissions since 2001.

Longyearbyen

In Longyearbyen, by far the largest settlement on the island, the pollution can be divided roughly into three: the coal and diesel power plant, open coal piles at the operating mine and at the harbour, and all vehicles, including cars and snowmobiles. Thus, two types of carbon substances are seen. The first is the finer EC particles from combustion, while much coarser coal particles originate from the coal mining activity. As reviewed in Section 2.7, the finer EC particles straight from combustion have a size of about $50\,nm$. In comparison, the coal dust particles can be up to several millimetres in diameter.

As seen in Table 2.1, about $2/3$ of all vehicles in Longyearbyen are snowmobiles. They are only in use during the winter season. The increase in quantities of lead free gasoline 95 octane and extra gasoline 98 octane sold in Longyearbyen during the winter (see Figure 2.3) is most likely solely due to these snowmobiles. Most used snowmobiles have a two-stroke internal combustion engine, while new models sold in the recent years are four-stroke. In comparison, cars have four-stroke engines. Heavy machinery runs normally on diesel. The winter months makes construction virtually impossible leading to increased activity in summer. The spiking in diesel consumption during summer is likely due to this.

The power plant is the only Norwegian power plant driven by coal, consuming about $26700\,tons$ of $coal/year$ during the 2007/08 season (see Table 2.2). In addition, the power plant has a reserve power plant running on diesel. Whenever, the main power plant is down due to repairs and malfunctions, the reserve produces electricity and district heating. As discussed by Bond *et al.* (2004), high-emitting events can occur during combustion. The smoke from the power plant can typically be classified as either black or white. These differences in the smoke indicate different processes that will result in variable emission factors. An episode of no cleansing of the exhaust, and, thereby, production of black smoke is seen in Figure 2.4(a).

Reimann *et al.* (Submitted) monitored some aromatic volatile organic hydrocarbons (VOCs) in the centre of Longyearbyen. They found extremely high concentrations of VOCs in the mornings and

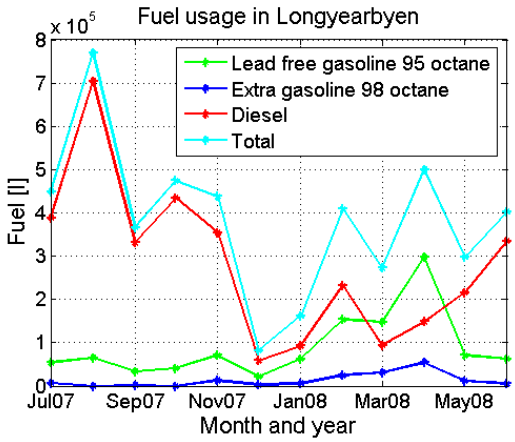

Figure 2.3: The fuel usage in Longyearbyen on a monthly basis for July 2007 to June 2008 according to Frank Jakobsen in Leonhard Nilsen & Sønner AS (Lns) Spitsbergen. This company is the only distributor of fuel in Longyearbyen.

Table 2.2: The fuel usage for the power plants in Longyearbyen and Ny-Ålesund from July 2007 to June 2008. Odd Jostein Sylte at Bydrift Longyearbyen and Frank Jakobsen from Leonhard Nilsen & Sønner AS (Lns) Spitsbergen are the sources behind the data for Longyearbyen, while Knut Breivegen from Kings Bay gave information for Ny-Ålesund.

Month	Longyearbyen coal power plant	Longyearbyen diesel power plant	Ny-Ålesund diesel power plant
Unit	ton coal	1000 litre diesel	1000 litre diesel
Jul 2007	1.552	98.289	67.514
Aug 2007	1.885	81.896	68.180
Sep 2007	1.939	162.717	81.120
Oct 2007	2.304	178.986	99.558
Nov 2007	2.332	136.831	96.631
Dec 2007	2.501	7.505	107.749
Jan 2008	2.501	22.122	107.845
Feb 2008	2.350	33.498	107.870
Mar 2008	3.091	3.822	106.932
Apr 2008	2.245	1.764	121.397
May 2008	2.025	3.729	88.139
Jun 2008	1.975	4.580	67.813
Total	**26.700**	**735.739**	**1.120.748**

(a) Smoke from the power plant (b) Coal pile

Figure 2.4: (a): Black smoke from the coal power plant in Longyearbyen on the 30th of March 2009. During that particular episode, the exhaust was not cleansed. (b): Airborne coal dust seen as black smoke at the coal processing plant nearby Longyearbyen on the 19th of February 2008. Photo by Åsmund Aamaas.

afternoons from mid-April to mid-May, the peak season for snowmobile driving. That is due to the usage of outdated two-stroke engine technology without any catalytic converter systems. The total yearly emissions of hydrocarbons was estimated to $80.8\,tons$, in which snowmobiles contribute with $88\,\%$. Since snowmobiles are driven over vast distances on Spitsbergen, the emissions will be spread out over large areas. The average concentrations in Longyearbyen in spring are almost as high as in Zurich, a city inhabited by around 100 times more people than Longyearbyen.

The local mining activity leads to various piles of coal situated at several places around the town. Some coal was during the 2007/08 winter stored just outside the mine entrance at Mine 7 about 13 km east of Longyearbyen, while some coal is found at the shipping harbour. In Figure 2.4(b), a coal pile at a coal processing plant is shown. This processing plant is by the harbour. An overview photo of the harbour and the processing plant is seen in Figure 2.5. The coal piles are the very dark areas to the left. Consistent south-easterly winds make a clear fan downwind. A study by Bøggild *et al.* (2007) states that snowmelt starts before temperature reaches zero due to extremely high coal dust and EC concentrations downwind of the processing plant. This is caused by a "snow/ice based green house effect," which was first described by (Bøggild *et al.*, 1995). The local coal mining company, Store Norske Spitsbergen Kulkompani (SNSK), is well aware of the large quantities of coal dust transported from the open coal piles. SNSK is planning to reduce the coal dust transport by using silos to store the coal instead of piles unprotected by the winds. More information about this can be found in Svalbardposten, the local newspaper (Amundsen, 22. August 2008). In February 2009, SNSK even halted the mining operations temporary due to significant coal dust loss from Mine 7 to the surroundings (Amundsen, 20. February 2009).

Ny-Ålesund

Ny-Ålesund is electrified and heated by a diesel power plant where the consumption for the 2007/08 winter is given in Table 2.2. The number of vehicles is only $2\,\%$ of what found in Longyearbyen.

Figure 2.5: A view of Svalbard Airport taken on March 10th 2008. The black areas are coal deposits and the coal processing plant. Downwind of these, a clear fan of coal dust discolours the surface snow. Photo by Markus Eckerstorfer.

Ny-Ålesund was established as a coal mining town, but closed down in 1963 (Arlov, 2003). Mine entrances and rock piles from the mining are close to the settlement. Rocks of coal and coal dust are laying around these sites.

Svea

Svea is a company town with considerable mining activity by SNSK. The author failed to get access to the fuel consumption data for the diesel power plant, which provides energy to the settlement. On Cape Amsterdam, several hundred thousand tons of coal is stored regularly. Windblown coal dust from the site is considerable. A study by Myhr (2003) estimated from snow samples that $54.1\,tons$ of "organic carbon" is lost to the snow pack downwind, i.e. southwest, of the coal pile. This "organic carbon" is thought to be mostly coal dust. Since he took measurements in only the most affected area, the total amount of coal dust in the snow is much higher. The snow downwind of the open coal pile is heavily darkened in a similar fashion to what is observed in Longyearbyen (see Figure 2.5). Myhr (2003) observed this miscolouring at least $4\,km$ downwind of Cape Amsterdam. Further, he observed a decrease in coal dust concentration in the snow by about $8\,\%$ for every $250\,m$ away from the coal pile. Coal dust is also lost during transport from the Svea Nord mine to Cape Amsterdam. Myhr (2003) estimated a yearly loss of about $30\,tons$ of coal dust along this road. In comparison, $116\,ton/year$ of sediments were made airborne in the same area. These sediments are mostly lose gravel from the road. After the trucking distance between the mine and Cape Amsterdam was halved in 2004, lower values of coal dust and sediment fallout was measured in 2006 (Stokkan, 2007).

Barentsburg

No measurements were taken around Barentsburg; however, local EC pollution is clearly visible around the settlement. The coal power plant in the settlement does not include any cleansing of its smoke. Black smog is visible downwind of the power plant, and the snow around the settlement is visibly discoloured (see Figure 2.6(a) and 2.6(b)). Forsström *et al.* (Submitted) measured a mean EC concentration of $254.0\,\mu g/l$ on Linnébreen, $15\,km$ southwest of Barentsburg.

(a) Smoke from the power plant (b) Smog over Isfjorden

Figure 2.6: (a): Barentsburg and its surroundings on the 18th of April 2009. The black smog on the left side of the photo originates from the coal power plant. The snow is clearly darker in the vicinity of the settlement, and that is mostly due to soot. Mining operations were closed at the time; hence, there is little coal dust on the snow surface. (b): The view of Isfjorden seen from Cape Linné on the same date. A clear dark smog layer is above the fjord. The thin and slender cloud seen above the smoke is distinctly discoloured. That particular cloud was considerably darker than any other cloud observed over the horizon when this photo was taken.

Hornsund

Hornsund is considered as an insignificant pollution source and has not been assessed here. However, this small research station gets electricity produced by small diesel generators and heating by coal combustion.

2.7 Deposition of EC to snow

EC particles are emitted to the atmosphere, transported by the winds, and finally deposited. Where there is snow, the EC particles will be incorporated in the snow pack. The EC particles are normally emitted with a mix of other pollutants varying with the type of the source. Most EC is emitted as hydrophobic, i.e. insoluble particles (Lund, 2008). Once emitted, these particles will be aged. The aging turns the particles hydrophilic. Since hydrophobic particles are unlikely to be deposited by precipitation, how the aging of the particle is proceeding is crucial to determine the atmospheric lifetime of EC. The aging is governed by physical and chemical processes (Croft *et al.*, 2005). Among the possible physical processes is the condensation of sulphuric and nitric acid onto the EC aerosols. SO_2 is co-emitted with EC, and the size of this concurrent emissions gives sensitivity to the aging process. An abundance of sulphuric acid will promote aging. The other physical process is the coagulation with other species that are soluble, e.g. sulphates. The chemical process is oxidation, which leads to surface groups that form hydrogen bonds. Aging is promoted if concurrent emissions of SO_2 are elevated and if effective production of sulphuric acid is occurring. While the EC is aged, it is also transported in the atmosphere. This transport includes large-scale motions (e.g. synoptic weather systems) and smaller scale processes (e.g. convection and turbulence). The transport is faster and more effective during the winter than summer, which partly explains the highest EC concentrations in the Arctic during the winter (see Section 2.8.1).

Bond *et al.* (2006) listed a number of combustion particle size studies. From that, a newly emitted EC particle is typically $0.05\,\mu m$ in size, while an aged particle has a diameter of about $0.2\,\mu m$. In comparison, the typical aerosol particle size at Zeppelin during the spring months is found in the

accumulation mode of about $0.15\,\mu m$ (Ström *et al.*, 2003). The less polluted summer air contains smaller Aitken size range aerosols around $0.03\,\mu m$. The shift between the spring and summer regimes happens in the end of May at the Zeppelin station. Lund (2008) modeled that freshly emitted EC particles, Aitken mode size of about $0.01\,\mu m$, are mostly removed by growing into accumulation mode particles of size $\sim 0.1\,\mu m$. In that study, the concentration of the accumulation mode EC was much higher near the emission sources than the Aitken mode EC. However, this relationship is turned around for the remote Arctic during winter. This indicates that events bring fine EC particles into the Arctic during the Arctic Haze season.

Aerosols such as EC are removed from the atmosphere by wet and dry deposition Ogren & Charlson (1983); Lund (2008). In addition, wind pumping forces aerosol filled air through the snow pack (Jones *et al.*, 2001) and, hence, leads to dry deposition. Chemical reactions or phase changes can be neglected as a source (Ogren & Charlson, 1983) as Section 2.5 showed that EC is inert and non-volatile. EC can be incorporated in precipitation in several ways. The particle can act as a nucleus during the formation of the snowflake or droplet and can also be scavenged as the flake or droplet falls through the atmosphere. When the EC acts as nucleation particles, an encapsulated mixing is likely. Scavenged snow will rather be in an external mixture, since the EC particles will most likely be on the surface of the snow crystal. Lund (2008) model subcloud scavenging of EC to be of little importance with a contribution of about $0.5\,\%$ of the total fallout.

Wet fallout is the most important contributor to EC in snow from remote sources. As those EC particles have a typical dimension of $0.1\,\mu m$, they are mainly removed from the atmosphere by wet deposition (Raes *et al.*, 2000; Lund, 2008). Further, these particles tend to be washed out with the first precipitation event. Then, the transport pathway described by Stohl (2006) as low-level transport followed by ascent in the Arctic would be the most effective path of transporting EC into the Arctic snow pack. Since the local sources are adjacent to the snow on Svalbard and the particle are coarser in size, dry fallout can be significant from the local sources. Moreover, wind can transport coal dust and highly elevated EC concentrated snow from the settlements in Svalbard to the surrounding areas. Jones *et al.* (2001) set the dry deposition velocity of EC to be in the range $< 0.2 - 0.55\,cm/s$. The dry deposition will increase the EC concentration in snow compared to the initial concentration when the snow precipitated.

The atmospheric lifetime of EC is defined as the average time an EC molecule remains in the atmosphere and varies between different atmospheric models. A typical range is found between 4.9 to $11.4\,days$ with an average of $7.3\,days$ (Schulz *et al.*, 2006). Lund (2008) observed a global mean EC lifetime of $7.3\,days$ with the Oslo CTM2 chemical transport model. That gives an atmospheric burden of $0.14\,Tg$. During Arctic Haze conditions, aerosol residence time of at least $30\,days$ is often observed (Suzuki *et al.*, 1996; Baskaran & Shaw, 2001). A similar lifetime for EC particles can be expected.

2.8 Measured and modeled concentrations in the Arctic

In order to model concentrations of species and their climatic effects, we make two assumptions (Bond & Bergstrom, 2006). The first is a predictable relationship between emissions and a spatially distributed concentration. That is depending on advection, chemical transformation, and removal processes in the atmosphere and depositional and post-depositional processes for the snow cover. The second paradigm is that there is a relationship between a species concentration in the atmosphere or in the snow and its effects on the radiation budget.

One of many chemical transport models is the Oslo CTM2 model (Lund, 2008). That is a 3-

dimensional global model that calculates the transport and distribution for a range of chemical species in the atmosphere, including EC. The meteorological data driving the transport comes from the European Centre of Medium Range Weather Forecasts (ECMWF). The input parameters are temperature, pressure, humidity, precipitation, and cloud coverage. The resolution of the model can be selected among some choices, where the finest resolution is $1^\circ x1^\circ$ horizontally and 60 layers vertically. A variation of chemistry modules can be included in the modeling. The dynamical and chemical processes in the model are as following: Convective and advective transport, dry deposition, wet removal, chemistry, and boundary layer mixing. Due to the crudeness in the currently available models, local sources in Svalbard and the effect of these sources in the nearby surroundings are badly modeled. A typical gridded resolution of emissions is $1^\circ x1^\circ$ (see e.g. Dentener *et al.* (2006)). However, the general transport of EC into Svalbard from long-range transported sources is modeled rather accurately. R. B. Skeie (personal communication) has added a routine that describes deposition and accumulation of EC in snow. A more detailed model description and results from model runs of the Oslo CTM2 model are shown in Section 3.6 and Section 4.7, respectively.

2.8.1 EC in air

In the period 1998 to 2007, the measured EC concentrations in the air at the Zeppelin station, Ny-Ålesund, had an annual mean of $39\,ng/m^{-3}$ and median of $27\,ng/m^{-3}$ (Eleftheriadis *et al.*, 2009). There is a high monthly variability with the maximum observed in February and March of about $80\,ng/m^{-3}$ and a minimum in June through September of 0-27 ng/m^{-3}. Spikes are seen all-year around, although the most severe in winter and spring. EC concentrations of maximum $\sim 300\,ng/m^{-3}$ can last for several days. The highest 12-hr concentration ever measured, $1020\,ng/m^{-3}$, was measured in early May 2006. That event is described in Section 2.6.1 and was due to agricultural fires in Eastern Europe (Stohl *et al.*, 2007). The concentrations and annual cycle are comparable to the stations in Alert, Canada, and Barrow, Alaska, (Sharma *et al.*, 2006). Sharma *et al.* (2006) stated that there has been a decrease in EC of about 54% in the air at Alert and $27\,\%$ in Barrow from 1989 to 2003. A similar trend in Svalbard is likely; however, there is a lack of data which could confirm this. Eleftheriadis *et al.* (2009) found a small decreasing trend in the period 2001-2007. Hence, the EC concentrations in the Arctic have most likely decreased from the 1980s.

2.8.2 EC in snow

In addition to the decline in EC concentration in the snow pack seen from studies given in Table 2.3, a gradual decline has also been seen in the same time period from an ice core study in Western Greenland (McConnell *et al.*, 2007). In Svalbard, there is a significant drop from the Clarke & Noone (1985) study to the recent study by Forsström *et al.* (Submitted). Parts of the gap are likely a result of discrepancies between the analysing methods. The sampling sites differ between the two studies. Therefore, local variability within Svalbard may explain some of the discrepancy. The EC measurements at the SHEBA experiment in 1998 (Grenfell *et al.*, 2002) showed much lower values than Clarke & Noone (1985) found 15 years earlier. We must bear in mind that the location of the sites differs quite substantially. In conclusion, a decline in EC concentration in snow has occurred during the last decades. The background level of EC concentration for the winter 2007/08 in Svalbard is expected to be similar to the level observed by Forsström *et al.* (Submitted) during the 2006/07 winter, which was $4.1\,\mu g/L$.

Table 2.3: Measured EC concentrations in snow in the Polar Regions. The different analysis methods will lead to some discrepancies in the contamination concentrations. The optical method will measure a factor of 2 to 7 larger concentrations than the thermo-optical method (Watson *et al.*, 2005).

Study	Site and time	Min [μ g/l]	Mean [μ g/l]	Median [μ g/l]	Max [μ g/l]	Analysis method
Clarke & Noone (1985)	Svalbard Mar/May 1983	6.7	30.9	33.5	52.0	Optical
Clarke & Noone (1985)	The Arctic 1983-84	0	34.2	24.5	127	Optical
Grenfell *et al.* (2002)	SHEBA The Arctic basin Spring 1998	1	4.4	-	7	Optical
Warren & Clarke (1990)	South Pole 1986	0.1	0.2	-	0.3	Optical
Chýlek *et al.* (1987)	Camp Century, Greenland 1982-1985	2.1	2.4	2.4	2.6	Thermo-optical
Forsström *et al.* (Submitted)	Svalbard Feb-Apr 2007	0	8.7	4.1	80.8	Thermo-optical

Chapter 3

Instruments and methods

3.1 Area of focus: Svalbard

Svalbard is defined as all land masses between the latitudes of 74 and $80\,^{\circ}N$ and longitudes 10 and $35\,^{\circ}E$ covering about $61000\,km^2$ (see Figure 3.1). As Spitsbergen is where most of the human activities happen and, by far, the largest island on the archipelago, it is also the centre of this project's attention. Moreover, the local effect of the settlements in Svalbard on the EC concentration in snow and on snow albedo is the main focus. Hence, the transects were concentrated around some of those settlements, namely Longyearbyen, Ny-Ålesund, and Svea. For a detailed historic overview of the settlements and why they were build, the book by Arlov (2003) is recommended.

An initial study was set in the surroundings of Longyearbyen with a few measuring points in Adventdalen, as given in Figure 3.2. Later, one transect was set upwind and downwind of Ny-Ålesund on the southern shoreline of Kongsfjorden (see Figure 3.3). For a description of the physical environment around Ny-Ålesund, and especially the nearby fjord, see Svendsen *et al.* (2002). Another transect was taken all the way from Bjørndalen, via Svalbard Airport and Longyearbyen, through Adventdalen and Eskerdalen and far in Sassendalen. This transect covers the typical upwind and downwind direction of Longyearbyen. A third transect was set in Longyeardalen and Longyearbreen, which is directly south of Longyearbyen. Figure 3.2 shows all the sites around Longyearbyen, including those sampled at the initial study. Around Svea, a final transect was made on the north shore of van Mijenfjorden to the west and into Kjellströmdalen in the east (see Figure 3.4). The initial study was executed in February 2008, while the main bulk of the field work was accomplished during March and April the same year. The upper part of Longyearbreen was resampled in August 2008 since snow was still remaining at the snow pit sites. Snowmobiles, cars, and skis were the mean of transportation during the fieldwork in winter. In August, everything was done on foot.

3.2 Snow sampling

The basics in this project were to sample snow for further analysis together with some snow characteristics. The sampling was done along transects. To avoid contaminating the samples, snowmobiles and cars were left downwind and preferably at least $100\,m$ from the sites. Due to rough local topography, this was not always possible, but a minimum distance of $30\,m$ was always kept. The distance to nearby roads and scooter tracks was also kept at a preferable minimum of $100\,m$. Further, any contact with the sampled snow by hands or other possible sources of contaminants was avoided. A snow pit was excavated at every measuring point along all the transects, as drawn in Figure 3.5(a). A photo of a

Figure 3.1: A map of Svalbard. All settlements are found on Spitsbergen, and the areas around Longyearbyen, Ny-Ålesund, and Svea are the focus. The distance from the top to bottom of the map is about 670 km. Map by Erika Aamaas using data from the Norwegian Mapping Authority.

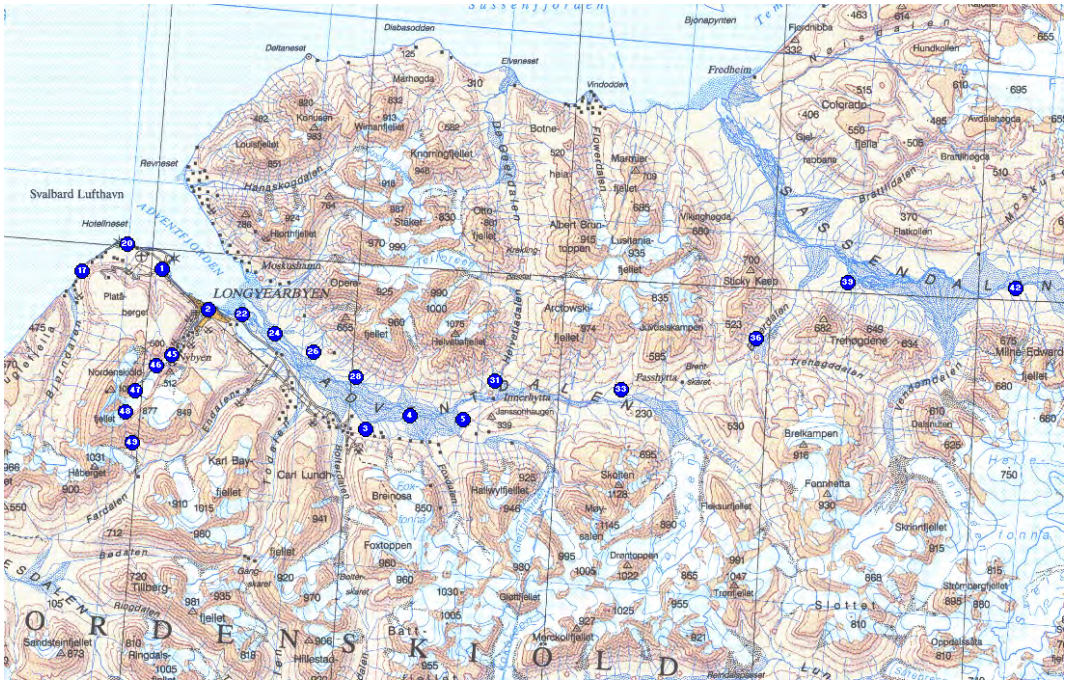

Figure 3.2: The blue dots numbered 1 to 5 are the positions of the snow pits in the initial study. The location was Longyearbyen and its surroundings. All the other points are from the main study. The main transect is the one going east-west from Sassendalen to Bjørndalen. A shorter one goes from Longyearbyen and south-westerly across Longyearbreen. Site 48 and nearby site 47 on Longyearbreen were resampled in late summer. Map source: Norwegian Polar Institute.

Figure 3.3: The blue dots show the location of the ten snow pits excavated in the surroundings of Ny-Ålesund. The total distance of the transect is approximately 30 km with Ny-Ålesund in the middle. Map source: Norwegian Polar Institute.

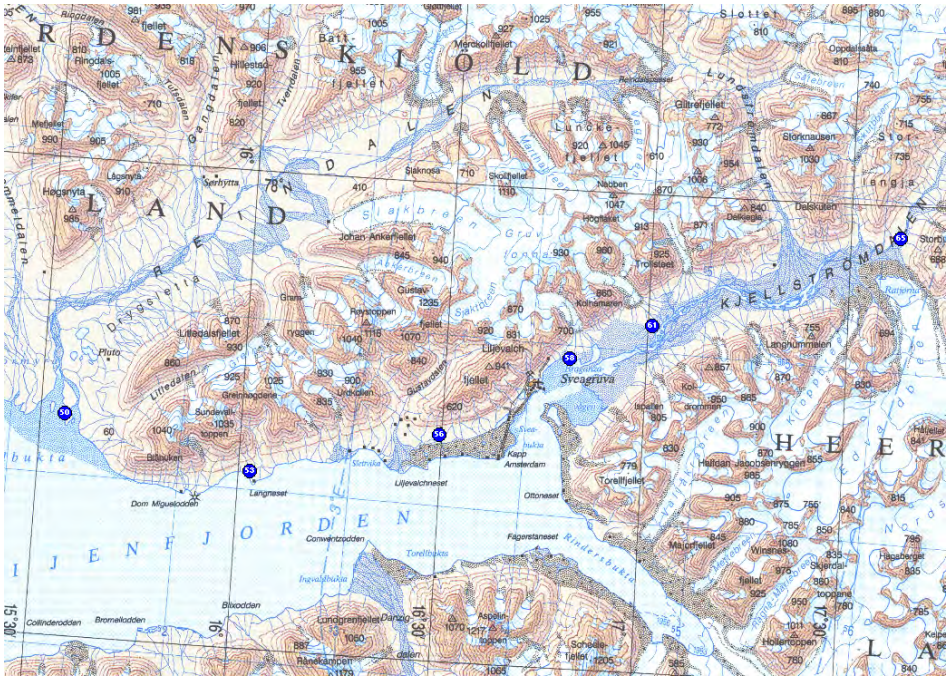

Figure 3.4: The blue dots are the positions of the snow pits taken around Svea. Map source: Norwegian Polar Institute.

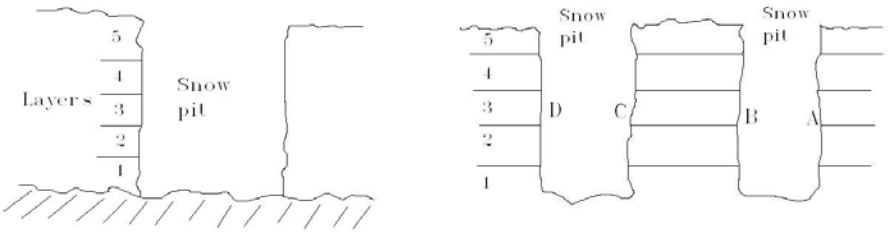

(a) A schematic snow pit (b) The snow at the site of the micro scale investigation

Figure 3.5: (a): The snow pits were excavated by removing the entire snow pack. The snow pack was typically divided into five snow layers with the numbering starting from the ground and upwards. (b): In the micro scale study, four point measurements were taken in a five meters long transect, at A, B, C, and D. This was carried out about $15\,km$ east of Longyearbyen in Adventdalen. This is snow pit Nr. 5 on the map given in Figure 3.2.

typical snow pit is shown in Figure 3.6(a). In addition, a micro scale study was included in the initial study. Here, two snow pits were excavated only a few meters apart, and snow samples were taken from the A, B, C, and D sides seen in Figure 3.5(b). By looking at the snow stratigraphy, the same snow layers were collected at the four vertical snow walls. The snow pack was divided into maximum five different layers. The maximum was set to five to limit the total number of samples, even though the snow pack could consist of more individual layers. When the snow depth was shallow, typically less than $40\,cm$, and only a few different snow layers were observed, the snow packed was divided more crudely. A snow sample equalling about a litre of melt water was gathered into plastic bags from every single layer (see Figure 3.6(b) for a typical snow sample). The snow characteristics of the layers were described, and divided into fresh snow, wind affected snow, ice lenses, and depth hoar. The samples were kept frozen until further analysis.

3.3 Snow melting and filtering

In the lab, the snow samples were melted in a microwave oven, and the melt water was immediately filtered through quartz filter (see Figure 3.7(a) and 3.7(b)). This was done to minimize the loss of EC particles to plastic and glass surfaces (Ogren *et al.*, 1983; Clarke & Noone, 1985). The filters used were the Munktell quartz microfiber disc with the grade T293 and $55\,mm$ in size. Blank filters were also run through the system to determine contamination from the melting and filtering process. The dried filters were packed in Petri dishes (see Figures 3.8(a), 3.8(b), and 3.8(c) for examples) and sent to ITM in Stockholm for final analysis. Everything except this final determination of the elemental carbon (EC) content was executed by the author of this thesis.

3.4 Filter analysis

The final analysis of the contaminated filters was done by the thermal-optical method at ITM in Stockholm. Through controlling the temperature and atmosphere following NIOSH protocol, the levels of organic, carbonate and elemental carbon are determined. Due to high temperatures, quartz fibre filters are required. Typically, a $1.5\,cm^2$ punch of the filter was analysed. The flame ionization detector

(a) A typical snow pit (b) A typical snow sample

Figure 3.6: (a): A snow pit in Sassendalen on February 20th 2008. Distinct layers are seen in the photo. The blue lines are ice lenses. Photo by Åsmund Aamaas. (b): A typical snow sample. This sample taken from Longyearbreen contained 918 ml of melt water and had an EC concentration of 5.28 $\mu g/l$.

(a) The melting and filtration instrument (b) A snow sample ready for melting

Figure 3.7: (a): and (b): Snow samples are placed in the microwave oven to be melted and, then, filtered.

(a) Highly EC contaminated sample (b) Clean sample (c) Sample contaminated by Aeolian dust

Figure 3.8: Filters with the contaminants from the snow samples. The value in the middle of the Petri dishes states the amount of melt water of the respective snow samples. (a): Sample taken close to Svalbard Airport that was highly contaminated with EC ($791.54\,\mu g/l$). (b): This snow was taken in Sassendalen, and the filter is very clean indicating a low EC value ($17.49\,\mu g/l$). (c): A sample taken on Larsbreen near Longyearbyen. Sand and dust give the distinct brown color seen. This sample contained too much Aeolian material to be EC analyzed.

(FID) reports in $\mu g/cm^2$, which can be converted to concentration ($\mu g/L$) with the knowledge of the punch area and total volume of melt water. The analysis consists of two stages. During the first, organic and carbonate carbon are volatilized in the pure helium atmosphere and gradually increasing temperature up to $820\,^oC$ (Birch & Cary, 1996). Then, evolved carbon is catalytically oxidized to CO_2 in a bed of granular MnO_2 and reduced to CH_4. In the second stage, the pyrolysis correction and EC are measured. The temperature has fallen and the atmosphere is changed to an oxygen (10%) - helium mix. Next, the temperature is raised up to $860\,^oC$. The oxygen in the oven will oxidize the pyrolytically generated EC char and lead to an increase in filter transmittance. The filter transmittance is monitored optically throughout the analysis. The point where the filter transmittance returns to its initial value is defined to be the split between OC and EC. Everything before the split is defined as OC, and everything after is EC. This is a pure operational definition. This results in a thermogram, and Figure 3.9 shows an example of that.

The precision of this analysing method increases with increasing EC burdens. For loadings greater than $0.8\,\mu g/cm^2$, Forsström *et al.* (Submitted) observed a precision less than $20\,\%$. The filter error was observed to be less than $130\,\%$ even for the lowest EC concentrations. $70.7\,\%$ of all samples in this thesis have values larger than $0.8\,\mu g/cm^2$. Any brown carbon that is found in a sample can be classified as an unknown mix of EC and OC by the analysis. The reason is that the brown carbon volatilizes over a wide range of temperatures (Andreae & Gelencsér, 2006). That gives additional uncertainty to the method. Forsström *et al.* (Submitted) observed that the combination of natural variability and uncertainties in the method produce a total uncertainty of $100\,\%$ for this exact analysing method for snow samples from Svalbard. In comparison, the optical method has according to Clarke & Noone (1985), an accuracy of about $50\,\%$ due to the filtering and the optical analysis.

As mentioned above, all snow samples were analyzed for both EC and OC. The OC measurements are the least trustful due to the simple sampling procedure and analysis handling. For instance, organic material could grow on the filter. While the blank filters were little or not at all contaminated by EC ($\leq\ 0.15\,\mu g/cm^2$), OC were detected on all blank filters, typically with a concentration of about

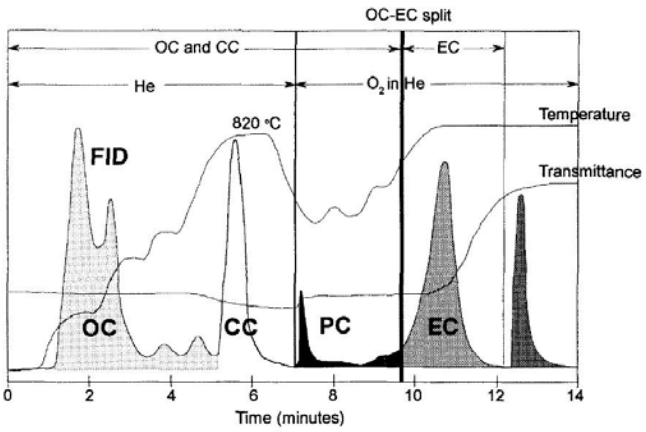

FIGURE 2. Example thermogram for sample containing rock dust (carbonate source) and diesel exhaust. Three traces correspond to temperature, filter transmittance, and detector (FID) response. Peaks correspond to organic (OC), carbonate (CC), pyrolytic (PC), and elemental (EC) carbon. The final peak is a methane calibration peak.

Figure 3.9: An example of a thermogram given by a flame ionization detector (FID). The figure is adapted from Birch & Cary (1996).

$0.5 - 1.0\,\mu g/l$. OC particles in the snow pack, in comparison to EC, absorb little solar radiation (see Section 2.5). Thus, OC concentrations will be neglected here, as biased snow surface albedo is the main focus in this thesis.

3.5 Alternative method of measuring EC

The analysis of filters for EC concentrations is both expensive and time-consuming. To see if an alternative method is possible, 81 of the filters that were analyzed at ITM were also checked in this other experiment. UNIS has an optical lab with no light sources. An artificial sunlight lamp (Daylight Power), which is very common to have in Svalbard, was used as a fixed light source. Such light is believed to be more stable and contain a richer spectrum than ordinary light bulbs (C.E. Bøggild, personal communication). The albedo was measured with a field spectrometer. The set up is schematically shown in Figure 3.10. Since EC is more sensitive than dust at the high end of the visible spectrum compared to the lower part (Warren & Wiscombe, 1980), the spectral albedo at $630\,nm$ was used. The impact of a contaminated filter was calculated as the difference in spectral albedo between the filter and an average of the blank filters.

3.6 Description of the Oslo CTM2 atmospheric chemistry model

The Oslo CTM2 model was run with a horizontally resolution of $2.8°x2.8°$ and 40 vertical layers. In addition, the model was run with full chemistry. A full description of an older version of the model has been given by Lund (2008), and she called this version the model with the original aerosol parameterization. The EC is emitted as $80\,\%$ hydrophobic and $20\,\%$ hydrophilic. According to R.B. Skeie (personal communication), two changes have been made compared to the model runs by Lund (2008). The aging from hydrophobic to hydrophilic particles is changed. This aging is governed by an exponential lifetime that depends on latitude and season. At high latitudes, this value is 5 days during winter and 1.5 days during summer. Those values are based on simulations of the M7 aerosol microphysical module (Vignati & Wilson, 2004; Grini, 2007) in the Oslo CTM2 model. The M7

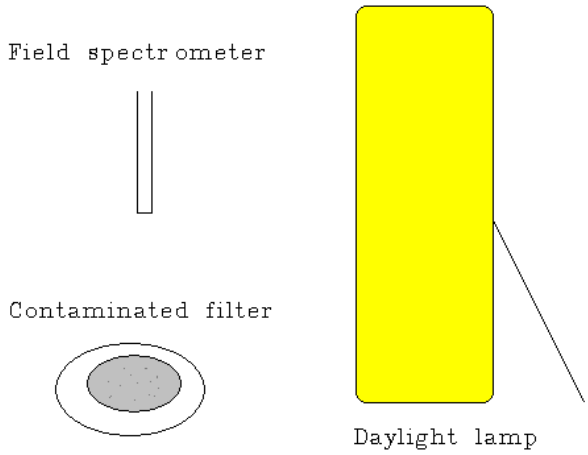

Figure 3.10: The set up for the spectral albedo measuring of the filters in the optical lab at UNIS.

module includes a realistic size distribution and mixing state for atmospheric aerosols. The other change is that a $100\,\%$ solubility in water clouds and $5\,\%$ solubility for ice clouds is assumed for hydrophilic EC particles in large scale precipitation.

Data for emission of EC by fossil fuel usage is taken from Dentener *et al.* (2006), while similar data from biomass burning were found in Randerson *et al.* (2007). The emissions are gridded in $1°x1°$, which was interpolated to the coarser resolution used here ($2.8°x2.8°$). The model separates between EC formed by fossil fuel burning and biomass burning and includes some local pollution from Svalbard.

The atmospheric transport model include a routine that describes deposition and accumulation of EC in snow and ice created by R.B. Skeie (personal communication). Snow precipitation from ECMWF is used to create snow layers, and the model allows a maximum of ten layers. If there is no snow falling within $24\,hours$ after an initial snow event, a new layer is created. The top layer is always maximum $1\,mm$ thick. If there are already ten snow layers, the two lowermost layers are merged. Hence, the model observes only the upper part of the snow pack since the total number of snow events during a winter is much higher than ten. Melting and evaporation is simulated using data from ECMWF, and the EC particles are accumulated at the surface during such conditions. For snow on sea ice, a constant melting from mid April to June 21st is assumed. All the EC is removed when the snow pack is completely melted or at the end of the melt season (August 30th). However, any remaining snow is not removed. Then, the EC concentration in the snow is set to zero.

Data of EC concentrations in snow from simulations with the Oslo CTM2 model was kindly provided by R.B. Skeie (personal communication) for the 2007/08 winter. The data is, here, analyzed and compared with measurements from this thesis. A direct comparison is not possible, since snow samples were taken from the entire snow pack while the model results only represent the top ten layers.

3.7 Analysis of $\delta^{18}O$

A sample volume of $10\,\mu l$ liquid water from all the 50 snow samples gathered in Ny-Ålesund was prepared in sealed bottles. These samples were taken from the melted water after the melting and filtering process described in Section 3.3. The $\delta^{18}O$ values were measured for these water samples

with the instrument Liquid-Water Isotope Analyzer including an Automated Injection. These measurements are based on high-resolution direct-absorption spectroscopy. Standards were used in the measurements to calibrate the results to the Standard Mean Ocean Water (SMOW).

The oxygen atom in the water molecule can vary between its three isotopes (^{16}O, ^{17}O, and ^{18}O). The natural occurrence of these isotopes in their relative proportions is $99.76\,\%$ of ^{16}O, $0.04\,\%$ of ^{17}O and $0.2\,\%$ of ^{18}O (Bradley, 1985). The vapour pressure of $H_2\,^{18}O$ is $10‰$ lower than that of $H_2\,^{16}O$. Hence, condensation of the vapour will favour the heavy isotope. Changes in temperature will affect the isotope ratio at condensation. Thus, isotopic concentration in the condensate is generally seen as a function of the temperature at which condensation occurs. When compared to a water standard (Standard Mean Ocean Water), this isotopic ratio can be used to calculate a departure from the standard (Bradley, 1985):

$$\delta^{18}O = \left[(\frac{^{18}O}{^{16}O})_{sample} - (\frac{^{18}O}{^{16}O})_{SMOW} \right] / (\frac{^{18}O}{^{16}O})_{SMOW} \cdot 10^3 ‰$$

A value of $\delta^{18}O = -10‰$ is depleted by $10‰$ of ^{18}O relative to SMOW. In equilibrium, the atmospheric water vapour will contain $10‰$ less ^{18}O than the SMOW due to different vapour pressures between ^{16}O and ^{18}O. This relation between temperature and isotope ratio is complicated by continuously exchange processes between atmospheric water vapour, water droplets in the air, and water at the surface.

Chapter 4

Results

4.1 Weather during the 2007/08 winter

A part of this project was to identify the major wind directions around local pollution sources, as well as precipitation and mild weather events during the winter of 2007/08. Observations from the Norwegian Meteorological Institute (Met) were used for this purpose. They observe weather every sixth hour in Ny-Ålesund, Svea, and Svalbard Lufthavn/Airport, which is situated $5\,km$ northwest of Longyearbyen. Unfortunately, none of the stations measured snow depth during the time period of interest.

At Svalbard Airport, the predominantly wind direction is from the southeast (see Figure 4.1(a)). The observation period is from the middle of August 2007 to the middle of July 2008. From the day of first snowfall (September 26th 2007) to the time of the field work (April 1st 2008), the wind came from southeast (between $90\,^\circ$ and $180\,^\circ$) in $60.0\,\%$ of the weather recordings. This corresponds to winds flowing out of Adventdalen. A second maximum is created by westerly winds, which also correlates well with the terrain. There is either outflow or inflow in Adventdalen.

Snow started to accumulate at Svalbard Airport on the 26th of September, and this snow stayed in the terrain for the rest of the winter. In the snow pack around Longyearbyen, three thick and complex ice lenses were typically found at the time of the field work. Each of these ice slabs, typically $5\,cm$ thick each, included several individual ice lenses. These ice lenses can be identified and dated when

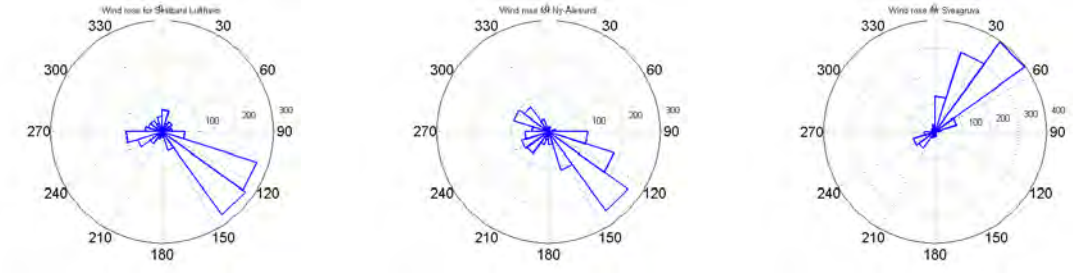

(a) Svalbard Airport (b) Ny-Ålesund (c) Svea

Figure 4.1: Wind rose for (a) Svalbard Lufthavn/Airport, (b) Ny-Ålesund, and (b) Svea in the period from August 15th 2007 to July 15th 2008. At Longyearbyen and Ny-Ålesund, the wind is south-easterly most of the time. At Svalbard Airport, a second maximum is seen with westerly winds. Two second maxima of south-westerly and north-westerly winds are observed in Ny-Ålesund. In Svea, a maximum is seen in winds from northeast and a second maximum with south-westerly winds. These winds follow the direction of nearby valley and fjord directions.

accurate meteorological data for the area is in hand. Temperature and precipitation events at Svalbard Airport are given in Figure 4.2.

Melting of snow and its rate depend on the energy balance at the snow surface. However, a much simpler concept in use is the degree day approach (Benson, 1962; Reeh, 1991). Then, we can state that melting, and, thus, ice layer formation, occurs most likely when the average temperature for a day is above zero (Benson, 1962). The strength of the melting can be correlated to the total degree days above freezing. Here, we assume those values are a minimum to create an ice lens. Figure 4.5(a) shows the positive degree days measured at Svalbard Airport. By using this definition, one might not detect events where the temperature spiked sharply over zero, but came back down again after a few hours' time. Due to no or little solar radiation during the winter, the diurnal cycle in temperatures is insignificant. Ice lens formation is also governed by rain events. More melting is taking place if it is raining than not for a given temperature. Further, there could be rain events on days when the mean temperature is below zero. Rain or drizzle occurring at temperatures below $0\,^{\circ}C$ are rare, occurring only once a year at Svalbard Airport. Førland & Hanssen-Bauer (2002) state further that the border between snow and rain goes on average at a temperature of $1.7\,^{\circ}C$. Thus, melting occurring due to rain at temperatures around $0\,^{\circ}C$ is unlikely. There are also large spatial variations. Weather can produce an ice layer at Svalbard Airport, while a bit further inland, it is too cold. Some ice lenses observed in Longyeardalen were not found at higher elevations on Longyearbreen. Thus, the big melting events are the most easy to investigate as these with great certainty lead to ice lens formation. At Svalbard Airport, such melt events were observed at the very beginning of the winter season, at September 28th and 29th 2007. Further, such days were seen on the 1st, 20th, 22nd, and 28th of October, 5th and 6th of November, and 23th of December. The last melt event before the field work in March and April was observed on January 1st and 2nd 2008. All these events were accompanied by precipitation, probably rain, which increases the probability of ice lens formation. Heavy ice lens formation was observed by Morgner (2009) in Adventdalen by the final melt event. Prior to the last warm spell, the coldest days so far in the winter were observed with temperatures close to $-20\,^{\circ}C$. Seven consecutive cold days must have cooled the snow pack significantly. The resulting cold snow would have slowed down the melt water percolation during the warm spell, and the top ice layer was most likely formed within $2\,cm$ of the snow surface. The snow above would experience a melt-freeze process and turn into an ice slab. Thus, all snow found over this ice slab precipitated consequently after January 2nd 2008. The interface between the newer wind packed snow and the ice slab with ice lenses was easily observed in most of the snow pits. This interface was actively used as a border between two different snow samples from different snow depths. The two other observed ice layers are likely formed in the period 20th to 23rd of October and November 5th and 6th, respectively. Ice layers were probably formed during the first days of snow on the ground; however, those must have been at the very bottom of the snowpack. Hence, it is less likely that those mild days have created any of the three major ice slabs observed.

The observed wind direction in Ny-Ålesund is given as a rose plot in Figure 4.1(b). The wind direction proves to be along the valley direction. The most frequent wind comes out the valley from southeast, while a second minimum is seen into the valley. A third direction is observed from south-west. This is due to the fact that Ny-Ålesund is at the bottom of small valley. From the first snowfall at October 1st 2007 to the time of field work at March 11th 2008, wind came from southeast (between $90\,^{\circ}$ and $180\,^{\circ}$) $61.2\,\%$ of the time.

If we consider pollution from Ny-Ålesund as a point source, airborne pollution is transported along these typical wind directions. Thus, the location of the snow pits was set along the southern side of Kongsfjorden, both outwards and inwards. Due to no sea ice at the time of the field work in March 2008, all measurements were on land. On the north-western side, the plumes originating

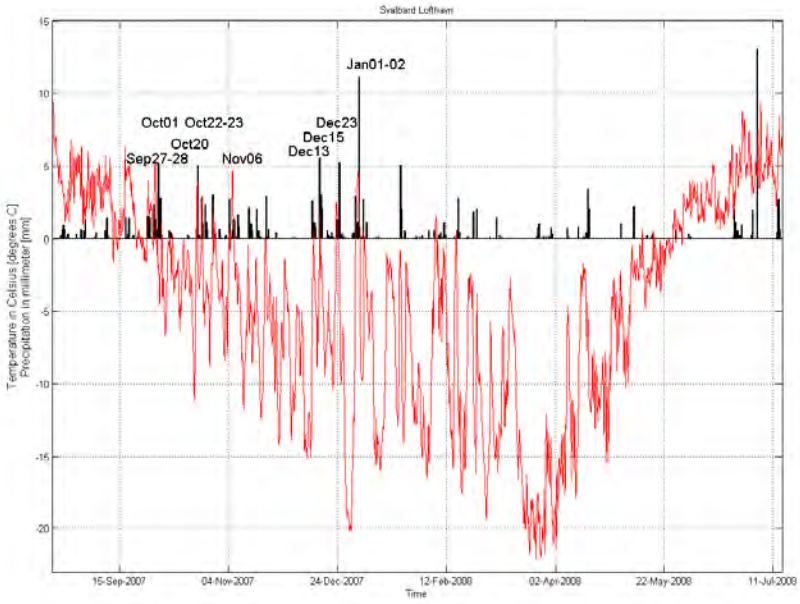

Figure 4.2: The red graph shows the temperature while the black bars give the measured precipitation at Svalbard Lufthavn/Airport, about $5\,km$ northwest of the centre of Longyearbyen. Melt events are indicated.

from Ny-Ålesund tend to go slightly offshore; thus, snow cannot be sampled directly downwind of Ny-Ålesund. The terrain around this research base is rough with rocky outcrops on the mountain slopes. This contributes to Aeolian transport, and the snow samples were taken in areas where this effect appeared to be minimal.

Temperature and precipitation events in Ny-Ålesund during the 2007/08 winter are given in Figure 4.3. There are several significant events during the early part of winter 2007/08 that most likely resulted in ice lens formation. As seen in Figure 4.5(b), there are seven melt days. Those are September 28th, October 1st and 28th, November 5th 2007, January 1st and 2nd, as well as February 7th 208. During the last event, the average temperature was just above zero, and no precipitation was measured. Hence, ice lens formation was less likely than at the other indicated days. In the two days of January 1st and 2nd, more than $40\,mm$ rain fell and the temperature rose well above $5\,^{\circ}C$. This must have caused melting and ice lens formation. As in Longyearbyen, the previous days were cold ranging between $-15\,^{\circ}C$ and $-20\,^{\circ}C$. Consequently, ice layers have probably been formed in the top snow layer. Thus, the top ice lens found in the snow pack at the time of field work was formed during that event. Further, all snow above that ice lens has fallen after that date. Around Ny-Ålesund, this ice lens was found close to the bottom of the snow pack. Hence, most of the snow pack dates from January, February, and March 2008.

The wind in Svea (see Figure 4.1(c)) is typically going out Kjellströmdalen from the southeast towards van Mijenfjorden. A second maximum is seen the opposite way. The temperature pattern, as given in Figure 4.4, is very similar to those in Longyearbyen and Ny-Ålesund. Since the distance to Longyearbyen is only approximate $70\,km$, the precipitation events are similar in Svea and Longyearbyen. The melt events in Svea in Figure 4.5(c) are almost identical to those seen in Longyearbyen. The exact same days are represented expect October 22nd and December 23th. Thus, a similar snow stratigraphy is expected. The temperature was somewhat lower than at Svalbard Airport during the

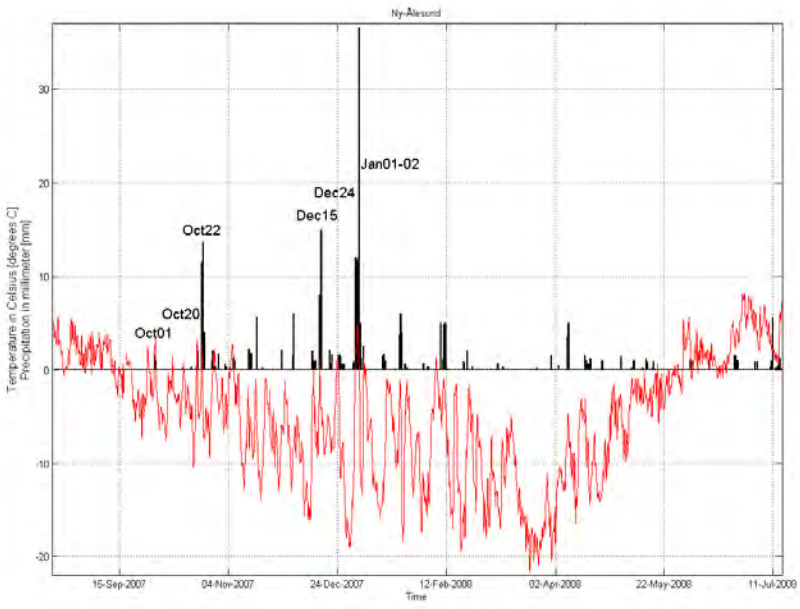

Figure 4.3: The red graph shows the temperature while the black bars give the measured precipitation in Ny-Ålesund.

melt events in October and November. That was also observed in the snow stratigraphy. As three typical thick ice slabs were seen in the snow around Longyearbyen, a thick ice slab with some minor ice layers beneath were noted in the snow around Svea.

4.2 Measured EC concentrations in snow

There is extreme spiking in the EC concentrations in and around Longyearbyen and Svalbard Airport, as observed in Figure 4.6(a), 4.6(b), and 4.7. These show the same data, emphasizing on the extreme EC concentrations, the range of concentrations, and low concentrations, respectively. Several samples contained concentrations of $> 1000\,\mu g/l$. Other samples were visibly found to contain so much coal dust that analysis would be impossible. The concentrations are out of scale. In comparison, Myhr (2003) measured coal dust concentrations varying between 78.8 and $312.5 mg/l$ in the most affected area downwind of the coal pile on Cape Amsterdam, which is about a factor 200 higher. Since the highest measured EC concentration was $2103.81\,\mu g/l$ in this thesis, a conservative estimate of those samples not analyzed is $2000\,\mu g/l$. This estimate is considered in the calculations of mean values. Even higher concentrations are likely; therefore, the spiking is even more extreme than Figure 4.6(a) shows. The most contaminated snow was found at the coal processing plant $3\,km$ northwest of Longyearbyen, seen as the area with the most discoloured snow in Figure 2.5. Freshly fallen snow from a snowfall three days before sampling had an EC concentration of $316.21\,\mu g/l$. The other snow samples from that snow pit are more contaminated than all the other samples in this project ($> 2000\,\mu g/l$). In comparison, the snow looks much cleaner to the right of the terminal building at the airport in Figure 2.5. From the measured samples, this was the area with the highest average EC concentration of this project, spiking to $1368.36\,\mu g/l$. That specific value is also an underestimate as the top snow layer at that site proved to be impossible to analyze. The snow sampled in February 2008

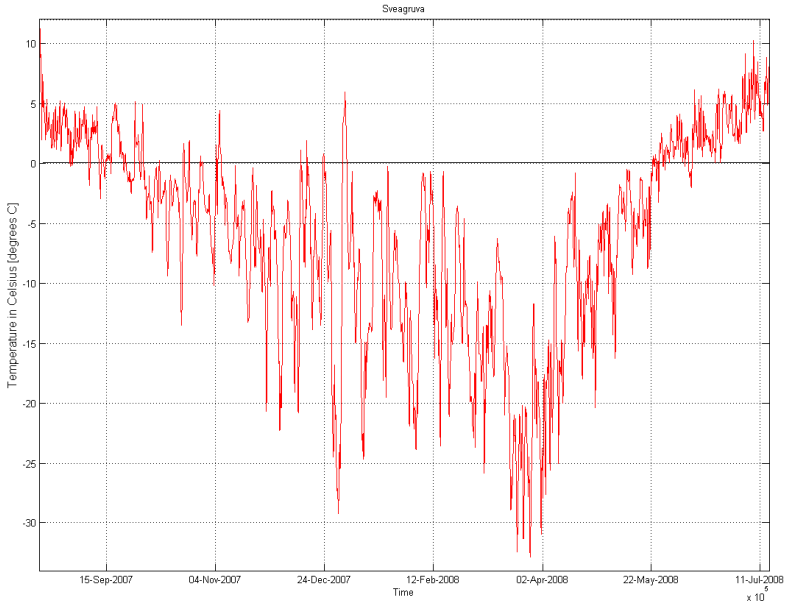

Figure 4.4: The red graph shows the temperature in Svea. Precipitation was not measured in this time period.

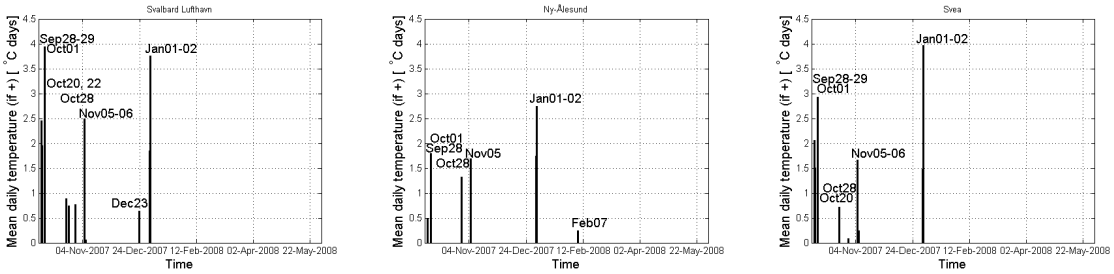

(a) Svalbard Airport (b) Ny-Ålesund (c) Svea

Figure 4.5: Days with melting for (a) Svalbard Lufthavn/Airport, (b) Ny-Ålesund, and (b) Svea during the winter 2007/08. A day with melting is defined to happen when the average temperature of the day is above zero as described by Benson (1962). The average is calculated as the mean of the maximum and minimum values measured four times a day. The height of the bars indicates the warmth at a particular day.

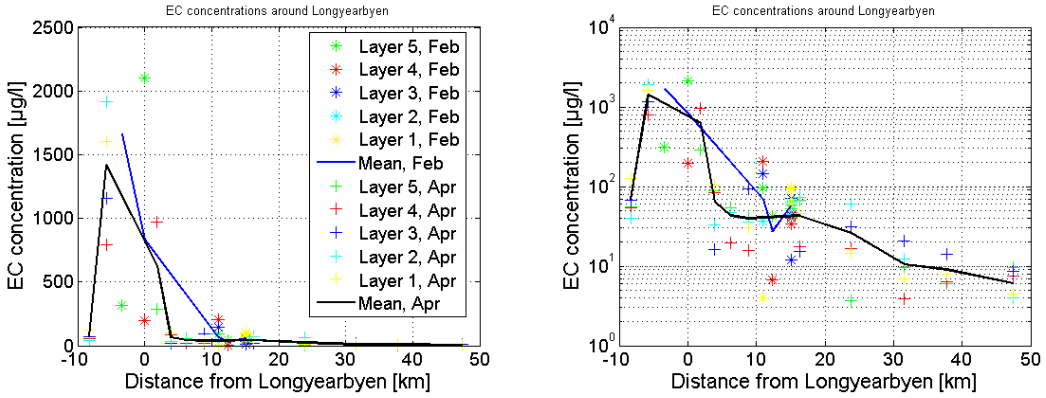

(a) Linear plot (b) Logarithmic plot

Figure 4.6: (a): The EC concentration around Longyearbyen. The city centre is at zero and the positive x-axis goes east into Adventdalen. For samples too contaminated to be analyzed, an EC concentration of 2000 $\mu g/l$ is assumed, and the mean value takes this into consideration. Figure (b) is identical to (a) with the exception of a logarithmic y-scale. The labelling is the same for these two figures. The location of the sites is shown in Figure 3.2.

shows higher concentrations than those sampled in April. The main reason is that the initial study was executed slightly closer to the trucking road between Longyearbyen and Mine 7 (see Figure 3.2), and, thus, closer to local sources. A plateau in the concentration is seen east of Longyearbyen and north of Mine 7 of about 40 to 55 $\mu g/l$. Further east, the mean concentration decreases. In Sassendalen, the gradient decreases, and the most remote site has a mean EC concentration of 6.09 $\mu g/l$. The variability also drops as we go eastward. The most contaminated samples in Sassendalen and Eskerdalen are those containing ice lenses and ice slabs, seen as blue plusses in Figure 4.7. The average snow depth around Longyearbyen, including Adventdalen, was 50 cm. Further east in Eskerdalen and Brentskaret, the mean snow depth was 104 cm and in Sassendalen 59 cm.

The measurements from the transect crossing Longyearbreen are given in Figure 4.8. The EC concentrations are much lower than those observed in Adventdalen. The mean value of all the samples gathered from Longyearbreen is 17.06 $\mu g/l$. A decrease is seen from Nybyen and onto Longyearbreen, while the concentration is nearly constant on the glacier. Thick ice lenses were observed in the lowest part of the glacier. The snow samples containing this ice show elevated concentrations. The top snow layer (the green stars in Figure 4.8) is the most contaminated. The samples were gathered in beginning of April, the peak season of snowmobile driving in the area. These samples are, therefore, locally contaminated by this traffic, even though the sampling was done in the least utilized areas of the glacier. The spiking is too high to be caused by Arctic Haze events similar to those observed in Section 4.7. The average snow depth on Longyearbreen in April was 166 cm. The plusses in the same figure show the concentrations for snow sampled in August 2008. The mean concentration was 230.65 $\mu g/l$, which is a factor 12 of what observed four months earlier. The snow depth was only a couple of centimetres at 6 km southwest of Longyearbyen. At the site highest up on the glacier, at 546 m a.s.l., the remaining snow depth was 14 cm. In April, the same snow depth was 162 cm. Of the 14 cm, the top 3 cm contained 327.13 $\mu g/l$, while the lower 11 cm contained 70.63 $\mu g/l$. Hence, the top layer has a concentration 18 times higher than the mean April concentration, while it is a factor 4 higher for the lower layer. Consequently, the EC is concentrated in the surface layer as the snow melts.

As observed in Figure 4.9, there is a high variability of the EC concentrations around Ny-Ålesund. However, the average value does not vary to the same degree. The mean value of all 50 samples is

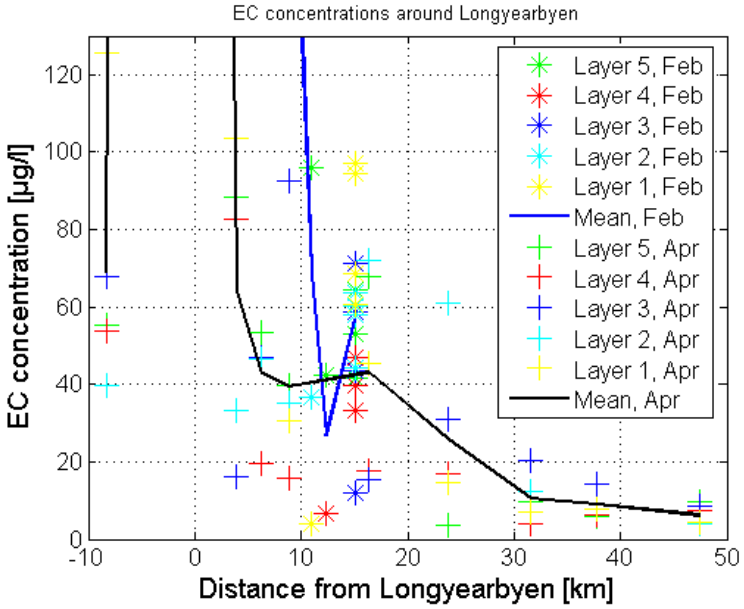

Figure 4.7: The same figure as Figure 4.6(a) with a closer look at concentrations less than 130 $\mu g/l$. A distinct gradient is observed between Sassendalen and Adventdalen. The location of the sites is shown in Figure 3.2.

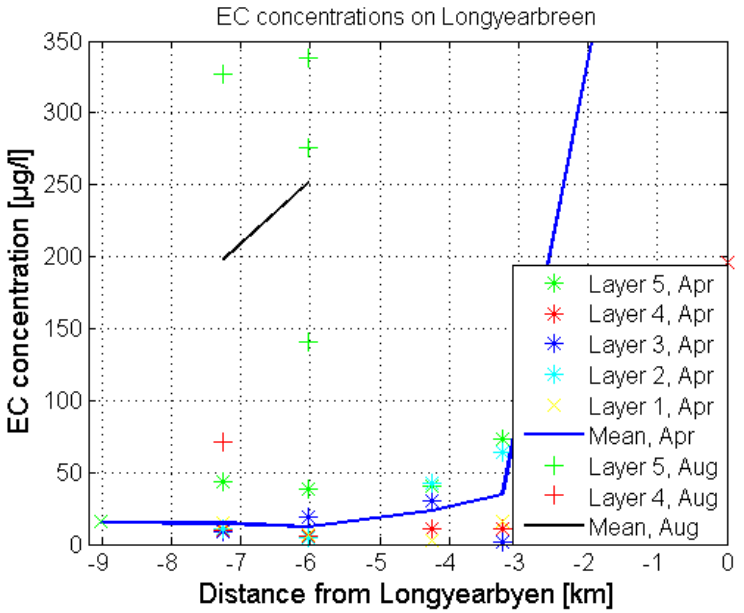

Figure 4.8: EC concentrations south of Longyearbyen, mainly on Longyearbreen. The snow was sampled in April and August 2008. The blue and black lines show the average values from April and August, respectively. The location of the sites is shown in Figure 3.2.

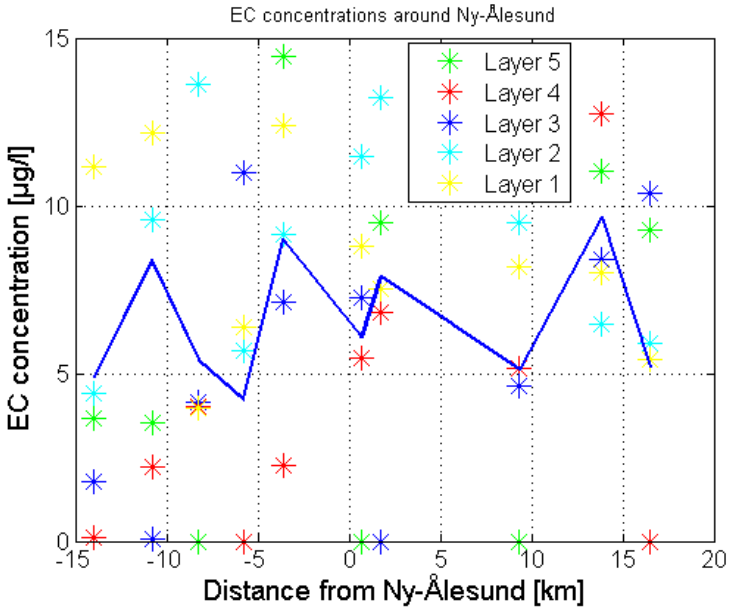

Figure 4.9: The measured EC concentration around Ny-Ålesund, where the settlement is at the zero mark. The location of the measurements is given in Figure 3.3. Positive direction of the x-axis is in south-easterly direction. The snow pack is divided into five layers, and the deepest layer is defined as Layer 1. The blue line represents the average value weighted by the thickness of the sampled snow layers.

$6.58\,\mu g/l$ with a standard deviation of $4.31\,\mu g/l$. The median value is $6.41\,\mu g/l$. The observed EC concentration is just a fraction of what measured around Longyearbyen. The centre of Ny-Ålesund is at the zero point on the x-axis; yet, no significant spiking in the EC concentration is observed in the nearby measuring points. The mean value looks to be randomly noisy around the total mean EC concentration along the transect. The median snow pit depth was $60\,cm$.

The measured EC concentration along a west-east transect with Svea in the middle is shown in Figure 4.10. All the six samples analyzed are from the top surface layer. The mean EC concentration was $46.86\,\mu g/l$ varying between $9.19\,\mu g/l$ and $158.08\,\mu g/l$. Minima are observed to the furthest east and west of Svea. The samples closest to Svea have an EC concentration of about $45\,\mu g/l$, while the absolutely highest concentration is measured further west. The snow southwest of the coal pile on Cape Amsterdam is visibly discoloured by coal dust in a similar manner as observed around Svalbard Airport. Hence, EC concentrations of $> 1000\,\mu g/l$ is probable in that area. Snow on the sea ice of van Mijenfjorden was not sampled due to safety reasons. The median snow pit depth for all pits was $56\,cm$.

As part of the initial study, a micro scale study was executed $15\,km$ southeast of Longyearbyen in Adventdalen (blue dot number 5 in Figure 3.2). The result of this is given in Figure 4.11. The mean value of the EC concentration for all 20 samples is $56.88\,\mu g/l$, with a standard deviation of $19.59\,\mu g/l$. The median value of $55.59\,\mu g/l$ correlated well with the mean value. These concentrations are well above those seen in Ny-Ålesund. The snow depth ranged between 108 and $127\,cm$.

The EC analysis indicated that Aeolian sediments were present in several snow samples, especially in those taken around Longyearbyen. A pinkish color of the filter after analysis confirms this. Almost all the samples contained dust taken from the transect from Bjørndalen in the west through Adventdalen and Sassendalen in the east. In summertime, organic materials is found in the snow and lives on photolysis. Some of the samples from Longyearbreen gathered in August 2008 contained red

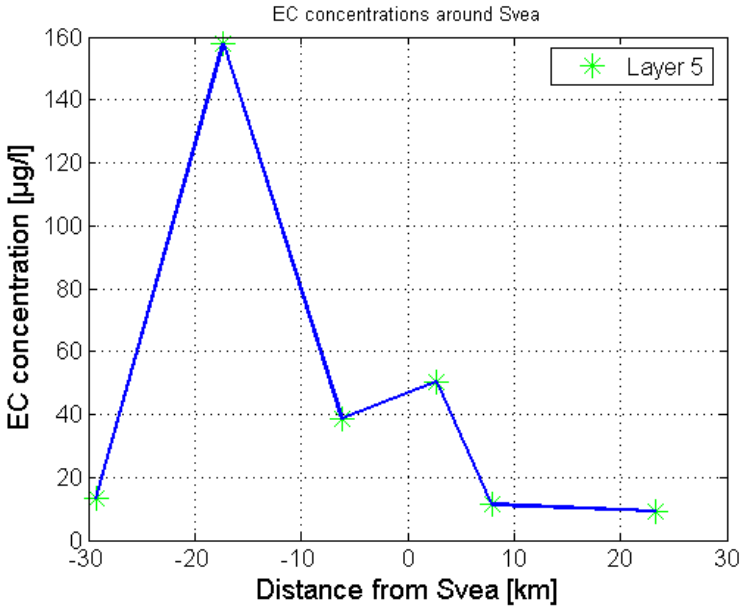

Figure 4.10: The measured EC concentration around Svea. The location of the sites is given in Figure 3.4. Svea is placed at zero.

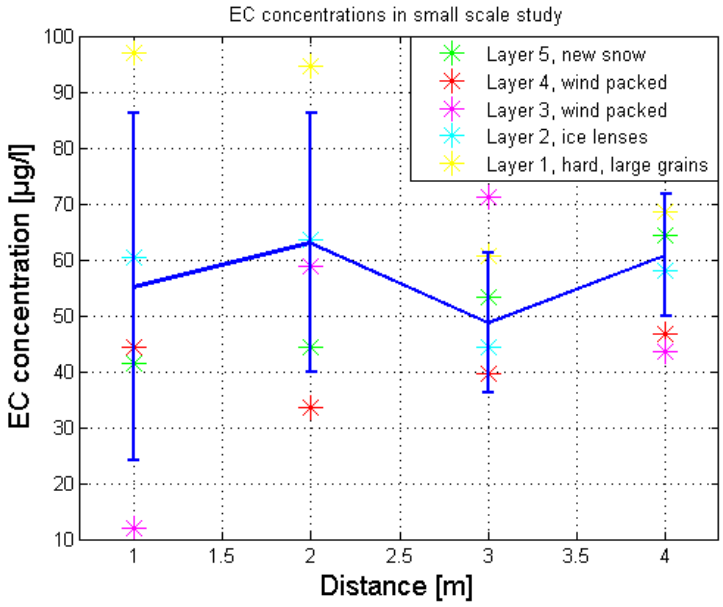

Figure 4.11: A small scale study at approximately 15 km southeast of Longyearbyen (blue dot number 5 in Figure 3.2). This is the same measuring point as the one 15 km east of Longyearbyen in Figures 4.6(a), 4.6(b), and 4.7. The blue line is the mean value which the standard deviation indicated at every single snow pit.

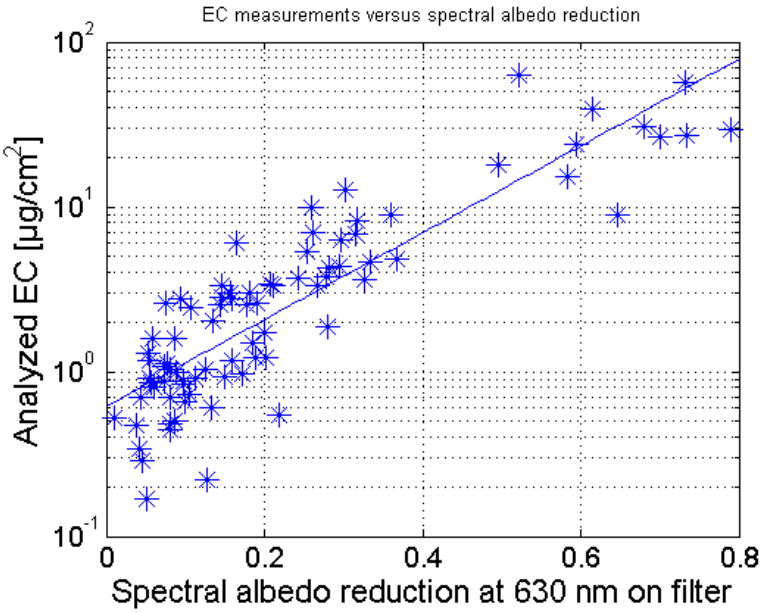

Figure 4.12: A comparison between the two EC measurement methods on the same filters at a spectral albedo of $630\,nm$. The blue line is an exponential regression with the function $y = 0.613 * \exp^{6.07x}$ with $r = 0.872$.

particles. These are green algae (Jones *et al.*, 2001).

4.3 Measured EC concentrations with the alternative method

The correlation between the easy alternative method and the proper EC analysis is nicely observed in Figure 4.12. The best regression to the points was an exponential fit. The EC burden on the filter is

$$EC_{amount} = 0.613 * \exp^{6.07 \cdot \alpha_{red,630\,nm}}$$

where EC_{amount} is the EC amount on the filter given in $\frac{\mu g}{cm^2}$ and $\alpha_{red,630\,nm}$ is the reduction in spectral albedo compared to a blank filter at a wavelength of $630\,nm$. The correlation coefficient is $r = 0.872$. Hence, the highest albedo sensitivity is at the lowest EC concentrations, as also observed by the albedo model plotted in Figure 4.19(a). Clarke & Noone (1985) used a similar method to estimate the dust amount from variations in the spectral albedo. They found that the relative absorption difference between $660\,nm$ and $535\,nm$ could be used as a proxy of the dust content. Such a relationship was not found for this experiment, even though several of the filters did contain dust and sediments. That was observed by visible examination and in the EC analyses. The root mean square is

$$rms = \sqrt{(1 - r^2)} \cdot \sigma_y = \sqrt{(1 - 0.872^2)} \cdot 11.62 \frac{\mu g}{cm^2} = 5.69 \frac{\mu g}{cm^2}$$

where $\sigma_y = 11.62 \frac{\mu g}{cm^2}$ is the standard deviation for the observations. The high correlation is promising and further research might use this simplified analysing method.

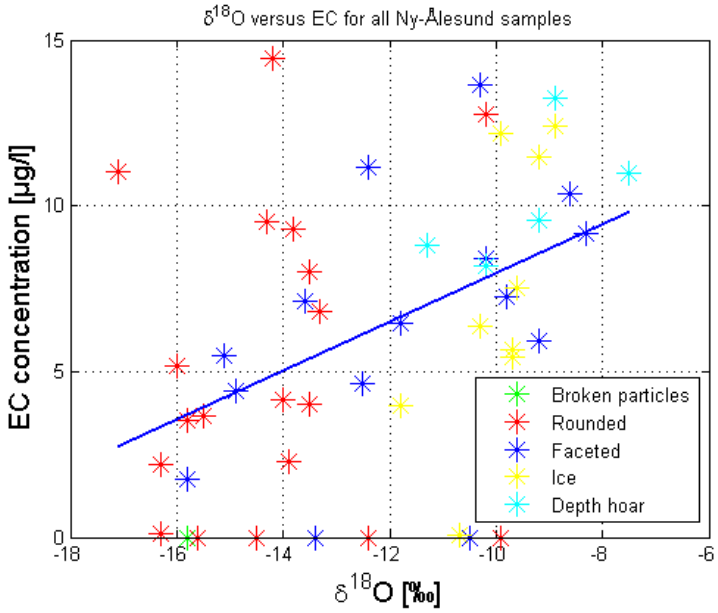

Figure 4.13: The relationship between $\delta^{18}O$ (x-axis) and EC concentration (y-axis) for all 50 samples gathered in the vicinity of Ny-Ålesund. The blue line is the linear regression of all points with the formula $y = 0.736x + 15.34$ with $r = 0.451$. The correlation is statistical significant. The snow samples have a colour coding according to their snow crystal type.

4.4 Measured $\delta^{18}O$

For all the 50 samples taken around Ny-Ålesund, $\delta^{18}O$ measurements were done in addition to EC analysis. The relationship between those two parameters is given in Figure 4.13. There is a clear signal indicating a higher EC concentration for snow with a warmer $\delta^{18}O$ ratio. A linear regression of all the data gives a correlation coefficient of $r = 0.451$. Snow crystal types normally found in the upper layers of the snow pack looks to be found in the lower left corner, while older snow particles are both more contaminated by EC and show a warmer temperature according to the isotope ratio.

4.5 Comparing EC, $\delta^{18}O$, and snow type

When comparing the EC concentrations with snow types (see Figure 4.14(a)) and $\delta^{18}O$ values with snow types (see Figure 4.14(b)), a similar trend is observed. The snow crystals have been given a number according to this scale: 1 = precipitation snow, 2 = broken particles, 3 = rounded, 4 = faceted, 5 = ice, and 6 = depth hoar. The correlation coefficient is 0.389 and 0.705, respectively, for those two relationships. The snow types normally found in the lower part of the snowpack, as depth hoar, has greater EC concentrations than those found in the top layers, like broken particles and rounded crystals. The variability observed is very large. The snow observed as relatively warm according to the isotope ratio is also found in the lower snow layers, while the cold isotopic ratio is found in less metamorphosed snow. The variability in the $\delta^{18}O$ versus snow type ratio is large, but somewhat less than for the EC and snow type relation. If we for simplicity assume that the isotopic ratio is only governed by EC concentration and snow crystal type, an empirical expression can be set up:

$$\delta^{18}O = -19.3 + 0.128 \cdot EC + 1.59 \cdot snow$$

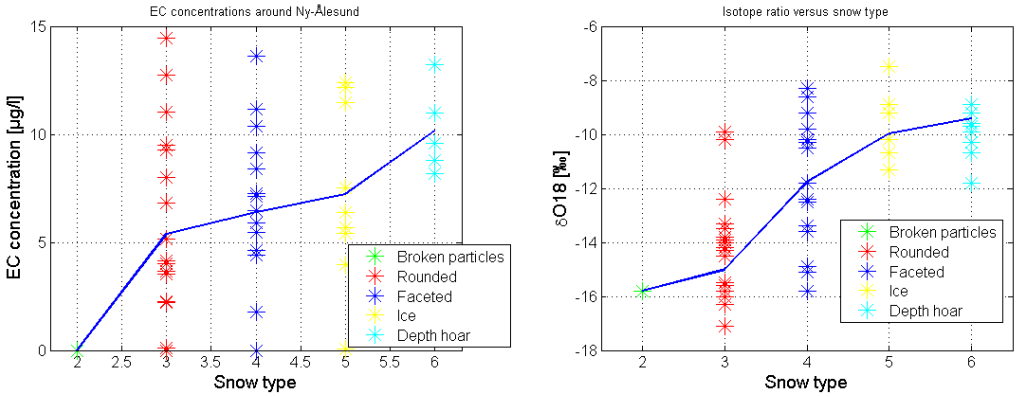

(a) EC concentration versus snow type in Ny-Ålesund

(b) $\delta^{18}O$ values versus snow type in Ny-Ålesund

Figure 4.14: (a) and (b): The relationship between EC concentration, $\delta^{18}O$, and snow type for all samples gathered around Ny-Ålesund. Due to the low EC concentrations measured, the impact of the settlements on these parameters is negligible. The correlation coefficient between EC and snow crystal type is 0.389, while it is 0.705 for $\delta^{18}O$ and snow crystal type. These correlations are calculated from the idea that every snow crystal type is given by an integer number. Both correlations are statistical significant.

This equation is a resulted of multiple regression, and the correlation coefficient between the measured and modeled $\delta^{18}O$ is $r = 0.730$. EC stands for the EC concentration in $\mu g/l$ and snow for the snow crystal type (1 = precipitation snow, 2 = broken particles, 3 = rounded, 4 = faceted, 5 = ice, 6 = depth hoar). For typical EC concentrations measured (between 0 and 15 $\mu g/l$), the most sensitive parameter is the snow type. Thus, snow metamorphism is important for the isotopic ratio. Further, metamorphosed snow crystals contain in average more EC and have a warmer isotope ratio than unmetamorphosed snow.

4.6 Comparison of EC and snow type

For a comparison of EC concentration and snow type at the micro scale study, see Figure 4.15. The variability is large and no clear trend is observed, as opposed to the data from the samples gathered around Ny-Ålesund. Local pollution has affected these snow samples which could bias the snow type versus EC concentration relation.

A closer look at two individual snow pits, one in Sassendalen and one in Longyeardalen, is done in Table 4.1. The weighted average EC concentration at the snow pit in Sassendalen was 8.97 $\mu g/l$. The EC concentration is slightly higher in the lower part of the snow pack. The snow sample consisting of several thick ice layers is clearly the most contaminated (14.17 $\mu g/l$). The weighted mean EC concentration at the other snow pit is considerably higher (34.86 $\mu g/l$). The main reason is the site's proximity to Longyearbyen and a major snowmobile track. The snowmobile traffic is especially high in late winter (March and April) and that is explaining the contaminated top layer. Otherwise, the results are similar to what observed in Sassendalen. The EC concentration is significant higher in the snow sample consisting of ice layers (64.29 $\mu g/l$). Trends in EC depositions throughout the winter are difficult to assess as post-depositional processes are significant. That is partly explained by the sampling procedure where every snow samples consisted of snow from several precipitation events, which would smear out any signals in the data. The ice layers are from the early part of winter. As observed in Section 4.1, the last formation of an ice lens was during the melt of January 1st and 2nd 2009. The top two layers from the Sassendalen snow pit and top three from the Longyeardalen snow pit must, therefore, consist of snow precipitated after January 2nd 2008. The lowest layer represents

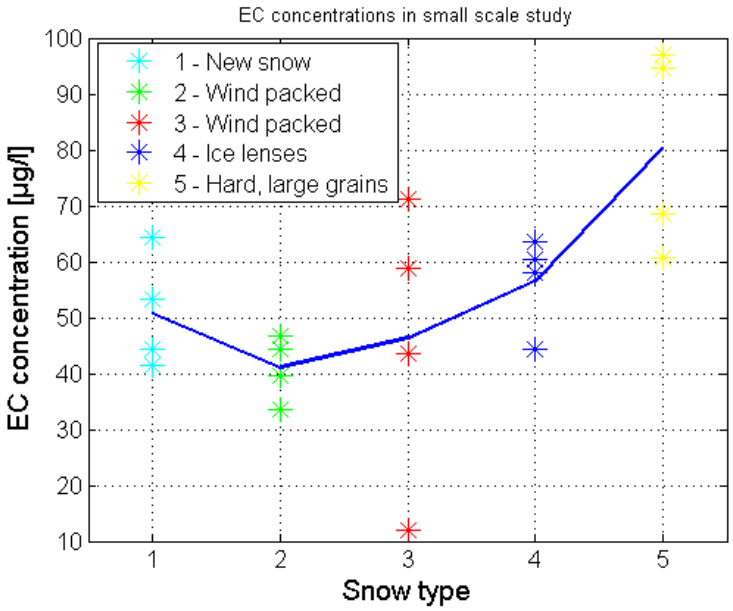

Figure 4.15: EC concentration with depth at the micro scale study in Adventdalen. The snow samples from the top layer, Layer 1, are given the value 1 and so forth until the bottom layer, which has a value of 5.

the oldest snow from both snow pits and was probably formed in October and November 2007.

4.7 Modeled EC concentrations with the Oslo CTM2 model

The data from runs of the Oslo CTM2 model has been provided by R. B. Skeie (personal communication). Since the model has such a coarse resolution, only three grid points cover entire Svalbard. A comparison between these is given in Figure 4.16. The top nine snow layers in the model for April 1st 2008 are included, and they show similar EC concentrations and profiles in the snow for all three sites. The numbers given are the total EC concentrations. All the sites have a clear spike in EC concentration of about 25 to 30 $\mu g/l$ in about the same depth. With the exception of this spike, the EC concentration is seen to be hovering around 5 $\mu g/l$ or slightly more. The mean EC concentration for the western site is 5.00 $\mu g/l$, while the middle and eastern sites have concentrations of 5.87 $\mu g/l$ and 5.93 $\mu g/l$, respectively. Such an east-west gradient is expected according to Forsström *et al.* (Submitted). Since there is so little local variability, the local EC sources cannot be significant in this model. Further, one of the grid points represents entire Svalbard rather well. In the rest of this section, data from the grid point 79.53 $^\circ N$, 14.06 $^\circ E$ is used. That is near Liefdefjorden in the northern part of Spitsbergen.

The EC content in the snow pack varies significantly through the winter. In Figure 4.17, the vertical profile of the EC concentration in the snow pack is given on a monthly basis. Some spikes are seen. They are caused by single events that brought large quantities of EC in the precipitation. These spikes are especially pronounced in February, March, and April, in the Arctic Haze season (Shaw, 1995). The highest modeled EC concentration in a single snow layer is observed in the April 1st plot with a value of 29.11 $\mu g/l$. The spike in the surface on May 25th is caused by melting. The melted snow will drain while the EC particles stay on the snow surface. The mean EC concentration is at its lowest during the three first months of about 1 $\mu g/l$ and then increases until April with a mean of 5.87 $\mu g/l$. A dip is seen in May; however, that is reversed as soon as the melt starts. The mean

Table 4.1: The EC concentration and snow type for different horizontal snow layers from a snow pit in Sassendalen (SA4) and in Longyeardalen (L4), in the middle between Nybyen and Longyearbreen. The lowest 10 cm from the snow pit L4 was not sampled due to visible contamination of Aeolian sediments.

Sassendalen	Snow depth [cm]	EC concentration $[\mu g/l]$	Snow type
5	59-68	6.04	New and freshly deformed snow
4	47-59	6.35	Hard windblown
3	32-47	14.17	Hard, 4 thick ice layers
2	20-32	-	Hard, melt-freeze
1	0-20	7.97	Depth hoar
Longyeardalen	**Snow depth [cm]**	**EC concentration $[\mu g/l]$**	**Snow type**
5	62-70	73.12	New snow
4	50-62	10.41	Wind packed
3	38-50	1.44	Hard, wind packed
2	19-38	64.29	Hard, 2 thick ice lenses
1	10-19	15.86	Faceted snow

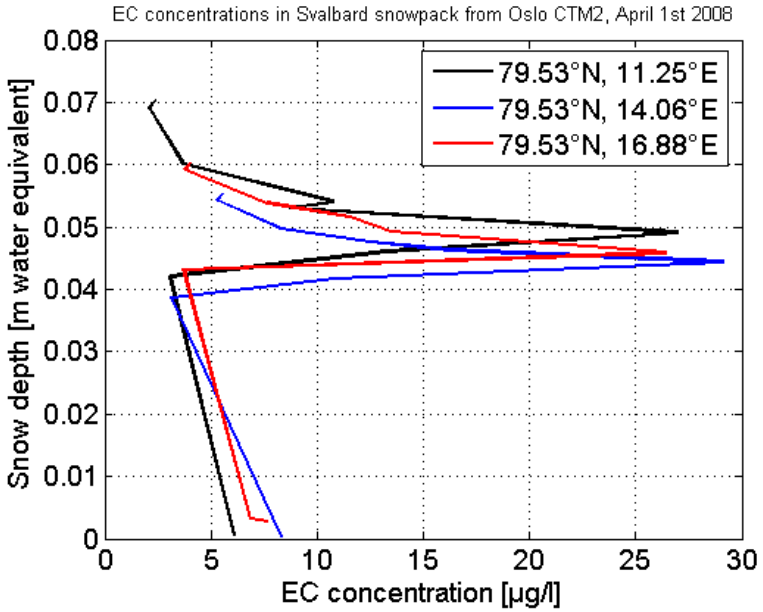

Figure 4.16: A comparison in EC concentrations between different grid points in Svalbard by running the Oslo CTM2 chemical transport model (R. B. Skeie, personal communication). Three of the grid points in the model are placed in Svalbard. The coordinates are $79.53\,^\circ N$, $11.25\,^\circ E$, $79.53\,^\circ N$, $14.06\,^\circ E$, and $79.53\,^\circ N$, $16.88\,^\circ E$. The vertical profile of EC concentrations in snow is given for the top nine layers on April 1st 2008. The EC concentrations here are the total output from the model.

concentration at May 25th was $6.43\,\mu g/l$. The fossil fuel burning is the dominant source. Early and late in the season, when forest fires is expected, biomass burning contributes with about $8\,\%$ of the total EC burden. In mid-winter, this share is as low as $1.0\,\%$.

The average concentration in the top five snow layers throughout the winter is seen in Figure 4.18. Five snow layers were used since that will represent the surface snow EC concentration and the optical properties fairly well. The snow depth of these five layers was typically $3.5\,cm$ water equivalent. The results are similar to what presented in Figure 4.17; however, the temporal resolution is about a week. Since the average of five individual snow layers is used, any spiking is smeared out. The EC is divided into according to their origin, fossil fuel and biomass burning. The mean EC concentration for the entire winter in total was $5.35\,\mu g/l$. Fossil fuel contributed with $5.11\,\mu g/l$, while biomass burning is only responsible for $4.5\,\%$ of the total or $0.24\,\mu g/l$. In general, the EC concentration is low during the early part of the winter while events cause some spiking in February, March, and April. That is a result of Arctic Haze (Shaw, 1995). A clear spike was observed on February 2nd 2008 (from $4.14\,\mu g/l$ to $8.69\,\mu g/l$ in $24\,hours$), while the largest increase happened from March 10th to 11th (from $5.83\,\mu g/l$ to $17.48\,\mu g/l$). The spring melt dramatically increases the EC concentration in the snow pack since the model assumes that EC particles remain in the snow pack. On May 31st 2008 all the top nine layers snow layers were melted. There was more snow; however, the model is, unfortunately, not able to include the rest of the snow pack. The last reading gave an EC concentration of $46.28\,\mu g/l$. Hence, the EC concentration will continue to increase until all the snow is melted or the melt season is over.

4.8 A comparison of measured and modeled EC concentrations

In Section 4.7, the mean modeled EC concentration during the 2007/08 winter was $5.35\,\mu g/l$. That is agreement with the background EC level in Svalbard, $4.1\,\mu g/l$ (Forsström *et al.*, Submitted). This modeled value compares well to what observed in locations with little local pollution. The mean of all samples from the area around Ny-Ålesund was $6.58\,\mu g/l$ (see Section 4.2). Unfortunately, the model only includes data for the upper part of the snow pack. Hence, a comparison of the vertical profile of EC concentration is not possible. The snow samples gathered from Ny-Ålesund was typically showing more EC the older and more metamorphosed the snow was. This is not seen in the model, since the EC concentration was at its lowest during the early part of winter. The model also fails to include melt events during the winter. The melt events early in the season led to an increase in EC concentration and are the main reason for the increased EC concentrations in the lower snow pack.

A comparison between surface snow samples and the mean EC concentration of the top five snow layers is seen in Figure 4.18. In Ny-Ålesund, snow was samples on the 11th and 12th of March 2008. The mean EC concentration of the top snow layer was $4.33\,\mu g/l$ and $5.97\,\mu g/l$ during those two days, in chronological order. That is similar to what the model predicted on March 10th, $5.83\,\mu g/l$. However, the model spikes ($17.48\,\mu g/l$) on the 11th due to a snow event with highly EC contaminated precipitation. Precipitation was not observed during the field work, and no precipitation is registered at the weather station in Ny-Ålesund. The grid point used here is not in Ny-Ålesund, so that local differences in weather within Spitsbergen are causing this misfit. During the field work in Svea, two snow samples were taken that is believed to be more or less pristine. On March 25th, an EC concentration of $9.19\,\mu g/l$ was registered and on March 26th $13.38\,\mu g/l$. That is accordance with the model, which predicted an EC concentration of $10.95\,\mu g/l$ and $9.63\,\mu g/l$, respectively. This comparison is based on only two snow samples; hence, there is a significant error margin. Finally, some samples were gathered in Sassendalen on March 29th that are insignificantly biased by local pollution. The three snow samples have a mean EC concentration of $8.42\,\mu g/l$, which agrees very

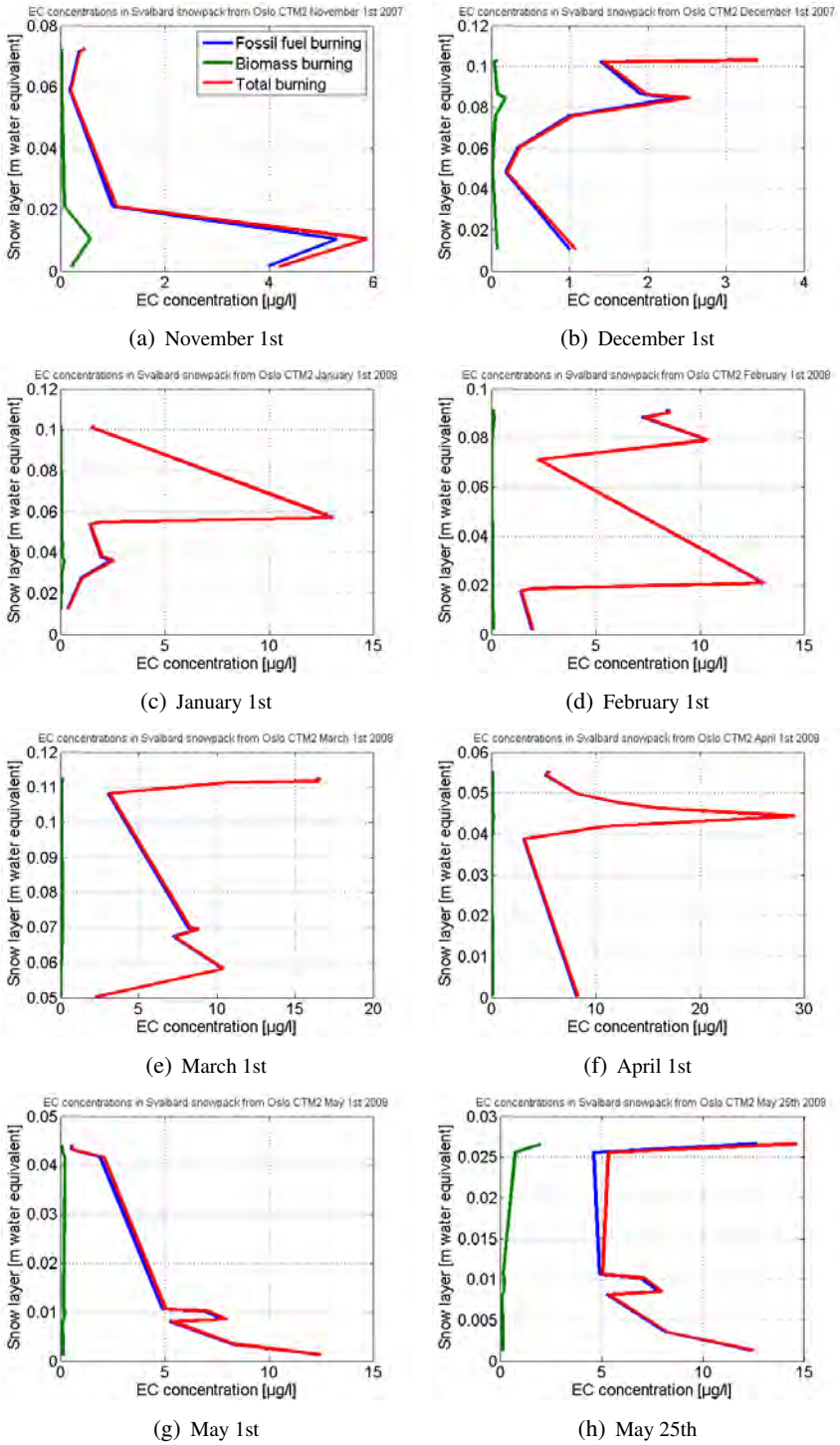

(a) November 1st (b) December 1st

(c) January 1st (d) February 1st

(e) March 1st (f) April 1st

(g) May 1st (h) May 25th

Figure 4.17: (a), (b), (c), (d), (e), (f), (g), and (h): The modeled EC concentration in the snow pack at $79.53\,^{\circ}N$, $14.06\,^{\circ}E$ during the winter 2007/08 (R.B. Skeie, personal communication). The top nine snow layers are included for the first day in every month between November 2007 and May 2008. Melting started in the end of May, and May 25th is chosen as the last plot according to this.

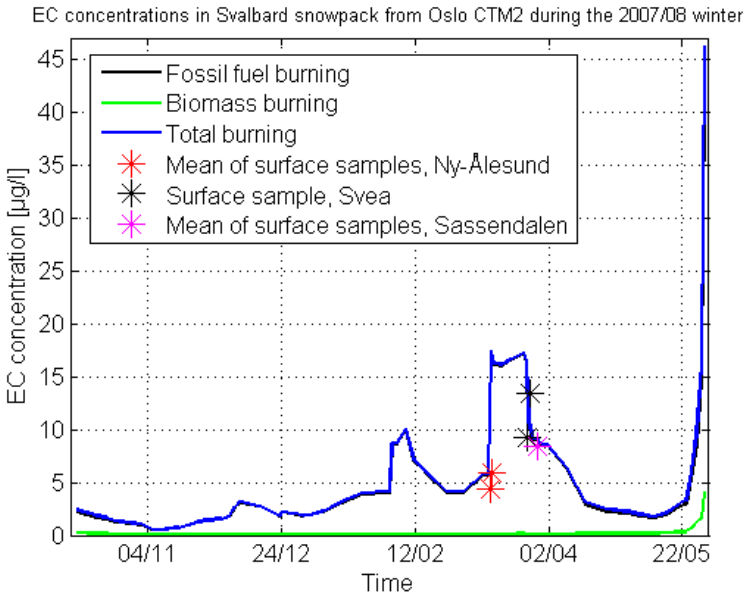

Figure 4.18: The EC concentration in the top five snow layers at $79.53\,^{\circ}N$, $14.06\,^{\circ}E$ during the winter of 2007/08 (R.B. Skeie, personal communication). The plot stops on May 31st 2008, the day all the top nine snow layers were melted. The points are EC measurements from background sites.

well with the model ($8.71\,\mu g/l$).

4.9 Relating EC concentration with snow albedo reduction

EC reduces the snow albedo, and the reduction is greater the greater the EC concentration is in the snow. A model of this spectral albedo reduction for different wavelength bands has been acquired from Rypdal *et al.* (Submitted). The data set is shown in Figure 4.19(a), and a linear relation is assumed between the data points. The model results were given by G. Myhre (personal communication), and the model is here considered as a "black box." However, the relation between the EC concentration and albedo effect is governed by optical properties as those discussed in Sections 2.4.1 and 2.5.1. A similar snow albedo model with impurities is discussed by Warren & Wiscombe (1980) and Wiscombe & Warren (1980). The model shows that the snow albedo is the most sensitive to changes in EC concentrations when these concentrations are low, and there is not a clear linear dependence between albedo change and EC concentration. Further, the albedo is most affected in the visible spectrum, while the effect is negligible in the infrared. The effect is greater for older and more coarse grained snow (optical grain size around $500\,\mu m$) than for new and fine-grained snow (optical grain size $50\,\mu m$). Temperatures around or above zero is rarely observed in February, March, and April in Svalbard; hence, the values for new, fine grained snow ($50\,\mu m$) is used in the calculations of the EC's albedo effect and in the calculations of the local impact of EC pollution.

The model by Rypdal *et al.* (Submitted) only shows the spectral albedo reduction. The total albedo reduction is calculated by weighing the different spectrum bands according to their relative strength in the solar spectrum on the ground surface. The solar spectrum used in this thesis is shown in Figure 4.19(b). From this, the albedo reduction for the 350 to $2500\,\mu m$ spectrum was found, which is a good proxy of the total albedo reduction. This albedo reduction as a function of EC concentration con is given by

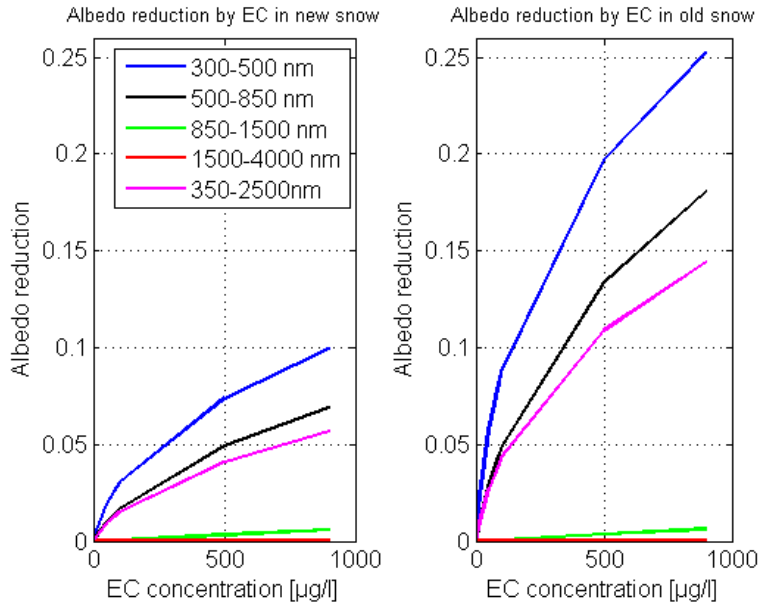

(a) Albedo reduction for spectrum bands

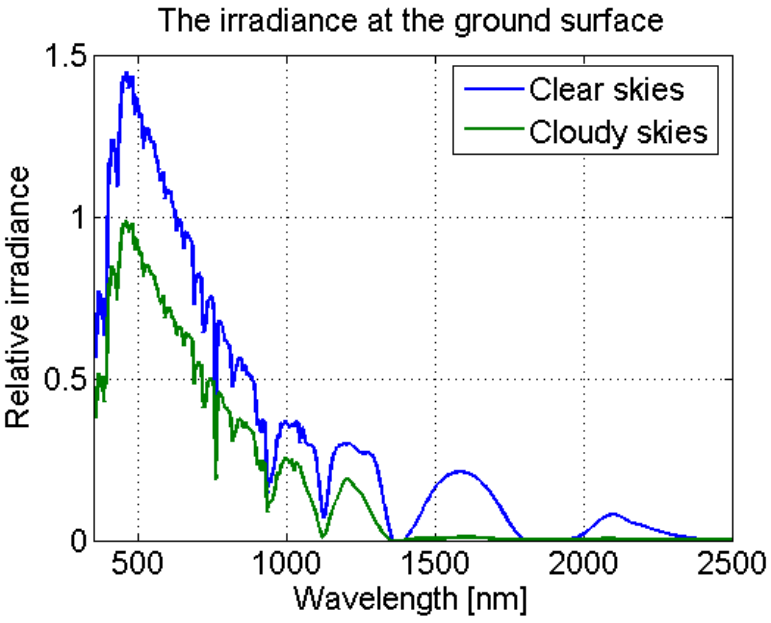

(b) Solar spectrum at the ground

Figure 4.19: (a): Modeled albedo reductions for new and old snow with optical grain radii of 50 μm and 500 μm, respectively. This model is based on a data set of 12 specific values for this relation given by (Rypdal *et al.*, Submitted), and, here, a linear relation is assumed between the data points. The spectral albedo effect for the 350 to 2500 μm band was calculated with a weighted solar spectrum. (b): The solar spectrum at the ground surface (C.A. Pedersen, personal communication). The solar spectrum is here given with relative values in order to compare the strength between various spectrum bands. This irradiance varies with time and space; however, the values given represent the conditions in Svalbard fairly well.

Table 4.2: The reduced albedo for different EC concentrations in the snow for new, fine grained and old, coarse grained snow, with optical grain size of $50\,\mu m$ and $500\,\mu m$, respectively. No albedo reduction is given for fine-grained summer snow on Longyearbreen since the snow grains at site were wet and coarse grained. The model parameters used in the calculations are based on data from Rypdal *et al.* (Submitted) and C.A. Pedersen (personal communication).

Case	EC concentration	Albedo reduction (α) new snow ($50\,\mu m$)	Albedo reduction (α) old snow ($500\,\mu m$)
Background level, median (Forsström *et al.*, Submitted)	$4.1\,\mu g/l$	0.0011	0.0033
Background level, mean (Forsström *et al.*, Submitted)	$8.7\,\mu g/l$	0.0021	0.0066
Typical concentration in Adventdalen (Section 4.2)	$\sim 50\,\mu g/l$	0.0091	0.0267
Typical concentration around Svalbard Airport (Section 4.2)	$\sim 1000\,\mu g/l$	0.0608	0.153
Mean concentration on Longyearbreen in summer (Section 4.2)	$230.65\,\mu g/l$	-	0.0646

$$\alpha(con) = \left[a(con)\cdot \sum_{i=350}^{500} ir_i + b(con)\cdot \sum_{i=500}^{850} ir_i + c(con)\cdot \sum_{i=850}^{1500} ir_i + d(con)\cdot \sum_{i=1500}^{2500} ir_i\right] / \sum_{i=350}^{2500} ir_i \quad (4.1)$$

where ir is the irradiance at the surface according to C.A. Pedersen (personal communication) with the subscript i that is the wavelength in nanometres (see Figure 4.19(b)). $a(con)$ is the albedo reduction for different EC concentrations in the 350-500 nm wavelength band, $b(con)$ for the 500-850 nm band, $c(con)$ for the 850-1500 nm band, and $d(con)$ for the 1500-2500 nm band (Rypdal *et al.*, Submitted). The sky is assumed to be clear; hence, the ir values for clear skies is used in the calculations. The spectral composition would be somewhat different in cloudy conditions with a relative richer visible spectrum. That would give higher albedo sensitivity. From this, the albedo effect of EC from local sources in Svalbard snow (Eff) was calculated with this formula:

$$Eff = \sum_i \sum_j A_{i,j}[\alpha(con_{i,j}) - \alpha(con_{back,j})]/A_s \quad (4.2)$$

where the subscript i is settlement and subscript j is a small finite area in Svalbard. $\alpha(con)$ is the albedo reduction for an EC concentration of con (see Equation 4.1) at a certain point that is assumed to be valid for the surrounding area given by A. The Thiessen method used here states that a point measurement j is set to be representative for an area halfway to the next point (Boots, 1980). con_{back} is the EC background level. This background value varies, and values fitting to the observations from Forsström *et al.* (Submitted) are used. Table 4.2 shows how the mean and median EC value found in her study give clearly different albedo effects. The estimated importance of local pollution for Longyearbyen, Svea, Ny-Ålesund, and Barentsburg is given in Table 4.3.

Based on the median EC value of $4.1\,\mu g/l$ observed by Forsström *et al.* (Submitted), the albedo reduction for new snow due to long-range transported EC to Svalbard was calculated to be 0.0011 (see Table 4.2). The mean value from the same study is higher ($8.7\,\mu g/l$), and that almost doubles the albedo effect. The EC background level will naturally vary throughout Svalbard. Around Longyearbyen, the background level is assumed to be about $6\,\mu g/l$ in the calculations as snow in

Table 4.3: An estimate of the albedo effect from measured EC concentrations around the settlements in Svalbard. These values are calculated by Equation 4.2. Barentsburg is included since its pollution is believed to be important for the total local effect in Svalbard. All numbers are given in percentage relative to the effect of long-range EC. The low estimate is a very conservative evaluation, while the high estimate includes areas that are likely to be affected by local pollution, but is lacking data. The last column gives an estimate where snow covered sea ice is assumed on Isfjorden. The effect of local EC sources compared to the total EC sources can be calculate in percentage as $e = eff_i/(100 + \sum_j eff)$, where eff_i is one or more local sources and $\sum_j eff$ are all local sources. The total is the summation of local and long-range transported EC. The model parameters used in the calculations are based on data from (Rypdal *et al.*, Submitted) and C.A. Pedersen (personal communication).

Settlement	Low estimate	High estimate	If sea ice
Longyearbyen	2.2 %	3.5	9.6 %
Svea	5.4 %	6.2	6.2
Ny-Ålesund	0 %	0 %	0 %
Barentsburg	~ 5 %	~ 7 %	~ 10 %
Total	**12.6 %**	**16.7 %**	**25.8 %**

inner Sassendalen contained $6.09\,\mu g/l$ (see 4.2). The EC background level was set to $9\,\mu g/l$ around Svea. That is based on the most remote samples in the area came close to that level (see 4.2) and that Forsström *et al.* (Submitted) observed a concentration of $9.8\,\mu g/l$ in Inglefieldsbukta, east of Svea. These spatial variations in EC concentrations could as well be a result of the snow sampling did span over several weeks. Then, the spatial variability may actually be temporal variability. However, the entire snow pack was sampled with snow from the entire winter accumulation period. Hence, the variability seen is mostly due to actual spatial variability.

The total albedo effect from local sources is shown in Table 4.3 to be $12.6\,\%$ of the effect by long-range transported EC. That is a conservative estimate since it only includes areas that have been measured and that are locally contaminated. Areas that are likely to be contaminated are included in the high estimate. That increases the local effect to $16.7\,\%$ of the long-range effect. The estimate would be even greater if snow covered sea ice is present in the fjords around the settlement, which increases the estimate to $25.8\,\%$. In the conservative estimate, the local effect of Longyearbyen for Svalbard is about $2.2\,\%$ of the long-range effect. Svea has a much bigger effect of $5.4\,\%$. However, this number is based on only six snow samples; therefore, the uncertainty is much larger than for the Longyearbyen estimate. The estimate of EC pollution from Svea does not consider the visible high EC concentrations around Cape Amsterdam and is, thus, likely underestimating. EC pollution from Svea has a larger albedo impact than contaminants from Longyearbyen since a much larger area is affected around Svea. Van Mijenfjorden is a fjord that freezes over every winter. As seen in Section 4.1, the main wind direction is north-east; hence, the pollution is efficiently spread out onto the snow pack covering the sea ice of van Mijenfjorden. Similarly, the south-east wind in Longyearbyen carries the pollution out on Isfjorden, a wide fjord. That fjord was nearly ice free during the winter of 2007-08. Elevated EC concentrations were not observed in the snow pack around Ny-Ålesund. As seen in Section 4.2, the mean EC concentration was only $6.58\,\mu g/l$. Thus, the local pollution effect is negligible, and the estimate is set to $0\,\%$. An educational guess of the effect by Barentsburg is included. No samples were taken at Barentsburg; however, the snow is visibly discoloured by soot in the settlements' vicinity. The effect is believed to be comparable of that by Svea, and a $5\,\%$ of the long-range effect is estimated as the local effect.

The calculations in the previous paragraph are based on EC in new snow. As seen in Figure 4.19(a), the sensitivity of EC in old, wet, coarse-grained snow is much larger than in new, fine-grained snow. For typical background level concentrations of EC, the albedo reduction is a factor 3 larger after melting has initiated (See Table 4.2). The albedo reduction at the background level of $4.1\,\mu g/l$ is

0.0033. At extreme high concentrations as those found around Svalbard Airport, the factor is a little less at about 2.5. Thus, the albedo effect from local EC sources is larger in coarse-grained snow than fine-grained snow, but the relative impact compared to long-range transported EC is slightly smaller. In addition to the higher EC sensitivity in melting snow, the EC concentration in the surface layer will increase during melting. That will increase the strength of the albedo reduction. In Section 4.2, an increase of a factor 18 was seen in surface snow on Longyearbreen from April to August. The EC concentrations measured on Longyearbreen during late summer will reduce the albedo by 0.0646.

Chapter 5

Perspectives

In this chapter, factors that affect the EC concentration in snow are analyzed. Among those factors are depositional and post-depositional factors. Then, a budget for local and long-range transported EC can be given. The snow albedo is also affected by dust particles. An overview of local and long-range sources of dust and its impact is, therefore, shown in this chapter. How all these factors affect the results in this thesis will be discussed in Section 6.

5.1 Factors affecting EC concentrations in snow

In section 2.8.2, temporal and spatial variations in EC concentrations in snow were discussed. As observed in Section 4.2, there are large spatial variations within Svalbard. Temporal variations are also modeled, but at a smaller extent (see Section 4.7). These variations are from the global to micro scale and from inter-annually to daily variations. Here, the factors determining deposition and post-depositional effects will be analyzed.

5.1.1 Depositional effects

The simplest explanation of variations in EC concentrations in snow is that there are variations in the sources. The study by McConnell *et al.* (2007) shows clearly a historic covariance between source output from industries in North America and EC concentrations in snow during winter in western Greenland. Although there are many different and complicating deposition processes, a study of ions in Spitsbergen snow (Semb *et al.*, 1984) showed that there is a consistent relationship between transport from sources and concentrations in the snow pack on temporal and spatial scales. The next step is to postulate that the transport of the pollution varies. Differences in precipitation events and the large-scale dynamics of the atmosphere will alter the initial EC content in different ways.

Different transport pathways to Svalbard were discussed in Section 2.6.1. Eneroth *et al.* (2003) and Forsström *et al.* (Submitted) observed that air reaching Svalbard from the east contained more pollution and EC than from the west. Further, a similar picture is seen in the snow samples as the EC concentrations were higher in the eastern part of Svalbard than the western. Eleftheriadis *et al.* (2009) modeled that EC contaminated air came from Northern and Central Russia to Svalbard. An air parcel can travel relatively unaffected from Northern Europe and Northern Russia to Svalbard where mountains on the eastern side will cause uprising of air. EC will be washed out, and the air is cleaner once it reaches the western side of Svalbard. Air arriving on the western side of Svalbard is more

likely to have crossed over the Atlantic Ocean. Due to the cyclonic activity related to the Icelandic Low, EC will to a great extent be washed out before reaching Svalbard.

The EC concentration in snow depends on the atmospheric burden of EC and the amount of precipitation. In order to find the total EC mass transport, we need to know the total mass of snow falling over Svalbard. Hence, a high EC concentration indicates either an abundance of EC or a dry climate with little precipitation. There are large variations in precipitation in Svalbard; however, measurements are sparse. In all, there are only a handful of stations measuring precipitation, including Longyearbyen and Ny-Ålesund. Most of these stations are close to large water masses and near the sea level. In the mountain areas, the precipitation is increased by an orographic effect and the forced uplift of air by the mountains (Førland *et al.*, 1997b). In addition, measuring precipitation is difficult in the Arctic. For instance, $190\,mm$ of blowing snow was measured as precipitation during 3 days at Hopen, an island southeast of Spitsbergen (Førland *et al.*, 1997a). In general, solid precipitation and winds tend to cause an underestimate of precipitation for most precipitation gauges (Legates & Willmott, 1990; Ungersböck *et al.*, 2000). A campaign study by Hanssen-Bauer *et al.* (1996) in Ny-Ålesund revealed that the true precipitation during snowfall was almost $190\,\%$ of the measured. Further, the annual precipitation was $50\,\%$ over the uncorrected value. That would shift the annual precipitation upwards from $385\,mm$ (Førland *et al.*, 1997a) to about $550\,mm$. Humlum (2002) used a $100\,\%$ correction for the precipitation in a precipitation modeling study. He modeled the annual precipitation in central Spitsbergen with the use of topographic maps and vertical precipitation gradients (see Figure 5.1). The average annual precipitation in this area is about $870\,mm$. All snow samples gathered around Longyearbyen and Svea were taken inside this area. The model shows a minimum in precipitation in Adventdalen, which incidentally is the area most heavily EC polluted area in Svalbard. The surrounding mountains receive much more precipitation. The vertical precipitation gradient is typically between 5 and $25\,\%$ per every $100\,m$ (Winther *et al.*, 1998; Humlum, 2002). Førland *et al.* (1997b) measured $45\,\%$ more precipitation on the elevated glacier Austre Brøggerbreen than nearby Ny-Ålesund by the shoreline. This can be explained by orographic effects which bring more snow in the mountains than along the coast. Further, the survey by Winther *et al.* (1998) found about 38 to $49\,\%$ more snow accumulation on the east coast of Spitsbergen than the west coast. Moreover, 40 to $55\,\%$ less snow accumulation is seen on the northern side of Spitsbergen than the southern. A maximum in precipitation is seen on the eastern coast of Spitsbergen. That is the same location as higher EC concentrations are found (Forsström *et al.*, Submitted). Hence, the effect of more EC available from Siberia out wins the effect of more precipitation. The study by Winther *et al.* (1998) was extensive and measured snow accumulation on glaciers just before the melting started in 1997. At a representative height of $400\,m\,a.s.l.$, the average water equivalent was $785\,mm$. The winter precipitation for Svalbard Airport and Ny-Ålesund was in average $82\,\%$ of the normal. A climatic normal snow pack would, therefore, contain $957\,mm$ water equivalent. In conclusion, the precipitation in Svalbard is highly variably; however low ($\sim$ 200-500 mm/yr) in the sampled areas. The average snow pack depth for entire Svalbard is $957\,mm$ water equivalent. Further, the precipitation is under measured, and for snowfall the true precipitation is about $190\,\%$ of the measured.

The median snow depth at the snow pits excavated around Ny-Ålesund was $60\,cm$ in the middle of March, while the mean snow depth for the entire field work was $67\,cm$. That is in accordance with a snow depth of $70\,cm$ with a standard deviation of $40\,cm$ observed in a large study by Bruland *et al.* (2001) west of Ny-Ålesund shortly before the melt season in 1998. For a normal year, the snow depth (D) can crudely be estimated by

$$D = P \cdot [A_{snow} + \frac{1}{2} A_{sleet}] \cdot corr/\rho$$

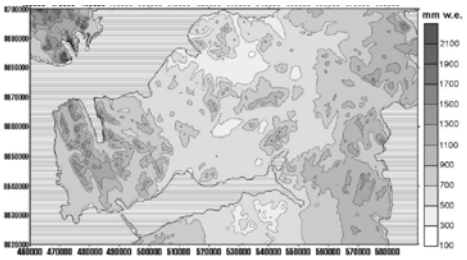

Figure 5.1: Modeled late 20th-century annual precipitation for Nordenskiöld Land. This area is in the middle of Spitsbergen and includes both Longyearbyen and Svea. Adventdalen, in the upper central part of this figure, is among the driest areas ($< 500\,mm/yr$). The average precipitation for the entire area is $870\,mm/yr$. The figure is from a study by Humlum (2002).

Table 5.1: The annual precipitation (Førland *et al.*, 1997a) and estimated snow depth by the end of a typical winter is here given for Svalbard Airport, Ny-Ålesund, and Svea. Half of the registered sleet is here assumed to stay in the snow pack as snow. The amount of solid and mixed precipitation was taken from Førland & Hanssen-Bauer (2002). The precipitation is under measured on Svalbard. In the column "corrected," the precipitation is increased by $90\,\%$ (Hanssen-Bauer *et al.*, 1996). In the last column, a sublimation of 53 cm for the winter is included as based on calculations by Jaedicke (2001). The sublimation term is calculated and discussed in Section 5.1.2. In comparison, the mean snow pit depth for the field work was $67\,cm$.

Settlement	Annual precipitation	Snow depth	Corrected	With sublimation
Svalbard Airport	190 mm	30 cm	57 cm	4 cm
Ny-Ålesund	385 mm	62 cm	119 cm	66 cm
Svea	260 mm	51 cm	97 cm	44 cm

where P is the annual precipitation, A_{snow} the percentage that comes as snow, and A_{sleet} that comes as sleet, $\rho = 0.371\,g/cm^3$ the typical snow density (Winther *et al.*, 1998), and $corr = 1.9$ the correction factor from measured to real solid precipitation. If no melting and no loss of snow due to wind drift are assumed, typical snow depths by the end of winter is given in Table 5.1. Values from Førland *et al.* (1997a) and Førland & Hanssen-Bauer (2002) are used in the calculations. The results of these calculations given in Table 5.1 show good agreement to the measured snow depths.

The precipitation from September 2007 to April 2008 was $104.9\,\%$ and $138.4\,\%$ of the normal at Svalbard Airport and in Ny-Ålesund, respectively. Thus, a slightly thicker snow pack than normal was expected at the time of the field work. However, the combination of dry snow, strong winds, and open tundra makes the snow depth measurements in this thesis highly inaccurate, as pointed out by Førland & Hanssen-Bauer (2002). The snow depth measurements were slightly biased since the snow pits were excavated in areas suitable for snow sampling and not necessary representative for the surrounding areas. Even so, snow depths agreed well with precipitation. The mean snow depth was $67\,cm$, with less snow in wind-exposed and dry areas and more snow in elevated areas.

As explained in Section 2.7, snowflakes scavenge impurities such as EC particles when falling from the sky. In the case of an aerosol rich air in the lower part of the atmosphere, the snow will get more and more contaminated as the snowflakes fall. Then, the EC concentration in the snow on the ground would be decreasing with altitude. Lund (2008) believes this subcloud scavenging is minimal, and she modeled this contribution to be about $0.5\,\%$ of the total deposition. Hence, subcloud scavenging will be neglected in this thesis.

EC particles are normally wet deposited, but could also be introduced to the snow pack by dry fallout. For remote areas in Svalbard, this is probably an insignificant effect due to the small size of the EC particles. On the other side, much coarser EC particles are found near the local sources, such as coal dust. Then, dry deposition is important for the understanding of the overall EC concentration in the snow pack.

Rain will, as snow, bring EC particles to Svalbard. If there is a snow cover on the ground, the rain water will either be drained out of the snow pack or freeze and form ice lenses in the snow pack. The EC particles stay on the snow surface. Rain events in the winter are rare, but they do occur. The greatest rain event during the winter of interest happened on January 1st and 2nd 2008 (see Section 4.1). That lead to elevated EC concentrations in the snow pack, as observed in Section 4.6. These events will lead to spiking in the EC concentration; however, the impact is low for the entire snow pack as these events are rare. Therefore, the contribution of EC in such rain events during wintertime is neglected in this thesis. On the other hand, rain will be an important source of EC for the remaining snow in summer.

5.1.2 Post-depositional effects

The EC concentration in a snow pack is influenced by snow metamorphism, surface exchanges between the snow and air, chemical reactions within the snow pack, and exchange processes with the ground soil (Jones *et al.*, 2001). Wind above the snow cover and the resulting snow drifts can also alter the EC concentrations. These processes will be discussed and quantified in this section.

Snow metamorphism can be divided into three different processes according to the temperature and temperature gradient in the snow pack. These are melt-freeze, equitemperature, and temperature gradient metamorphism (Male, 1980; Flanner & Zender, 2006), and the snow grain size evolution caused by these processes was discussed in Section 2.4.2. The snow metamorphism is, in general, increasingly quicker with increasing temperatures. As observed in Section 4.1, air temperatures are often ranging around -15 to $-20\,^{\circ}C$ in Svalbard. Even though the snow surface is cold, the ground surface has a temperature not far off $0\,^{\circ}C$. Hence, the temperature gradient metamorphism is important for the snow pack in Svalbard. This large temperature gradient can be maintained because of the low thermal conductivity of the snow pack and that the soil in the ground was initially relatively warm and wet (Jones *et al.*, 2001). The shallower the snow pack is, the larger the temperature gradient. There can even be a high temperature gradient between adjacent snow crystals. The saturated water vapour pressure over a flat ice surface goes exponential with the temperature. As a result, a temperature gradient will create a water vapour pressure gradient, which leads to diffusion of water vapour from the lower cold snow crystals to the shallower warm crystals. Hence, mass is moved within the snow pack while the non-volatile EC particles stay. Pomeroy & Gray (1995) argue that the density could decrease by $50\,\%$ in the lowest snow layers during a winter in High Arctic conditions. That would double the EC concentration. As the vapour flux will be reduced by a factor of 2 for every $8\,^{\circ}C$ temperature drop (Male, 1980), this mechanism is fastest in the lowest snow layers. Depth hoar crystals will be formed at temperature gradients larger than $0.15\,^{\circ}C$ (Jones *et al.*, 2001), while smaller gradients results in faceted crystals. When liquid water is present in the snow pack, melt-freeze metamorphism is occurring and leading to rapid grain growth. At the time of the field work in February, March, and April 2008, the temperature was well below $0\,^{\circ}C$ and, hence, no melt-freeze metamorphism occurred in that period. Snow metamorphism tends to move the impurities, such as EC particles, from the inner part of the snow grain to the surface (Rosenthal *et al.*, 2007). That will reduce the potential albedo reduction due to the light-absorbing impurities (Chýlek *et al.*, 1983). In Section 2.5.1, an external mixture of snow and EC particles was explained to be less absorptive than an internal/encapsulated mixture. In conclusion, snow metamorphism will increase the EC concentration in the lower part of the snow pack by as much as $100\,\%$ as snow is transported upwards, while the change in mixing will nearly halve the albedo effect. Melting will dramatically increase the EC concentration on the snow surface since the EC particles are not drained out.

Observations of snow types and crystals types were given in Sections 4.5 and 4.6. Depth hoars

were seen in the lowest part of the snow pack in most snow pits indicating temperature gradient metamorphism. The upper layers contain newer snow that is less metamorphosed and typical have rounded grains from equitemperature processes. The ice lenses observed have been formed by melt-freeze metamorphism when there was an abundance of liquid water. The snow samples gathered in August 2008 contained large rounded grains in the order of several millimetres, as is expected after the presence of liquid water throughout the melting season. Elevated EC concentrations were observed in the lower part of highly metamorphosed snow packs and after melting, especially in the snow surface layer.

Parts of the snow pack sublimate during the winter since the vapour pressure is well below saturation except under foggy conditions or during precipitation events. Then, loss of snow will result in a higher EC concentration. As discussed above, water vapour is transported in the snow pack and, in particular, in the snow closest to the ground. This sublimated snow is relocated further up in the snow pack. In addition, the snow pack can be increasing in mass by water vapour movement from the ground to the snow (Pomeroy & Gray, 1995). This process is relatively unknown. Takeuchi *et al.* (1995) measured a sublimation rate of $0.01 - 0.03\,mm/h$ at the snow surface in early June in Ny-Ålesund. The rate will be lower in winter due to lower temperatures. Jaedicke (2001) calculated the sublimation rate at the snow surface in Adventdalen for a period from January to May in 2000, and it was about $0.01\,mm/h$. For a six month period, from the first snow cover to the time of the field work, about $52\,mm$ water equivalent is, then, sublimated from the snow pack. That would reduce the snow pack in Adventdalen by about $25\,\%$, and, thus, sublimation increases the EC concentration significantly in dry areas.

As reviewed by Male (1980), very light dry snow can start drifting when the wind speed at $10\,m$ height is only $1.9\,m/s$. For wind-hardened snow, the limit is $10.5\,m/s$. This variability is governed by the cohesive forces of ice bonds between snow crystals in the very top of the snow pack (Jaedicke, 2001). From the time of snow on the ground on September 26th 2007 to June 1st 2008, the wind speed was above $1.9\,m/s$ for $87.2\,\%$ of the time and $9.0\,\%$ of the time for $10.5\,m/s$ at Svalbard Airport. At Ny-Ålesund the numbers were $73.0\,\%$ and $8.5\,\%$, respectively, while in Svea $72.8\,\%$ and 10.7, respectively. That is in accordance to what observed by Forsström (2008). The average wind speeds at Longyearbyen Airport, Ny-Ålesund, and Svea are $5.9\,m/s$, $4.9\,m/s$, and $5.3\,m/s$, respectively. A study by Jaedicke (2001) found similar numbers in Adventdalen during the winter of 2000 with an average wind speed of $5.2\,m/s$. He also observed the dominating wind direction to be from southeast. The wind came from that direction during about $80\,\%$ of the time, which corresponds well to the $60\,\%$ seen at Svalbard Airport during the winter 2007/08. Snow drifting is observed at approximately $15\,\%$ of the weather observations at Svalbard Airport (Førland *et al.*, 1997a). Pomeroy & Gray (1995) stated that the sublimation rate in blowing snow will increase exponentially with wind speed. From the work by Jaedicke (2001), we can find the total sublimation rate for blowing snow and from the snow surface to be $0.046\,mm/h$ in Adventdalen during winter. This corresponds to a loss of snow equal to $197\,mm$ water equivalent or about $53\,cm$ of snow cover for a six months period. That is significant since this loss is in the same order as the annual measured precipitation at Svalbard Airport (Førland *et al.*, 1997a). An estimate of the snow pack thickness including this sublimation estimate is given in Table 5.1. In Ny-Ålesund, almost half the snow pack would sublimate. Pomeroy & Gray (1995) show that the sublimation rate at Regina in Canada is $41\,\%$ of the total snow pack, and the winter climate is there similar to what found in Svalbard. At that location, $10\,\%$ of the snow have been through saltation and $26\,\%$ suspension. All this has the possibility of alter the EC concentration in the snow pack. The snow drift leads to a loss of mass to the open fjords and oceans surrounding Svalbard. Jaedicke (2002) observed that about $0.2\,\%$ of the annual precipitation is lost from Adventdalen, while the value for entire Spitsbergen is seen less than $1.1\,\%$. Hence, the loss of snow to fjords is in this thesis neglected.

The snow drift can redistribute the precipitation unevenly. By modeling, Jaedicke & Sandvik (2001) showed that additional snow mass from snow drift is needed for the survival of several glaciers in Nordenskiöld Land. They estimated that the accumulation could be about $10\,cm$ of water equivalent snow during a winter, which is in accordance with Bringedal (2004). The measurements taken on Longyearbreen are affected by this wind induced snow accumulation. Hence, to set the precipitation at a spot as a function of snow depth is not straightforward. Wind drift will redistribute the snow. The wind will increase the sublimation rendering a reduction of the snow pack by about $50\,\%$ in the areas sampled and even by a greater share in the driest areas. Since the EC particles are not lost, this results in a doubling of the EC concentration.

Wind pumping (see Jones *et al.* (2001) and Flanner & Zender (2006)) could also alter the EC concentration. Winds can introduce cyclic movement between the atmosphere and the snow pack. As EC-containing air is filtered through the snow pack, an increase in the EC concentration is likely in the snow. One could also theoretically think that pockets of EC-enriched snow is somehow removed and, thus, leading to a decreasing EC concentration. Temperature gradients as those discussed above can lead to thermal convection inside the snow pack. That could be a part of this cyclic air movement. Estimates of how this wind pumping alters EC concentration do not exist, and this effect is here assumed to be insignificant.

The wind will lead to abrasion of rocks by the snow drift (Seppälä, 2004). Samuelsson (1921) was the first to propose this abrasive ability of snow and ice particles. Abrasion is mechanical wearing and grinding of rock surfaces due to friction and impact of colliding particles, here wind-transported snow and ice grains. Seppälä (2004) explains that cold ice can be as hard as glass, and that the hardness of drifting snow increases as the temperature falls. However, snow abrasion has been observed at temperatures as high as $-2.5\,^oC$. Cavities in rocks have been measured to grow at a rate of up to $1.5\,mm/year$. Such faceted, fluted, and grooved surface have been observed on rocks in Svalbard (Åkerman, 1980). Since the vegetation is sparse in Svalbard, the surface is easily exposed to this abrasion process. Hence, this is a local source of dust and possibly a source of light-absorbing particles (e.g. coal dust) from the local geology in Svalbard. In an experiment at Cape Linné on the west coast of Spitsbergen, Åkerman (1980) observed that the wind abrasion takes place mainly from January to April due to low temperatures and strong winds. Aeolian sediments were found in the snow pack in November and December as well; however, no significant abrasion was measured during those months. Abrasion will increase the dust amount in snow; however, there exist no study of how this may alter the EC concentration. This will be discussed in Section 5.3.2, which concludes that this effect is minimal.

During melting events, melt water will percolate the snow pack. Jones *et al.* (2001) describe how melt water will leach solute species. Hence, ions will be concentrated in the melt water. EC particles can partly be assumed to behave similarly. When refreezing occurs, the snow most affected by the melt will form ice slabs. Ice lenses will be formed where excessive amounts of melt water are trapped in the snow pack. These ice lenses could be spots with elevated EC concentrations. In this work, EC concentrations were typically higher in depth hoar and ice lenses (Section 4.5). Those were found in the lowest layers. They were affected by several melt events with rain (see Section 4.1). Several snow samples from ice slabs formed after the rain event on the 1st and 2nd of January 2008 had elevated EC concentrations. The higher EC concentration observed is, thus, following the argument above.

On the other side, EC particles tend to stay in the snow pack during melting. The removal of EC described above can only happen by thoroughly flushing. The EC particles stay in contact with the snow crystals similar to the way contaminants was sticking to the laboratory equipment during melting and filtering of the snow samples. Then, there will be an increase in the EC concentration as the snow pack melts away. As the top layer of the snow pack melts, an increase in the EC concentration

is in particular seen in the snow surface. On Longyearbreen, the EC concentration of the surface layer increased by a factor of 18 from April to August. In April, the EC amount in the snow pack was $9.07\,mg/m^2$ if we assume a snow density of $\rho = 0.371\,g/cm^3$ (Winther *et al.*, 1998). The snow pack was in August soaked with water, and, thus, much denser. With an assumed density of $\rho = 0.5\,g/cm^3$, the EC amount in the snow pack was about $8.79\,mg/m^2$. In addition to the remaining snow pack of $14\,cm$, there is superimposed ice formed from the last winter's snow. This layer is typically 10 to $20\,cm$ thick. Hagen & Liestøl (1990) observed such thicknesses on the glaciers Brøggerbreen and Lovénbreen close to Ny-Ålesund. Superimposed ice $10\,cm$ in thickness with density $\rho = 0.9\,g/cm^3$ and an EC concentration similar to the lower part of the snow pack will increase the total EC amount to $15.15\,mg/m^2$. Thus, about the same amount of EC is found in the snow pack. If the superimposed ice is included, the estimate indicate an increase in the EC burden by about $67\,\%$ from April to August. Local pollution, especially heavy snowmobile traffic on Longyearbreen, and additional snow fall would have increased the total EC amount. EC from rain will also add to the EC burden in the snow pack. On the other side, the summer snow density estimate is on the lower side. Hence, most of the EC particles stay in the snow pack during the snow melt. Thus, snow melting will increase the EC concentration, and in particular in the surface layer. This results in a significant increase of the albedo reduction. Snow melt will lead to very quick snow metamorphism and snow grain growth. From Section 4.9, the albedo sensitivity of EC is greater for old melting snow than for new snow. That will further enlarge the radiation perturbation from the EC in the snow pack.

5.2 Estimate of amount of EC in Svalbard snow

5.2.1 Long-range transported EC

There are a range of different EC sources found globally and a large variability in transportation to Svalbard. Forsström *et al.* (Submitted) found a median value of $4.1\,\mu g/l$ which represents the entire archipelago fairly well, and that value is used in the calculations here of the long-range source. Further, the total mass of snow fall over Svalbard has to be estimated to find the total EC burden. The typical snow pack depth was in Section 5.1.1 found to be $957\,mm$ water equivalent. As Svalbard covers about $61000\,km^2$ of land, the total EC deposition through a winter is approximately $240\,tons$. That is $0.03\,‰$ of the annual global production of EC estimated by Bond *et al.* (2004). If the mean value of $8.7\,\mu g/l$ calculated by Forsström *et al.* (Submitted) is used, the estimated EC loading is $509\,tons$. That study concludes that the mean values describe the general EC concentration best. Thus, the best estimate is that $240\,tons$ of long-range transported EC accumulates during the winter in Svalbard.

5.2.2 Locally produced anthropogenic EC

The locally produced EC in the snow pack will be calculated using two different methods. First, the emissions from the amount of fuel consumed will be estimated. Due to wet and dry deposition, most of the emissions will be distributed in the surroundings, and in this case mostly in the snow pack. The second way to estimate this is to use the measured EC concentrations in the snow pack as typical values for the surrounding areas.

Calculated from emission estimates

As discussed by Bond *et al.* (2004), calculating EC produced from combustion is not straightforward. One cannot use a ratio of fuel and air at the time of combustion to estimate EC. The EC values are governed by kinetics, not equilibrium states; thus, by small-scale mixing and not average composition. Another difficulty is that every car, snowmobile, and combustion engine is different. There tend to be a few cars and other vehicles or engines, typically old, that emit much more EC per each unit fuel than others. Those "super emitters" can be responsible for a large share of the total emission. Here, the values given by Bond *et al.* (2004) will be used in the estimate of local produced EC in Svalbard. They state in their study that the total uncertainty expected is about a factor of 2. The total EC emission from Svalbard is

$$Em = \sum_k \sum_l \sum_m FC_{k,l,m}[\sum_n EF_{k,l,m,n} X_{k,l,m,n}] \tag{5.1}$$

where the subscripts k,l,m, and n stands for settlement, sector, fuel type, and fuel/technology combination, respectively. Further, Em is the emissions, while EF is the emission factor given by Equation 5.2 and X is the fraction of fuel for a certain sector consumed by a specific technology. The emission factor can be calculated from this formula

$$EF_{EC} = EF_{PM} F_{1.0} F_{EC} F_{cont} \tag{5.2}$$

EF_{PM} is the bulk particulate emission factor given in g/kg. Moreover, $F_{1.0}$ is the fraction of the emitting particles with a diameter of less than $1.0\,\mu m$, F_{EC} the amount of the particles that are EC, and F_{cont} the amount that is not removed by cleansing. Since none of the diesel power plants in Svalbard have cleansing, this value is set to $F_{cont} = 1.0$. The coal power plant in Longyearbyen has cleansing, and a value of $F_{cont} = 0.05$ is assumed. In the calculations, it is assumed that the values estimated by Bond *et al.* (2004) for BC particles can be used for EC particles. Further, the values found in Table 5, 7, and 8 in Bond *et al.* (2004) are used, and a technology division identical to North America (seen in Table 8) is used to represent Svalbard. Svalbard certainly differs from North America; however, the values for North America are used since no better assessment exists. The calculated EC emissions from Longyearbyen, Ny-Ålesund, and Svea are given in Table 5.2. The emissions are calculated from the time of the first snow fall (around October 1st 2007) to the approximate time of the snow sampling (around April 1st 2008). The emissions will be spread and scavenged. If we assume that all the EC ends up in the snow pack after some time, we can compare the local pollution estimates with the EC concentration found in the snow nearby to the three settlements in question.

The largest sources in the settlements investigated are the power plants running on diesel in the settlements. In general, the diesel off-road components do also contribute significantly. The off-road component is much larger than the on-road because $75\,\%$ of the diesel goes to off-road and the emission factor is much larger. Bond *et al.* (2004) explained the higher emission factor by fewer regulations and higher fuel sulfur content for off-road vehicles than on-road vehicles. Most of the EC pollution is caused by diesel consumption. The coal power plant in Longyearbyen have a smaller, but still a significant effect. Snowmobiles contributes less, but are more important than other vehicles running on gasoline. Svea is the largest EC source of about $5.4\,tons$, Longyearbyen a bit smaller with $3.9\,tons$, and Ny-Ålesund has the least EC emissions ($2.2\,tons$).

Kallenborn *et al.* (2009) have conducted a pollution inventory for Svalbard on behalf of the Norwegian Pollution Control Authority (SFT). The assumptions in the report vary some from those used here; however, the emission estimates are somewhat similar. All emissions within the area defined as Svalbard, also vast ocean areas and emissions from transport from Tromsø to Svalbard, is included in

Table 5.2: Estimates of the local EC sources in Longyearbyen, Ny-Ålesund, and Svea are here given as calculated from emission estimates and EC concentrations measured in the snow pack. All values are shown as $10^{-3}\,tons$ of EC. The first estimate is divided into different sources as according to Bond *et al.* (2004) and the data given in section 2.6.2. The calculations are based on Equation 5.1. For Ny-Ålesund and Svea, the numbers for the transport sector have been calculated as a scaling to Longyearbyen according to the number of registered vehicles. All values are given in kg EC produced in the period 1st of October 2007 to 1st of April 2008. The category "diesel, off-road' is assumed to be 75 % of the total diesel consumption as specified by Bond *et al.* (2004) and includes ships and industry. As a educational guess, 60 % of the snowmobiles are thought to have a two-stroke combustion engine, while 40 % have a four-stroke, as other types of vehicles do. The share of snowmobiles having a four-stroke engine is increasing by every winter. These two types of snowmobiles are assumed to be driven similarly, and a consumption of $0.25\,l/km$ for two-stroke and $0.16\,l/km$ for four-stroke is used (K. Johansen, personal communication). Since no information about the power plant in Svea has been found, the consumption of diesel is a scaling to Ny-Ålesund in regards of number of vehicles. That might be an underestimate because the highly active mining activities in Svea would probably need much more electricity than the research stations in Ny-Ålesund. In the second estimate, the Thiessen method is used (Boots, 1980). Every snow pit is assumed to represent the area halfway to the next snow pit. The snow density was set to $\rho = 0.371\,g/cm^3$ (Winther *et al.*, 1998).

Sector Unit	Longyearbyen [$\cdot 10^{-3}$ t]	Ny-Ålesund [$\cdot 10^{-3}$ t]	Svea [$\cdot 10^{-3}$ t]
Coal power plant	209.0	-	-
Diesel power plant	1108.0	2133.9	5071.2
Diesel, on-road	226.6	10.3	26.8
Diesel, off-road	2185.9	99.4	258.3
Gasoline, vehicles	25.7	0.6	3.5
Gasoline, snowmobiles	182.6	3.8	1.8
Total	**3937.8**	**2247.9**	**5361.6**
From EC measurements in snow	4004	0	1453

the inventory estimate. Thus, aviation and shipping have been encompassed in contradiction to this thesis' calculations. The report estimates an annual EC emission from all local sources of $79\,tons$ in 2007 for entire Svalbard. That is nearly a doubling from 2001. The largest relative increase in any pollution type was seen for particulate matter in this very time period. A further increase is anticipated. The estimate is more than a factor 3 higher the one presented in this section. That is mainly due to that this thesis' estimate did include neither Barentsburg nor shipping. Shipping stands for the major share of the total EC emissions. Energy production and vehicles both consuming diesel were also important contributors. This estimate is much higher than the given in this thesis; however, a smaller relative portion of the emissions will be deposited in snow and ice in Svalbard because a larger portion of the emissions happens offshore. Since the ships spend considerable time in the fjords in Svalbard, some of these emissions will be settling onto the nearby snow packs. Hence, the local EC sources in Svalbard are not only restrained to its settlements.

In Longyearbyen and Svea, coal mining is still ongoing. Thus, coal particles and coal dust are also polluting the local environment around the coal mines, open coal piles, and transport pathways. An estimate of the EC source from these operations has not been assessed in this thesis. Myhr (2003) found $54.1\,tons$ of coal dust lost from the coal pile on Cape Amsterdam rendered by snow samples in only the most affected areas.

Calculated from measured EC concentrations in the snow pack

In calculating the total amount of EC found in the snow pack, the assumption is that the snow depth and EC concentration of every snow pit represent the surrounding area and halfway to the next pit (the Thiessen method as described by Boots (1980)). A mean snow density of $\rho = 0.371\,g/cm^3$ was used (Winther *et al.*, 1998). In addition to the background EC, about $4.0\,tons$ of EC was estimated to origin

from Longyearbyen and $1.5\,tons$ from Svea (see Table 5.2). Since no elevated EC concentrations were observed around Ny-Ålesund, the estimated EC source from the settlement is set to zero.

Comparison of methods

With the exception of Ny-Ålesund, the estimates for the two methods are in the same order of magnitude. The two methods show almost the same number for Longyearbyen, while the emission estimate is clearly the largest for Svea. The discrepancy for Svea occurred since snow samples were not gathered in the most polluted areas. Due to safety precautions, no snow samples were taken on the sea ice. Parts of the sea ice on van Mijenfjorden were visibly clearly discoloured. We must remember that the fuel consumption estimate disregards sources of coal dust, and is, therefore, a lower limit. This coal dust is locally a large EC source since the extreme spiking in EC around Longyearbyen Airport can only be explained by this coal dust. Coal mining ceased in Ny-Ålesund in 1963 (Arlov, 2003), and little coal dust is available for wind transport. The first described method give the magnitude of emissions to the atmosphere, while the second method show the EC content in snow. Not all the EC emitted will contaminate the snow. Some will be transported away and some will deposit over open water. However, the two methods match fairly well, and a relation between EC emissions and EC in snow is observed.

5.3 Aeolian dust in the snow

5.3.1 Dust from long-range transported sources

By using the numbers given in Section 5.2.1, the annual accumulation of EC from long-range transported sources is calculated to approximately $3.9\,mg/m^2$. In comparison, the long-range transported flux of mineral aerosols to the Svalbard area has been modeled to be a factor 25 larger at about $0.1\,g/m^2yr$ (Harrison *et al.*, 2001). Andersen & Genthon (1996) state that this deposition of mineral dust was up to 200 times greater during the last glaciation, which resulted in a significant flux. The same study modeled a peak in transportation during spring, summer, and autumn, which partially can be explained by the Arctic Haze (Shaw, 1995) in spring and by local sources.

5.3.2 Dust from local sources

The local source of Aeolian sediments is much larger than the long-range transported source. Newly exposed surficial deposits from former glaciated areas and little vegetation result in significant wind erosion (Seppälä, 2004). Any degraded material will come in a range of particle sizes. Sand grains as large as $2\,mm$ will be deposited close to its source, will dust ($< 0.1\,mm$) can be suspended in the atmosphere and transported much farther. The author of this thesis sees discoloured snow around rocky outcrops whenever he is out in the Svalbard nature. A study in British Columbia, Canada, observed a local rate of dust deposition of $11\,g/m^2yr$ in terrain and climate similar to Svalbard (Owens & Slaymaker, 1997). That is a factor of about 110 larger than the long-range transported source. This particular study indicated that others have measured typically in the range between < 10 and about $200\,g/m^2$. A study by Czeppe (1966) at Hornsund, on the southern tip of Spitsbergen, found an Aeolian deposition of $100\,g/m^2$ during the four winter months and about 300-400 g/m^2 for a year. A rather extensive study at Cape Linné, on the west coast of Spitsbergen, found the Aeolian deposition in snow to equal $270\,g/m^2yr$ (Åkerman, 1980). The precipitation during the sampling period was

$400.8\,mm/yr$, which is a bit lower than the normal of $480\,mm/yr$ (Førland *et al.*, 1997a). The author states that the dust deposition might be overestimated since the snow samples were exclusively taken from snow patches, which tend to accumulate sediment particles. Moreover, a snow density of $0.6\,g/cm^3$ is used. Old melting snow is likely to have a lower density, typically around $0.4\,g/cm^3$ (Wiscombe & Warren, 1980). Hence, $270\,g/m^2yr$ in dust deposition might be an overestimate. Due to the strong winds (see Section 5.1.2) and lose sedimentary rocks found in Svalbard, the $11\,g/m^2yr$ measured in British Columbia can be seen as a conservative lower limit in Svalbard. The lithology around Longyearbyen consists mainly of horizontally oriented sedimentary rocks, such as shale, siltstone, and sandstone (Hjelle, 1993). Further, the bedrock is relatively soft, fine-grained, and easily eroded by mechanical weathering. Åkerman (1980) observed that the wind abrasion was negligible during summer compared to winter, as explained in Section 5.1.2. The abrasion is mostly active from January through April, but the sediments are found throughout the snow pack due to its abundance. In this thesis, dust was found in all snow layers with a maximum in the lowest part. That particular snow came most likely in late September and October. Snow and Aeolian sediments are then in a mixture termed niveo-aeolian (Seppälä, 2004). That is in accordance with Dijkmans (1990) that found niveo-aeolian sedimentation to be most dominant in shallow snow packs. In conclusion, the local source of dust in Svalbard is conservatively estimated to approximately $11\,g/m^2yr$; however, much higher values are seen locally. The dust concentration in snow is at its highest in the lowest part of the snow pack and near any rocky outcrops.

Wind erosion and transport of dust is in particular significant in arid and semi-arid areas such as Adventdalen. Fine-grained soil deposits above the river bed in the lower part of Adventdalen can only be described in terms of Aeolian deposition (Bryant, 1982). The same study observed active Aeolian transport in the area. A seasonal dust storm is seen every fall in Adventdalen (Landvik, 1998). Such events are present once the ground has frozen, but not yet covered by snow, as shown in Figures 5.2(a) and 5.2(b). As a result, Aeolian sediments were seen in the snowpack, especially in the lowest layers. To sample snow with a minimum of this dust in Adventdalen proved to be a challenge. A satellite photo (Figure 5.3(a)) shows that large quantities of sand are present in the top snow layer in Adventdalen even by the end of the winter season. A similar brownish discolouring is not seen around Capp Linné on the west coast of Spitsbergen, were an annual dust deposition of $270\,g/m^2$ was measured. Most of the snow samples gathered from Adventdalen showed indications of sediments in the analysis. Thus, the high value of $270\,g/m^2yr$ in dust deposition found at Cape Linné is realistic for Adventdalen.

All the three settlements, Longyearbyen, Ny-Ålesund, and Svea, are or have been coal mining sites. The major coal horizons could be a source of EC as the rocks weather. These are found in the Tertiary rock formations, the yellow areas in Figure 5.4. In addition, the mudstone in those Tertiary rocks contain high concentrations of EC (Bøggild *et al.*, 2007). Further, the Jurassic, Cretaceous, and Triassic rocks on Edgeøya, Barentsøya and the east coast of Spitsbergen contain grey and dark shale (A. Braathen, personal communication). While the coal horizons are typical only $1\,m$ thick, the shale and mudstone layers can be tens of meters thick. Thus, the shale and mudstone are greater sources of EC than the coal horizons. Due to highly variable topography with steep hill sides, little precipitation (see Section 5.1.1), and strong winds (see Section 5.1.2), such rocks are exposed most of the year. Weathered grains from those EC contaminated rocks are most likely coarse and deposited in the nearby surroundings. If we assume an extreme case where an area with only dark shale and mudstone with an EC concentration of approximately $20\,\%$ (Bøggild *et al.*, 2007) that weathers with a dust deposition of $11\,g/m^2yr$ (Owens & Slaymaker, 1997) and a typical snow depth of $957\,mm$ (Winther *et al.*, 1998) water equivalent, the potential EC concentration can be estimated to about $2300\,\mu g/l$. That is a maximum value since a mix of different rocks, typically observed in nature, will

(a) View from Nybyen (b) View from Adventdalen

Figure 5.2: (a) A sand storm sweeps over Adventfjorden on the 12th of October 2008 as sediments are made airborne in Adventdalen during strong south-easterly winds. The mountain in the back, Hiorthfjellet, is blurred out in this photo due to large quantities of airborne sediments. The atmosphere over Svalbard is rarely hazy due to cold and dry air, as well as its remoteness from long-range transported pollution sources. About one hour after this picture was taken, the maximum wind speed was recorded to be $7.1\,m/s$ and the maximum gust to be $8.7\,m/s$ at Svalbard Lufthavn/Airport. Such events are typical once the ground has frozen, but is still not covered by snow. (b): A similar sand storm seen from the old Aurora Station in Adventdalen on October 8th 2008. Airborne sediments are clearly seen as a brownish layer just above the surface of Adventdalen. The typical depth of such a dust layer is $1\,m$ (Seppälä, 2004). The maximum wind speed that day was $6.1\,m/s$ and the maximum wind gust $7.1\,m/s$. Photo by Carl Egede Bøggild.

result in lower concentrations. Thus, the local effect can be significant. That has not been assessed in the literature and can, hence, not be verified. Local contamination by such rocks did not influence the measurements of the samples used in this thesis. Therefore, the source of EC from rocks is here seen as negligible.

5.4 Processes affecting $\delta^{18}O$ in snow

The observed covariance between EC and $\delta^{18}O$ could either be explained by an actual covariance from the source point of EC and $\delta^{18}O$, or could be due to natural processes in the snow pack affecting both EC and $\delta^{18}O$. An overview of different processes relating $\delta^{18}O$ in the snow pack is given here and further discussed in Section 6.4.

In ice core studies (for instance in Isaksson *et al.* (2003, 2005)), $\delta^{18}O$ is used to tell the climate of the past. Hence, this variable should reflect the actual weather. Bradley (1985) states that $\delta^{18}O$ values in precipitation, in general, show geographical variations that reflect variability in temperature. As the heavy isotopes in water are more likely to be lost than lighter ones on the way to higher latitudes, a latitudinal gradient is seen in the $\delta^{18}O$. The same process of losing heavy isotopes is seen when distance from moisture source and elevation is considered.

When snowmelt and percolation occur, differences in the isotopic ratios are smoothed out due to isotopic exchanges as the snow and ice refreezes (Bradley, 1985; Koerner, 1997). As observed from stratigraphy and weather data analysis, snowmelt and percolation through the snow pack did occur. The isotopic ratio is, thus, expected to be averaged. In addition, rain events, especially the one happening on the 1st and 2nd of January 2008, added liquid with a potentially different isotope ratio. When cold weather came after this warm spell, some of that rain water refroze with the original snow pack. This could change the isotopic ratio signature of a snow layer, and Koerner (1997) states that in this example, the isotopic ratio temperature will increase. The lowest layer in the snow pack has probably its isotopic ratio temperature biased to the warmer. However, studies have shown that

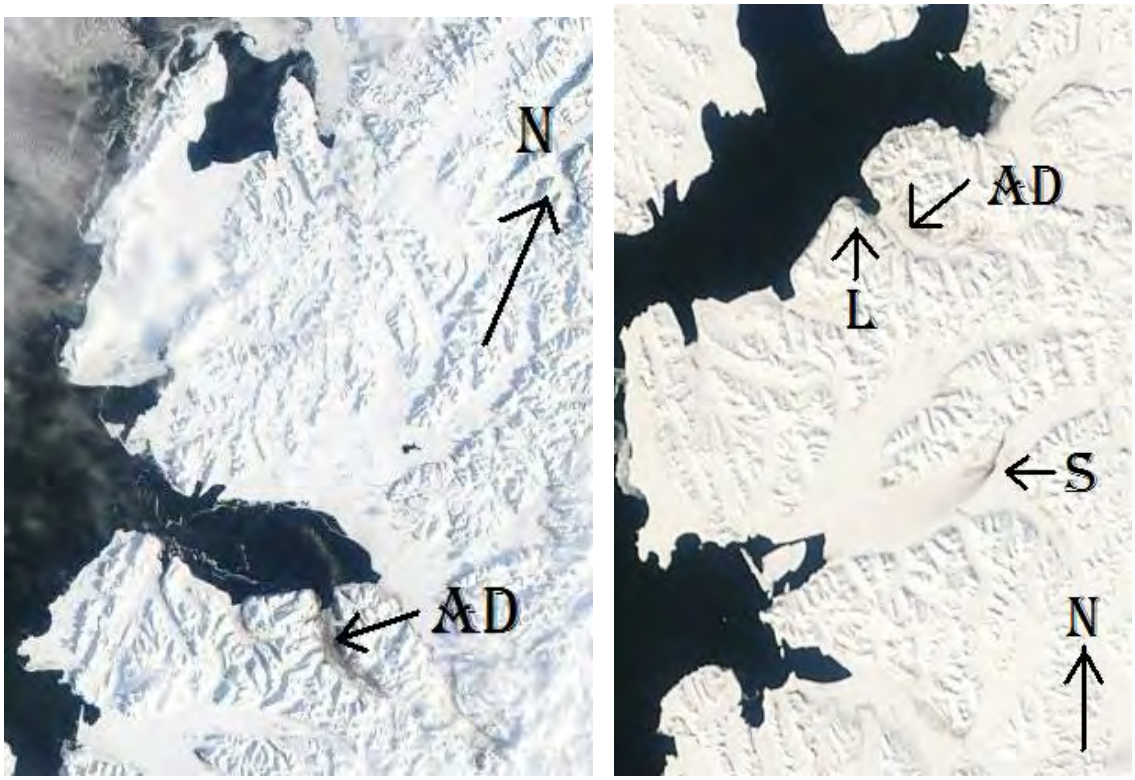

(a) View from Nybyen (b) View from Adventdalen

Figure 5.3: (a): A satellite image of parts of Spitsbergen on May 18th 2004. North on the image is shown with the N arrow. The open water in the lower part of the photo is Isfjorden. Adventdalen (AD in the image) is seen as the grey area under Isfjorden. Longyearbyen is situated where Adventdalen and Isfjorden meets each other. Source: MODIS (http://modis.gsfc.nasa.gov/) (b): Another satellite image of Central Spitsbergen from MODIS Terra taken on May 19th 2008. North is upwards in the image (see N arrow). The other arrows show Adventdalen (AD), Longyearbyen (L), and Svea (S). The dark area in the upper part of the photo is Isfjorden. On the right side of the image (at arrow S), a black fan can be observed. That is the fan of coal dust that is blown downwind from the coal pile on Cape Amsterdam. The road between the mine in Svea and this coal pile is the black line to the northeast of the fan. Mine 7 can vaguely be seen as a dark spot outside of Longyearbyen. The road between the mine and Longyearbyen is clearly visible in the upper part of the image, on the southern shoreline of Isfjorden (near arrow AD). The area around Svalbard Airport is also very dark (arrow L). At that time, there was only partly snow cover around Svalbard Airport while most of Svalbard was covered in deep snow. Source: MODIS (Retrieved May 25th 2009 from http://rapidfire.sci.gsfc.nasa.gov/subsets/?subset=AERONET_Hornsund.2008140.terra.250m.jpg)

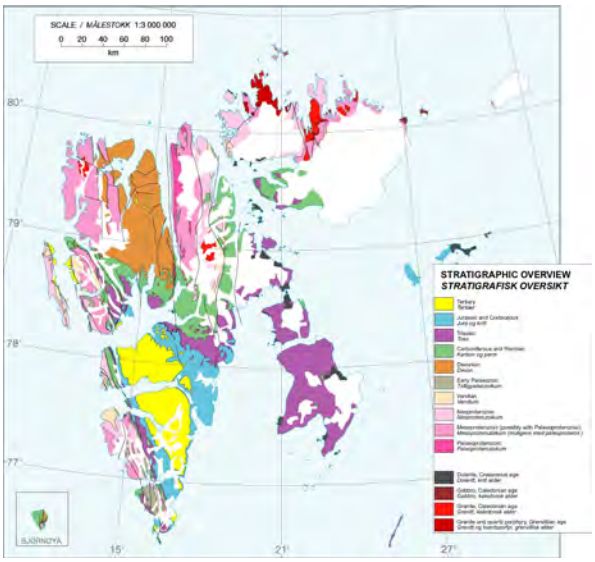

Figure 5.4: A geological map of Svalbard. The coal layers are mostly found in the yellow areas, which are Tertiary rock formations. Dark and grey shale is found in the blue and purple areas, dominantly found in south-eastern Svalbard. Map source: Norwegian Polar Institute.

annual signals are partly preserved in ice cores from glaciers that are affected by melting in Svalbard (Isaksson *et al.*, 2003; Pohjola *et al.*, 2002). Hence, some of the isotopic ratio variations in the snow samples investigated in this thesis should be conserved.

Bringedal (2004) stated that the heavy wind drift seen in Svalbard can change the initial isotopic ratio. Further, water vapour is transported in the snow pack due to a large temperature gradient between the ground and snow surface (see Section 5.1.2). Typically, the temperature at the ground can be slightly below zero, while it is $-20\,^{\circ}C$ at the surface temperature. This will bias the isotope ratio as time goes. Due to different vapour pressures, the lighter isotope $H_2\,^{16}O$ is more likely to vaporize than the heavier $H_2\,^{18}O$. This leads to relatively more $H_2\,^{18}O$ than $H_2\,^{16}O$ and an increase in the isotopic temperature. Evaporation of snow affecting the isotopic ratio is concluded by Bringedal (2004) to be a negligible process in nature.

(Igarashi *et al.*, 2001) found no clear seasonal variety in $\delta^{18}O$ in Ny-Ålesund; however, a complex and highly varying pattern was observed. This pattern is linked to atmospheric circulation pattern. Then, variations in $\delta^{18}O$ can be correlated weakly with temperature and correlated nicely with source region and temperature of the source regions. A study of precipitation in Longyearbyen and snow from Longyearbreen by Bringedal (2004) confirmed this. She found a weak $\delta^{18}O$-temperature relationship. The controlling factor for $\delta^{18}O$ was the source area of the precipitation. The precipitation samples in Longyearbyen varied between $-3.54\,‰$ and $-35.21\,‰$. (Igarashi *et al.*, 2001) found a similar variation in Ny-Ålesund between $-4.7\,‰$ and $-23.6\,‰$. These variations are smoothed out by post-depositional processes. Snow samples from snow pits on Longyearbreen varied less with values between $-7.13\,‰$ and $-18.85\,‰$ (Bringedal, 2004). A study from Midtre Lovénbreen shows also large variation for $\delta^{18}O$ between individual snow fall events, and that the signals are averaged out as time goes, but not lost entirely (Glasser & Hambrey, 2002). As a result, different snow types rendered from different post-depositional processes will give varying $\delta^{18}O$ values. In conclusion, there is a clear relationship between the source of the water vapour and the $\delta^{18}O$ parameter in snow. This relationship is partly lost in post-depositional processes in the snow. Based on this, the link between $\delta^{18}O$ values and EC concentrations is discussed in Section 6.4.

Chapter 6

Discussion

6.1 Snow albedo effects due to EC

In Section 4.9, the albedo effect of local EC pollution was compared to long-range transported EC. There is some uncertainty in what areas that are affected. The low estimate includes only areas that are found to be polluted. Unfortunately, very few measurements have been done in the surroundings mountains of the settlements. In the high estimate, some EC pollution in those mountains is added. The potential effect will also vary from year to year with changing sea ice conditions. This is particular important for pollution from Longyearbyen. Longyearbyen has a bigger impact than Svea if there is plenty of sea ice, while the impact is much smaller if there is little sea ice. van Mijenfjorden freezes over every winter; thus, changing sea ice conditions does not affect the estimate for Svea. During the winter 2007-08, Isfjorden and Adventfjorden did not freeze over except some minor icing in April 2008. Normally, the fjord is more or less ice covered. The current ice free conditions is due the intrusion of warm Atlantic water into the fjord during the winter 2005-06 (Cottier *et al.*, 2007) and not an effect of global warming (Forster *et al.*, 2007). There is natural variability in the climate, for instance on a decadal timescale (Keenlyside *et al.*, 2008). Then, the next winters might be colder, and, thus, sea ice is believed to return to the fjord system in the winters to come. Similarly, Kongsfjorden was at the time of the field work ice free; however, that has normally not been the case (Gerland & Renner, 2007). Since the plume from the power plant in Ny-Ålesund often goes out in the fjord, elevated EC concentrations might be detectable out on the sea ice. Thus, there might be a measurable impact of EC in snow by pollution from Ny-Ålesund. Snow covered sea ice was observed during short periods in March, April and May 2009 on Isfjorden. Kongsfjorden was also covered by heavy sea ice in the same period. Thus, the albedo effect of locally produced EC was larger in April 2009 than in April 2008, and the albedo effect could become larger in the coming years.

This estimate of the albedo effect is sensitive to the EC background level assumed. The study by Forsström *et al.* (Submitted) claims that the median level in their data set represents the EC concentration in snow better than the mean level. Hence, the median level has been used in this thesis ($4.1\,\mu g/l$). If the mean EC concentration is used ($8.7\,\mu g/l$), the relative significance of the local pollution will be halved. The background level of EC is varying, and that has been considered in the calculations. As a result, different background values have been used for Longyearbyen and Svea. The EC background level was generally found to be somewhat higher in measurements, for instance $6.58\,\mu g/l$ around Ny-Ålesund. Thus, the effect of local EC is likely overestimated by the low background level. However, the effect is likely underestimated by not including all likely affected areas in the low estimate as discussed in the previous paragraph. The local effect is modeled to be $12.6\,\%$ of

the long-range effect, and, that is, consequently, a reasonable estimate.

While the background EC level reduces the snow albedo only slightly (0.0011), the highly elevated concentrations observed near the settlements have larger impacts. Figure 5.3(b) is a satellite image of Central Spitsbergen, where extremely elevated EC concentrations are clearly visible. That has a strong impact on surface albedo. A dark fan is seen downwind of the coal pile on Cape Amsterdam outside Svea. The area around Svalbard Airport is significant darker than the surrounding area. At the time, May 19th 2008, the only area that was partly snow free in Svalbard was this specific area. A link between early snow melt and an extreme high EC concentration at this site has been observed by Bøggild *et al.* (2007). The EC concentrations measured on Longyearbreen during late summer will reduce the albedo by 0.05 to 0.09. That is significant and will lead to increased ablation in the summer. Thus, local pollution must be an important factor on the mass balance of Longyearbreen. Further, the extreme high EC concentrations cause a detectable earlier snow melt.

6.2 Depositional and post-depositional processes

In Section 5.1.1, variations in the EC depositions were analyzed. The snow samples were gathered in central and western Spitsbergen, so that the east-west gradient in EC concentration discussed cannot be clearly seen in this data set. However, the EC background level was observed higher around Svea than Longyearbyen and Ny-Ålesund, and this fits with the idea that EC concentrations are higher towards the east. EC is carried to Svalbard on event basis, and in particular in the Arctic Haze season (see Section 2.6.1). Such events were difficult to find in the snow samples because every snow layer sampled consisted of several snow events and post-depositional altered the initial conditions. However, results from the Oslo CTM2 model show that several events occurred during the winter and the Arctic Haze season was at its strongest in March 2008.

The variability in precipitation investigated in Section 5.1.1 was confirmed by snow pack depth measurements. Most of field work was done in dry valleys with thin snow packs, typically less than $60\,cm$. In elevated areas, the snow pack was much thicker. On Longyearbreen, about $500\,m$ a.s.l., the snow depth was almost $2\,m$. Adventdalen is among the driest areas in Svalbard, and the snow pack was shallow here. That will increase the impact of the local EC pollution since there is less snow to mix out the EC. Most of the local pollution is emitted in the dry areas of Svalbard, and the albedo effect of this EC is, hence, amplified.

The post-depositional processes in the snow reviewed in Section 5.1.2 will, in general increase the EC concentration. In total, about a doubling in EC concentration can be anticipated in highly metamorphosed snow. Sublimation of snow is the largest contributor. In snow samples containing thick ice lenses, the EC concentration was elevated by even more. Melt events are the most effective at increasing EC concentrations in snow on an event basis.

At a site on upper Longyearbreen, the EC burden in snow increased from $9.07\,mg/m^2$ in April to $15.15\,mg/m^2$. From the discussion in Section 5.1.2, virtually all EC particles stay during melt conditions. Then, the increase in EC burden in that period is explained by EC contaminated snow and rain, as well as local pollution from Longyearbyen and exhaust from snowmobiles. From snow started to accumulate in September 2007 to August 2008, $34.2\,\%$ of the precipitation occurred between April and August. $40.1\,\%$ of the EC came in the same period. The transport of EC to Svalbard in summer is smaller than in winter (see Section 2.8.1). That reduces the EC source from precipitation during summer. Thus, precipitation and local sources contribute with about the same amount of EC to the EC burden increase from April to August.

6.3 EC in Svalbard snow

First, the estimate of long-range transported EC calculated in Section 5.2.1 is discussed, followed by an analysis of the local produced EC estimate in Section 5.2.2. In this thesis, the measured background EC concentration was in general higher than the value given by Forsström *et al.* (Submitted). Thus, the estimate of $240\,tons$ could be on the lower side. Another uncertainty is the snow accumulation. $957\,mm$ water equivalent converts to a snow thickness of about $258\,cm$. That is much deeper than the $70\,cm$ measured by Bruland *et al.* (2001) in the relative dry area around Ny-Ålesund and the $67\,cm$ measured in this thesis. The field work was executed well before the start of the melt season and, more importantly, mostly in dry (Humlum, 2002) and low-levelled areas. Thus, the average snow depth in Svalbard is more those $67\,cm$, but $258\,cm$ is probably an overestimate. In these estimates, an even distribution of the EC particles in the precipitated snow is assumed. According to section 5.1.1 that is not true, but a fair approximation. The highest EC concentrations are according to Forsström *et al.* (Submitted) found in the areas with the most precipitation, namely the east coast of Svalbard. The average value used will, then, be underestimating the total EC burden. Since about $60\,\%$ of Svalbard is covered by glaciers (Winther *et al.*, 1998) and most of Svalbard is covered by snow during large parts of the year, the rain during summer will contribute in this estimate. The rain brings with it EC in the same manner as snow. While the rain water is drained out or refrozen in the snow pack, the EC particles will stay in the top part of the snow pack. That partly explains the increase EC burden on Longyearbyen observed during the summer months. At Svalbard Airport, $27.9\,\%$ and $26.7\,\%$ of the total precipitation comes as rain and sleet, respectively (Førland & Hanssen-Bauer, 2002). That is a significant source of EC. In total, these errors cancel each other out as they go both ways, and the rendered estimate of $240\,tons$ of EC is, thus, reasonable.

In the rest of this section, the assessment of the local source of EC is discussed. Due to its size, Longyearbyen is a natural candidate as the largest local EC source from combustion. However, the diesel power plant in Svea makes that settlement the largest source. The emissions from that power plant are based on several assumptions; hence, there is a large uncertainty in this calculation. All sources have been treated as point sources in this assessment. While the power plants are point sources, vehicles are not. They move around and pollute a greater area. Due to few roads in Svalbard, snowmobiles are the most mobile transportation units. A snowmobile can be driven from the west coast of Spitsbergen to the east coast in one day; thus, most of Svalbard is accessible by snowmobiles. Elevated EC concentrations in the snow pack are likely seen along all major snowmobile paths and not only in Longyearbyen and the other settlements. Hence, snowmobile trails can pollute an otherwise pristine area. The number and width of these snowmobiles trails made snow sampling a bit difficult around Longyearbyen due to topographic limitations. For instance, Longyearbreen can be seen as one big snowmobile trail in late spring. This trail can even be seen from satellites (Google Earth, retrieved 17. February 2009). Exhaust from these snowmobiles is spread out over a large area. Snowmobiles that are running on a two-stroke combustion engine emits about 23 more than a four-stroke engine. This is a direct result of the intake of fresh air and fuel is simultaneous with the exhaust (Bond *et al.*, 2004). Consequently, Reimann *et al.* (Submitted) found dramatic quantities of VOCs emitted from two-stroke snowmobiles in Longyearbyen. In conclusion, snowmobile traffic emits EC over large areas of Svalbard, and is, thus, important. Combustion of diesel gives large EC emissions, and the diesel power plants are the largest EC emitters in the settlements.

Coal dust is also a source of EC. The extreme spiking seen in EC concentrations is caused by coal dust. The magnitude of this coal dust has not been assessed, but it is large. A large part of the total EC burden found in the snow pack came from coal dust. The coal dust particles are much coarser than the soot particles, which leads to a deposition much closer to the source. That limits the area which is

impacted by the coal dust. Hence, coal dust should be included in EC estimates for Svalbard.

Although more EC was found in the snow around Longyearbyen than Svea, the albedo effect is the largest around Svea. One reason is the nonlinearity between EC concentration and albedo reduction. At high EC concentrations, as those observed in the vicinity of Longyearbyen, a further increase in EC concentration results only in a modest albedo reduction. The second reason is that the snow depth on the sea ice on van Mijenfjorden was assumed to be only $10\,cm$ deep. Then, a certain quantity of EC can cover a larger area with a certain EC concentration. There are large areas in Kjellströmdalen and on van Mijenfjorden that can be contaminated by pollution from Svea. That makes EC emissions from Svea important for the total albedo reduction effect from all local sources. Thus, the impact of EC emissions depends not only on the strength of the source, but also the area accessible for the pollution and the snow depth.

6.4 Covariance between EC and $\delta^{18}O$

As with $\delta^{18}O$, EC in snow depends on its source. However, the EC concentration is also affected by processes after deposition, as discussed in Section 5.1.2. Melt events will remove some of the snow while most of the EC particles remain in the snow pack. Thus, the EC concentration increases. While the snow sampling showed, in general, higher EC concentrations in the lowest part of the snow pack (see Section 4.5), the modeling from Oslo CTM2 indicates the highest EC concentration in snow that precipitated during late winter (see Section 4.7). The discrepancy is a result of the model failing to include the post-depositional processes accurate. In conclusion, post-depositional processes will make the temperature given by the isotopic ratio increase, as well as an increase in EC concentration. That explains the results seen.

On the other side, $\delta^{18}O$ is used as a temperature indicator (e.g. Isaksson *et al.* (2005)), and EC concentration is used to explain the magnitude of pollution (e.g. McConnell *et al.* (2007)). Even though there are post-depositional processes affecting both parameters, there might originally be a connection. We must bear in mind that the sources of EC and the oxygen isotope ratio do not need to be the same. The moisture, which determines the isotope ratio, could have been introduced to the air parcel before pollution sources affected the air parcel, or vice versa. Both soot and water vapour have a relatively short atmospheric lifetime, for EC it is about $7\,days$ (Schulz *et al.*, 2006) and about $10\,days$ for water vapour (Wallace & Hobbs, 2006). Thus, the sources of the soot and water vapour cannot be too distant to each other. A covariance between these parameters is plausible. Such a link between EC and $\delta^{18}O$ cannot be determined by the results found in this thesis.

6.5 Evaluation of field work strategy

The strategy for the field work is discussed in this Section. The most important question to ask is if the sampling covered the trends and variability in EC concentrations that exist in nature. Only a limited number of samples could be gathered. The two important parameters are the distance between the measuring sites and the total length of the transects. Noisy behaviour in EC concentrations is observed around Ny-Ålesund, which shows the spatial resolution is good enough. The transect is also long enough. For the transect around Longyearbyen, the mean EC concentrations show very little noise. The length of the transects could also have been longer. Isfjorden is situated west of Longyearbyen, which makes a longer transect impossible. Only six samples were analyzed from a $55\,km$ long transect around Svea, which is insufficient. The number of samples and density of samples is good for the Ny-Ålesund transect. Thus, a distance of $3\,km$ between points is preferable.

In this study, more snow samples from Svea should have been analyzed at the expenses of the transects around Ny-Ålesund and on Longyearbreen. That would have increased the certainty of the local EC estimate. The transects could have been repeated to give temporal variation; however, that is fairly well covered by sampling the entire snow pack. In conclusion, a distance of $3\,km$ between points is recommended and the transect should preferable go $50\,km$ out from the settlements to observe the local effect.

6.6 Uncertainties and errors

The natural variability of EC concentrations in the snow pack is large. The results from the small scale study show that. The standard deviation for all 20 samples was $35.6\,\%$ of the mean value. This variability is probably natural and exists everywhere. The samples taken around Ny-Ålesund has a higher standard deviation in percentage ($67.8\,\%$), but due to low values this is probably caused by errors in the analysis. The variability was observed for samples that were believed to come from the same precipitation events as well. Post-depositional effects, such as strong winds, can mix snow. Thus, an apparently uniform snow layer can exist of different precipitation events and vary on a scale of centimetres. According to Forsström (2008), the needed number of snow samples to determine the EC concentration for entire Svalbard with a confidence interval of $10\,\mu g/l$, $5\,\mu g/l$, and $1\,\mu g/l$ given a $95\,\%$ confidence level is 36, 142, and 3550 samples, respectively.

During the sampling procedure, there might have been a risk of contamination. Fibres from clothing was found in some of the filters, which may have biased the OC readings positively. Exhaust from the snowmobile can have contaminated the outer clothing, and this clothing could have further contaminated the samples. To avoid this, separate gloves and mittens were used for the driving and the sampling. Preferably overalls and rubber gloves should be worn; however, temperatures around $-20\,^{\circ}C$ throughout the time of the field work made this impracticable. The chance of getting frost bites is imminent when doing field work in the High Arctic.

The snow samples were kept frozen until further analysis to minimize the loss of EC particles. However, Forsström *et al.* (Submitted) showed that melting the samples overnight in glass jars did not cause significant losses of EC. These particles are sticky, and Ogren *et al.* (1983); Clarke & Noone (1985) discussed that these particles are lost to jar walls. Even as the snow is frozen, some particles might be lost to the plastic bag. In the melting and filtering process, more EC particles are lost to glass and plastic surfaces. Hydrophobic particles are especially prone to be lost in the melting and filtering process. To prevent this, the samples were filtered as soon as the snow was melted in the microwave oven. Clarke & Noone (1985) had a similar setup, and they estimated the loss of particles to be about $10\,\%$. We must keep in mind that the speed of the melt water through the filter system is given by the strength of the vacuum pump. For some samples, a hand-held pump was used, while an electronically pump was used at other times. Variations in filtration rates could affect the loss of EC particles in the process.

Another possible source of error is the filtration efficiency. In this work, the same melt water was filtrated twice for one single sample. While the EC concentration was $195.9\,\mu g/l$ for the original run, the second run failed to come over the detection limit. Hence, the filtration through the quartz filters is effective and the results trustful. Ogren *et al.* (1983) determined the filtration efficiency of the quartz filters to be 50-80 %. The numbers are even greater in this thesis, as Forsström (2008) with an identical setup as used here found a better filtration efficiency. In a report by Simonsen (2007), he found out that about $20\,\%$ of the EC particles ran straight through the typical filter (pore size of $0.4\,\mu m$) used in the optical method.

In some samples, large particles clogged the filter. In a few extreme cases, the filtration effectively stopped, and the filtration had to be aborted. This was either caused by an extreme high concentration of coal particles or Aeolian or organic matter. As explained in Section 5.3.2, some snow covered areas had high concentrations of Aeolian sediments in the snow.

6.7 The effect of EC in snow for Svalbard and the Arctic

Jaedicke (2002) points to the fact that Adventdalen is free of snow as soon as the winter season ends in late April or early May, while most of Svalbard will be covered in snow until June. This can partly be explained by little precipitation and heavy snow drift. Adventdalen is also the most polluted area in Svalbard with the highest EC concentrations in the snow. That will lead to an earlier snow melt. The direct link between highly elevated EC concentrations and early snow melt around Longyearbyen has been observed by Bøggild *et al.* (2007). Höganäsbreen is a glacier that is retreating noticeable faster than comparative glaciers. On this specific glacier there is a road that connects Svea with the coal mine, and this is the only road in the world that crosses a glacier. Aeolian sediment from the road, as well as coal dust lost during trucking the coal, is believed to be the reason for this elevated melting. In addition, water with high EC content is flushed from the mine and onto the glacier. Thus, EC has a local effect near local sources in Svalbard.

From Section 4.9, the effect from local EC sources was estimated to be responsible for about $11.2\,\%$ of the total albedo reduction seen from all EC in Svalbard snow. That is a low conservative estimate, and, hence, the local effect might even be as large as $20\,\%$ of the total. Svalbard is a tiny archipelago compared to the entire Arctic. While the land areas of Svalbard covers about $61000\,km^2$, the Arctic Ocean is $14056000\,km^2$ large. Thus, the Arctic Ocean is about 230 times bigger than Svalbard. In the Arctic Ocean, there is no pollution except from any shipping or aviation. Then, the albedo effect from the local sources in Svalbard is minimal for the entire Arctic. We can consider the entire Arctic ocean full of snow covered sea ice and the EC background level of Svalbard ($4.1\,\mu g/l$) to be valid for the entire area. If that is true, the local EC sources in Svalbard are responsible of $0.5\,‰$ of the albedo reduction caused by EC in snow. The sea ice is retreating swiftly in the Arctic Ocean (Forster *et al.*, 2007). That will open the area for commercial shipping. Kallenborn *et al.* (2009) estimated that the lion share of EC pollution in and around Svalbard comes from shipping. Hence, the local EC pollution may increase significantly within the High Arctic in the future.

In Table 6.1, estimates of the albedo effect in new snow for different EC and dust concentrations are given. The natural dust concentration in snow in Svalbard is three orders of magnitude higher than the background EC level. Even where the snow is highly contaminated by local EC sources, the dust concentration dominates over the EC concentration. However, EC is highly absorptive and about 50 times more effective than dust in reducing snow albedo (Warren, 1984). A dust deposition rate of $11\,g/(m^2yr)$ typical for alpine environments (Owens & Slaymaker, 1997), which results in a dust concentration of $\sim 11.5\,mg/l$ in Svalbard snow, reduces the snow albedo by 0.0096. That is a factor 8 larger than the effect of the background EC found on Svalbard. However, much larger dust deposition rates have been observed in Svalbard, typically a factor 25 larger (Åkerman, 1980). At such high contamination concentrations, the albedo model given here cannot be trusted. A likely albedo reduction due to such dust concentrations in snow is proposed in Table 6.1, but this value is not put any emphasize in this thesis. Hence, the importance of dust in snow may be larger than the calculated albedo reduction of 0.0096. Dust deposition is highly variable, ranging from large, visually detectable concentrations near rocky outcrops to much lower values in large snow covered areas. Coarse dust grains are observed in snow near its sources.

Table 6.1: A comparison of the reduced albedo effect for different EC and dust concentrations in snow. The snow depth is set to $957mm$ water equivalent (Winther *et al.*, 1998). For simplicity dust is assumed to be $1/50$ as effective as EC in absorbing sunlight (Warren, 1984). The albedo model (Rypdal *et al.*, Submitted) for new snow with optical grain size of $50\,\mu m$ discussed in Section 4.9 is used together with a weighted solar spectrum (C.A. Pedersen, personal communication). For concentrations above $900\mu g/l$, the albedo reduction is crudely assumed to increase linearly as between 500 and $900\,\mu g/l$. This will somewhat overestimate the albedo reduction. The albedo effect is only calculated for the EC for the dust that contains $20\,\%$ EC. The remaining $80\,\%$ dust will give an additional albedo reduction. The yearly Aeolian dust deposition rate of $11\,g/m^2$ (Owens & Slaymaker, 1997) is typical for alpine and subalpine environments. Higher deposition rates are observed in Svalbard, e.g. $270\,g/(m^2yr)$ at Cape Linné (Åkerman, 1980).

Case	Concentration	Albedo reduction (α)
Background level, EC (Forsström *et al.*, Submitted)	$4.1\,\mu g/l$	0.0011
Typical EC concentration in Adventdalen (Section 4.2)	$\sim 50\,\mu g/l$	0.0091
Typical EC concentration around Svalbard Airport (Section 4.2)	$\sim 1000\,\mu g/l$	0.0608
Local Aeolian dust (typical for alpine environments), $11\,g/(m^2yr)$ (Owens & Slaymaker, 1997)	$\sim 11.5\,mg/l$	0.0096
If 20 % of Aeolian dust is EC, only calculated for EC	$\sim 2300\,\mu g/l$	0.112
Local Aeolian dust (typically observed in Svalbard), $270\,g/(m^2yr)$ (Åkerman, 1980)	$\sim 282.3\,mg/l$	0.225

A range of contaminants is found in the snow pack. EC is the focus in this thesis since that substance is the most effective at reducing albedo for specific concentrations. As discussed above, the total effect of dust in snow is larger than EC in snow. Further, the ratio between EC and dust concentrations are important. C.E. Bøggild (personal communication) has observed that for increases in EC concentrations above $4\,\%$ of the total impurity mass, a similar increase in elevated absorption is not seen. Hence, EC is most effective at reducing albedo when its mass is less than $4\,\%$ of the total impurity mass. In Section 5.3.1, we estimated the ratio between the long-range transported flux of Aeolian dust to EC to be 25 to 1. In that perspective, the dust to EC ratio can be affecting the albedo sensitivity. However, the local source of dust is large. For a long-range transported flux of $0.1\,g/m^2yr$ (Harrison *et al.*, 2001) and local flux of $11\,g/m^2yr$ (Owens & Slaymaker, 1997), the local source is a factor 110 larger than the long-range source. With these typical values, the EC concentration in snow has to be greater than about $450\,\mu g/l$ to cross this $4\,\%$ level. Such values were only observed in the near vicinity of Longyearbyen and Svalbard Airport. Thus, we can, in general, neglect the effects of dust on the optical properties of EC in snow when calculating the albedo sensitivities.

The albedo reductions for different contaminant concentrations in Table 6.1 are given for new snow. For older, coarse grained snow, the effects are much larger. As melting progresses, EC particles will accumulate on the snow surface. That results in increasing EC concentrations and increasing albedo reductions. In the last part of the melt, the snow pack cannot be considered optically semi-infinite any longer, and the darker surface under the snow is impacting the albedo. That gives a positive feedback to the initial albedo reduction. Hence, the total climate effect is larger than the numbers in Table 6.1 indicate. Here, only the albedo effect from the EC in snow has been modeled, secondary effects are not included. The positive feedbacks will increase the effect. Flanner *et al.* (2007) indicated that the accelerated snow aging due to the presence of EC in the snow is as important

as the initial albedo effect. The total climate effect from locally produced EC in Svalbard snow will not be estimated in this thesis.

The climatic effect of EC particles depends on the location of the emissions. Emissions of EC particles within Svalbard has a much higher radiative effect on the snow pack in Svalbard per emitted particle than from any other source, e.g. from China. Studies such as Berntsen *et al.* (2006); Koch *et al.* (2007) show that there are regional and sectoral differences in radiative effects of short-lived species, e.g. aerosols. In general, the nearer a pollution source is to snow covered areas, the larger the potential radiative perturbation will be for those snow packs. That is also true within Svalbard. Due to the mobility, snowmobiles spread their exhaust over large areas in Svalbard. The climate effect from snowmobiles driven in Svalbard is, therefore, significant per emitted EC particle.

The climate system consists of a variety of parameters with varying importance. The EC concentration is only one of these parameters. A question could be if EC is important for snow depth in Svalbard. The snow depth varies greatly from year to year due to natural variations. The EC particles have no climatic effect during the dark season since there is no solar radiation to absorb. The EC background concentration gives such a tiny perturbation in albedo that this cannot be observed in the snow depth. On the other side of the scale are the extreme high EC concentrations observed in some of the settlements. Melting is seen earlier at Svalbard Airport than in the surroundings mainly due to spiking EC concentrations (Bøggild *et al.*, 2007). In early June 2009, the snow around Mine 7 was completely melted, while a continuous snow pack was observed in the surroundings. Then, the effect of EC can be noticed in the snow depth during late winter and spring around Svalbard Airport. EC concentrations as those measured in Adventdalen ($\sim 50\,\mu g/l$) are found over much larger areas than just the extreme spiking. Hence, it is important to see if those areas are measurably affected by EC. The albedo is reduced some, but is the reduction large enough to override natural variations in the climate? The snow in Adventdalen melts faster than most of Svalbard (Jaedicke, 2002); however, that is also caused by a dry climate and large quantities of dust in the snow pack. EC is a contributing factor that will have some effect on the snow depth, in particular during the melting season, in the area. In conclusion, EC is an important factor for snow depth in the most EC polluted areas, while EC has a negligible effect for most of Svalbard.

Chapter 7

Conclusions

7.1 Summary and conclusions

Svalbard is affected by pollution, mainly from sources in Europe and Northern Russia. Forsström *et al.* (Submitted) found the average EC background concentration on Svalbard to be $4.1\,\mu g/l$. In this thesis, the local contribution has for the first time been estimated. That is based on an extensive snow sampling programme. The effect of EC was calculated as the albedo reduction on snow due to its presence, and the conservative estimate here states that $11.2\,\%$ of all the EC pollution is local. The spatial distribution of the local pollution varies greatly. Darkened snow due to extremely high EC concentrations around Svea and Longyearbyen is easily observed in satellite images. The EC concentration around Svalbard Airport and the centre of Longyearbyen was above $1000\,\mu g/l$, which is a factor of 200 or more above the background level. Elevated EC concentrations were also measured around Svea, while no local pollution was found around Ny-Ålesund. In Ny-Ålesund the mean EC concentration in snow was $6.58\,\mu g/l$. The pollution from Svalbard has little significance to the overall EC content in the entire Arctic.

The snow samples gathered show that several tons of EC is in the snow around both Longyearbyen and Svea. The extremely high EC concentrations seen are due to coal dust from the mining activities. Combustion sources were estimated to produce about $11.5\,tons$ of EC during the winter period in the three studied settlements. Pollution from Longyearbyen will have a much greater effect if Isfjorden is ice-covered. In total, a minimum of $5.5\,tons$ of EC was found in the snow to be of local origin. That compares to an estimated $240\,tons$ EC in entire Svalbard from long-range transported sources.

Depositional and post-depositional processes are affecting the EC concentration in snow. The settlements in Svalbard are situated in relative dry areas; thus, local EC emissions will lead to relatively high EC concentrations in the snow pack. Sublimation and melting of snow will remove snow while the EC particles stay. This could double the EC concentration within a winter, and the EC concentration is, in particular, elevated in the surface snow layer. In addition, EC from rain events will increase the EC burden in the snow pack.

The albedo reduction from the EC particles has been modeled. The background EC level is reducing the albedo of fresh snow by 0.011. For old, coarse-grained snow the effect is a factor 3 larger. The local EC sources increase this albedo reduction. In Adventdalen, the typical EC concentration is $50\,\mu g/l$, which reduces the albedo of dry snow by 0.0091. All these numbers are based on the direct albedo effect of EC in snow. There are several secondary effects that have not been included in these estimates. Melting leads to a rapid growth in snow grain size, which increases the albedo effect. EC in the snow will promote snow aging and grain growth even more. This EC-induced grain growth feed-

back is approximately as important for the snow albedo as the initial albedo effect from EC. During melting, the EC particles will stay in the snow, especially in the surface layer, while the melt water runs off. That results in an increase in EC concentration. All this will magnify the forcing of EC in snow. On Longyearbreen, an increase by a factor of 18 in the EC concentration was measured in the surface snow between April to August. The albedo effect for Longyearbreen during late summer was about $0.05 - 0.09$, which is significant.

Aeolian sediments were observed in the snow pack, in particular near rocky outcrops and in the lowest part of the snow pack. The albedo reduction of dust in snow has roughly been estimated to be a factor 8 greater than the effect of EC. The high dust content is caused by sparse vegetation, plenty of glacial sedimentary present, and strong winds in a dry climate.

The measurements of EC concentrations in the snow pack have been compared to model runs from the Oslo CTM2 chemical transport model. An average concentration of $5.35\,\mu g/l$ given by the model for the 2007/08 winter fits with the observed EC background level. These two methods agree well for the surface samples. Strong melt events during the winter is badly modeled by the model; however, the spring melt gives a realistic increase in the surface snow EC concentration. The model shows that single events are important for long-range transported EC to come to Svalbard and that the Arctic Haze results in a maximum in this transport. The combination of an event based transport and a changing climate may lead to a deposition of EC in the future that we may not predict.

A relation between EC and $\delta^{18}O$ in snow was analyzed. A correlation was observed due to post-depositional processes in the snow pack, especially due to melting events. The alternative measuring method of EC introduced in this thesis showed a promising correlation with the traditional method and should be investigated in later research.

7.2 Further work

This work has estimated the significance of the local EC pollution in Svalbard; however, more can be done to improve this estimate. The importance of Aeolian sediments in the snow pack has been discussed here, but not analyzed in detail. The relation between EC and $\delta^{18}O$ in the snow has been looked into, and showed that more work is needed in the field. Some proposed studies that can be a follow up on this thesis are listed below:

- Snow samples were not taken in and around Barentsburg. A visual look of the discoloured snow around this settlement and the black smoke from its power plant reveal that Barentsburg is an important local EC source. An estimate of the pollution effect by Barentsburg could be done by taking snow samples in transects in the area and analyzing the data in a similar fashion to what is done here.

- Even though the effect of Longyearbyen, Ny-Ålesund, and Svea has been investigated, the total impact has not been assessed. Very few samples were taken in the surroundings mountains due to limited resources. These mountains might be affected by the local EC sources.

- Post-depositional processes in the snow pack are clearly having an impact on the EC concentration. More work is needed to understand these processes and how they impact EC particles in the snow. This could be done by selecting a site that is not affected by local pollution and regularly throughout the winter sample snow and investigate the snow stratigraphy. Such a study should including modeling. The Oslo CTM2 chemical transport model could be linked with a detailed snow pack model (e.g. SNOWPACK (Bartelt & Lehning, 2002)).

- Only the direct albedo effect from EC in snow has been calculated in this thesis. There are several secondary effects, where the most important one is the EC-induced grain growth feedback. This feedback should be investigated by looking at the microstructure in the snow pack and how EC affects this microstructure.
- There are a lot of Aeolian sediments in the snow in Svalbard. More research is needed to estimate how much there is and how this is reducing the albedo of snow. The reduced albedo effect of dust particles has to be accurately determined. That can be done by combining snow sampling and the use of sediment traps with in-situ albedo measurements. Dust concentrations in the snow are in some places so high that the dust content can be easily weighted.
- Some of the rocks on Svalbard contains EC, and several coal horizons is present. The weathering of these rocks will be a source of EC to the snow pack. This source is believed to be minimal, but might be measurable in places near these rock types. That should be investigated.
- This thesis found a covariation between EC concentration and $\delta^{18}O$. Here, post-depositional processes were discussed and argued to be dominant. However, there might be an initial correlation in freshly precipitated snow. That could be investigated by sampling fresh snow. A fitting site would be Larsbreen since it is both near Longyearbyen and in the mountains with no local EC sources. Such a study should include back-trajectory analysis to determine the sources of the water vapour and EC.

Acknowledgments

I would like to thank those that gave me economic support. Without grants from the University Centre in Svalbard (UNIS), University of Oslo (UiO), Svalbard Science Forum (SSF), the Jan Christiansen endowment, and the Swedish Research Council FORMAS, this project would not have been possible.

Further, I would like to thank all my supervisors. I'm grateful for all valuable information, ideas, and help that were given. My supervisors were Frode Stordal, Carl Egede Bøggild, Terje Berntsen, and Kim Holmén. The idea of studying dark matter in snow was first given by Carl Egede Bøggild. Johan Ström was officially not a supervisor, but for me he sure was one. I'm very thankfully about all the help he gave me concerning all problems relating to instrumentation. Some of his colleagues at the Norwegian Polar Institute (NPI) gave me also valuable support. I had the pleasure of following the footsteps of Sanja Forsström. Christina Pedersen and Sebastian Gerland were also giving me a hand. Gunnar Myhre is another supportive scientist. The Oslo CTM2 model was introduced to me by Ragnhild Bieltvedt Skeie. The discussion with fellow students, both in Oslo and Longyearbyen, has been rewarding.

A big thanks to everyone in the local community in Svalbard that provided me with data. Among them are Petter Braaten (the Governor of Svalbard), Knut Breivegen (Kings Bay), Frank Jakobsen (Lns Spitsbergen), Odd Jostein Sylte (Bydrift Longyearbyen), and Nils Bjerg Tokheim (SNSK). Erika Aamaas is hereby acknowledged for her work on some of the maps.

The field work would have been impossible without the help of the logistic department at UNIS and NPI's people in Ny-Ålesund. All the help I got from field assistants was crucial. The assistants were Åsmund Aamaas, Luis Aguilera, Willem van der Blit, Caroline Dupuy, Markus Eckerstorfer, Eli Anne Ersdal, Juho Pekka Vehviläinen, and Jago Wallenschus. Library and computer services by UiO and UNIS have also been helpful and highly appreciated.

I want to thank my parents for their interest in my education. They have always encouraged me to go further. When the plans of UNIS was made official 17 years ago, my father told the eight years old version of me that UNIS would be a cool place to study. He was also the one that told me about the meteorology studies at the University of Oslo. My parents also helped me with an ash on snow experiment set in Hjartdal.

I'm grateful I got the chance to study my favourite substance in the world, snow.

Bibliography

Åkerman, J.H. 1980. *Studies on periglacial geomorphology in West Spitsbergen*. PhD thesis, Department of Geography, The Royal University of Lund, Sweden.

Amundsen, Birger. 20. February 2009. *I nattens mulm og mørke in Svalbardposten, 61 (8), 4-5*.

Amundsen, Birger. 22. August 2008. *Mindre kullstøv fra Gruve 7 in Svalbardposten, 60 (33), 7-8*.

Andersen, K.K., & Genthon, C. 1996. Modeling the present and last glacial maximum transportation of dust to the Arctic with an extended source scheme. *Pages 123–132 of:* Guerzoni, S., & Chester, R. (eds), *The impact of desert dust across the mediterranean*. Oristano, Italy: Kluwer Academic Publishers.

Andreae, M.O., & Gelencsér, A. 2006. Black carbon or brown carbon? the nature of light-absorbing carbonaceous aerosols. *Atmospheric chemistry and physics*, **6**, 3131–3148.

Arlov, T.B. 2003. *Svalbards historie*. Trondheim: Tapir Akademiske Forlag.

Bartelt, P., & Lehning, M. 2002. A physical SNOWPACK model for the Swiss avalanche warning. part 1: Numerical model. *Cold regions science and technology*, **35**, 123–145.

Baskaran, M., & Shaw, G.E. 2001. Residence time of Arctic haze aerosols using the concentrations and activity ratios of ^{210}po, ^{210}pb and ^{7}be. *Aerosol science*, **32**, 443–452.

Beine, H.J., Engardt, M., Jaffe, D.A., Hov, Holmén, K., & Stordal, F. 1996. Measurement of NOx and aerosol particles at the Ny-Ålesund Zeppelin mountain station on Svalbard: Influence of regional and local pollution sources. *Atmospheric environment*, **30 (7)**, 1067–1079.

Benson, C.S. 1962. Stratigraphy studies in the snow and firn of the Greenland ice sheet. *In: Sipre research paper 70*.

Berntsen, T., Fuglestvedt, J., Myhre, G., Stordal, F., & Berglen, T.F. 2006. Abatement of greenhouse gases: Does location matter. *Climatic change*, **74**, 377–411.

Birch, M.E., & Cary, R.A. 1996. Elemental carbon-based method for monitoring occupational exposures to particulate diesel exhaust. *Aerosol science and technology*, **25**, 221–241.

Bøggild, C.E., Winther, J.-G., Sand, K., & Elvehøy, H. 1995. Sub-surface melting in blue ice fields in Dronning Maud Land, Antarctica: Observations and modelling. *Annals of glaciology*, **21**, 162–168.

Bøggild, C.E., Lüthje, M., & Holmes, J. 2007. Albedo observations with large concentrations of black carbon in High Arctic snow packs from Svalbard. *Pages 21–28 of: 63rd eastern snow conference*.

Bohren, C.F. 1987. Multiple scattering of light and some of its observable consequences. *American journal of physics*, **6**, 524–533.

Bond, T.C., & Bergstrom, R.W. 2006. Light absorption by carbonaceous particles: An investigate review. *Aerosol science and technology*, **40 (1)**, 27–67.

Bond, T.C., Streets, D.G., Yarber, K.F., Nelson, S.M., Woo, J.-H., & Klimont, Z. 2004. A technology-based global inventory of black and organic carbon emissions from combustion. *Journal of geophysical research*, **109**, D14203, doi:10.1029/2003JD003697.

Bond, T.C., Habib, G., & Bergstrom, R.W. 2006. Limitations in the enhancement of visible light absorption due to mixing state. *Journal of geophysical research*, **111**, D20211, doi:10.1029/2006JD007315.

Boots, B.N. 1980. Weighting Thiessen polygons. *Economic geography*, **56 (3)**, 248–259.

Bottenheim, J.W., Dangstoor, A., Gong, S.L., Higuchi, K., & Li, Y.F. 2004. Long range transport of air pollution to the Arctic. *Pages 13–39 of: The handbook of environmental chemistry*, vol. 4, Part G.

Bradley, R.S. 1985. *Quaternary paleoclimatology. methods of paleoclimatic reconstruction*. London: Chapman & Hall.

Bringedal, Å. H. 2004. *Oxygen isotopes from the surface of Longyearbreen, central Spitsbergen: Palaeoclimatic implications*. Master Thesis, Department of Earth Science, The University of Bergen.

Bruland, O., Sand, K., & Killingtveit, Å. 2001. Snow distribution at a High Arctic site at Svalbard. *Nordic hydrology*, **32 (1)**, 1–12.

Bryant, I.D. 1982. Loess deposits in lower Adventdalen, Spitsbergen. *Polar research*, **1982 (2)**, 93–103.

Chýlek, P., Ramaswamy, V., & Strivastava, V. 1983. Albedo of soot-contaminated snow. *Journal of geophysical research*, **88 (C15)**, 10837–10843.

Chýlek, P., Strivastava, V., Cahenzli, R.G., Pinnick, R.G., Dod, R.L., Novakov, T., Cook, T.L., & Hinds, B.D. 1987. Aerosol and graphitic carbon content of snow. *Journal of geophysical research*, **92 (D8)**, 9801–9809.

Clarke, A.D. 1981. Integrating sandwich: A new method of measurement of the light absorption coefficient for atmospheric particles. *Applied optics*, **21 (16)**, 3011–3020.

Clarke, A.D., & Noone, K.J. 1985. Soot in the Arctic snowpack: A cause for perturbations in radiative transfer. *Atmospheric environment*, **19 (12)**, 2045–2053.

Conway, H., Gades, A., & Raymond, C.F. 1996. Albedo of dirty snow during conditions of melt. *Water resources research*, **32 (6)**, 1713–1718.

Cottier, F.R., Nilsen, F., Inall, M.E., Gerland, S., Tverberg, V., & Svendsen, H. 2007. Wintertime warming of an Arctic shelf in response to large-scale atmospheric circulation. *Geophysical research letters*, **34**, L10607, doi:10.1029/2007GL029948.

Croft, B., Lohmann, U., & von Salzen, K. 2005. Black carbon ageing in the Canadian Centre for Climate modelling and analysis atmospheric general circulation model. *Atmospheric chemistry and physics*, **5**, 1931–1949.

Czeppe, Z. 1966. Przebieg głównych procesów morfogenetycznych w poludniowa-zachodnim Spitsbergenie. (Summary: The course of the main morphogenetic processes in South-west Spitsbergen). *Prace geograficzne, kraków*, **1**, 103–120.

Dahl, I.T. 1998. *Glimt av Tuddal - Før i verden*. Tuddal: Eige forlag.

Dentener, F., Kinne, S., Bond, T., Boucher, O., Cofala, J., Generoso, S., Ginoux, P., Gong, S., Hoelzemann, J.J., Ito, A., Marelli, L., Penner, J.E., Putaud, J.-P., Textor, C., Schulz, M., van der Werf, G.R., & Wilson, J. 2006. Emissions of primary aerosol and precursor gases in th years 2000 and 1750 prescribed data-sets for AeroCom. *Atmospheric chemistry and physics*, **6**, 4321–4344.

Dijkmans, J.W.A. 1990. Niveo-aeolian sedimentation and resulting sedimentary structures; Søndre Strømfjord area, Western Greenland. *Permafrost and periglacial processes*, **1 (2)**, 83–96.

Dunkle, R.V., & Bevans, J.T. 1956. An approximate analysis of the solar radiation reflectance and transmittance of a snow cover. *Journal of meteorology*, **13**, 212–216.

Eleftheriadis, K., Vratolis, S., & Nyeki, S. 2009. Aerosol black carbon in the European Arctic: Measurements at Zeppelin station, Ny-Ålesund, Svalbard from 1998-2007. *Geophysical research letters*, **36**, L02809, doi:10.1029/2008GL035741.

Elgmork, K., Hagen, A., & Langeland, A. 1985. Polluted snow in southern Norway during the winter 1968-1971. *Environmental pollution*, **4**, 41–52.

Eneroth, K., Kjellström, E., & Holmén, K. 2003. A trajectory climatology for Svalbard, investigating how atmospheric flow patterns influence observed tracer concentrations. *Physics and chemistry of the earth*, **28**, 1191–1203.

Flanner, M. 2007. *Effects of vertically-resolved solar heating, snow aging, and black carbon on snow-albedo feedback*. PhD thesis in Earth System Science, University of California.

Flanner, M.G., & Zender, C.S. 2005. Snowpack radiative heating: Influence on Tibetan Plateau climate. *Geophysical research letters*, **32**, L06501, doi:10.1029/2004GL022076.

Flanner, M.G., & Zender, C.S. 2006. Linking snowpack microphysics and albedo evolution. *Journal of geophysical research*, **111**, D12208, doi:10.1029/2005JD006834.

Flanner, M.G., Zender, C.S., Randerson, J.T., & Rasch, P.J. 2007. Present-day climate forcing and response from black carbon in snow. *Journal of geophysical research*, **112**, D11202, doi:10.1029/2006JD008003.

Førland, E.J., & Hanssen-Bauer, I. 2002. *Climate variations and implications for precipitation types in the Norwegian Arctic*. Tech. rept. 24/02. Norwegian Meteorological Institute.

Førland, E.J., Hanssen-Bauer, I., & Nordli, P.Ø. 1997a. *Climate statistics and longterm series of temperature and precipitation at Svalbard and Jan Mayen*. Tech. rept. 21/97. Norwegian Meteorological Institute.

Førland, E.J., Hanssen-Bauer, I., & Nordli, P.Ø. 1997b. *Orographic precipitation at the glacier Austre Brøggerbreen, Svalbard*. Tech. rept. 02/97. Norwegian Meteorological Institute.

Forsström, S. 2008. *Carbonaceous aerosol particles in Svalbard snow*. Master Thesis, University of Helsinki.

Forsström, S., Ström, J., Pedersen, C.A., Isaksson, E., & Gerland, S. Submitted. Elemental carbon distribution in Svalbard snow.

Forster, P., Ramaswamy, V., Artaxo, P., Berntsen, T., Betts, R., Fahey, D.W., Haywood, J., Lean, J., Lowe, D.C., Myhre, G., Nganga, J., Prinn, R., Raga, G., Schulz, M., & Van Dorland, R. 2007. Changes in atmospheric constituents and in radiative forcing. *In: The physical science basis. contribution of working group 1 to the fourth assessment report of the intergovernmental panel on climate change*. Cambridge University Press.

Gerland, S., & Renner, A.H.H. 2007. Sea-ice mass-balance monitoring in an Arctic fjord. *Annals of glaciology*, **46**, 435–442.

Giddings, J.C., & LaChapelle, E.R. 1961. Diffusion theory applied to radiant energy distribution and albedo of snow. *Journal of geophysical research*, **66 (1)**, 181–189.

Glasser, N.F., & Hambrey, M.J. 2002. δd-$\delta^{18}o$ relationships on a polythermal valley glacier: Midtre Lovénbreen, Svalbard. *Polar research*, **21(1)**, 123–131.

Grenfell, T.C., & Perovich, D.K. 2004. Seasonal and spatial evolution of albedo in a snow-ice-land-ocean environment. *Journal of geophysical research*, **109**, C01001, doi:10.1029/2003JC001866.

Grenfell, T.C., Warren, S.G., & Mullen, P.C. 1994. Reflection of solar radiation by the Antarctic snow surface at ultraviolet, visible, and near-infrared wavelengths. *Journal of geophysical research*, **99 (D9)**, 18669–18684.

Grenfell, T.C., Light, B., & Sturm, M. 2002. Spatial distribution and radiative effects of soot in the snow and sea ice during the SHEBA experiment. *Journal of geophysical research*, **107 (C10)**, 8032 doi:10.1029/2000JC000414.

Grini, A. 2007. *Including the M7 aerosol dynamics model in the global Chemical Transport Model Oslo CTM2*. Technical report, Report no. 133, ISBN 82-91885-37-0, University of Oslo.

Hagen, J.O., & Liestøl, O. 1990. Long-term glacier mass-balance investigations in Svalbard, 1950-88. *Annals of glaciology*, **14**, 102–106.

Hansen, J.E., & Nazarenko, L. 2004. Soot climate forcing via snow and ice albedos. *Pnas*, **101 (2)**, 423–428.

Hansen, J.E., & Sato, M. 2001. Trends of measured climate forcing agents. *Pnas*, **98 (26)**, 14778–14783.

Hanssen-Bauer, I., Førland, E.J., & Nordli, P.Ø. 1996. *Measured and true precipitation at Svalbard*. Tech. rept. 31/96. Norwegian Meteorological Institute.

Harrison, S.P., Kohfeld, K.E., Roelandt, C., & Claquin, T. 2001. The role of dust in climate changes today, at the last glacial maximum and in the future. *Earth-science reviews*, **54**, 43–80.

Haywood, J.M., Roberts, D.L., Slingo, A., Edwards, J.M., & Shine, K.P. 1997. General circulation model calculations of the direct radiative forcing by anthropogenic sulphate and fossil-fuel soot aerosol. *Journal of climatology*, **10**, 1562–1577.

Hjelle, A. 1993. *Geology of Svalbard*. Oslo: Norsk Polarinstitutt.

Humlum, O. 2002. Modelling late 20th-century precipitation in Nordenskiöld Land, Svalbard, by geomorphic means. *Norsk geografisk tidsskrift*, **56 (2)**, 96–103.

Igarashi, M., Kamiyama, K., & Watanabe, O. 2001. Stable oxygen isotope ratio observed in the precipitation at Ny-Ålesund, Svalbard. *Memoirs of national institute of polar research*, **54**, 169–182.

Isaksson, E., Hermanson, M., Hicks, S., Igarashi, M., Kamiyama, K., Moore, J., Motoyama, H., Muir, D., Pohjola, V., Vaikmäe, R., van de Wal, R.S.W., & Watanabe, O. 2003. Ice cores from Svalbard - useful archives of past climate and pollution history. *Physics and chemistry of the earth*, **28**, 1217–1228.

Isaksson, E., Divine, D., Kohler, J., Martma, T., Pohjola, V., Motoyama, H., & Watanabe, O. 2005. Climate oscillations as recorded in Svalbard ice core $\delta^{18}o$ records between AD 1200 and 1997. *Geografiska annaler*, **87 A (1)**, 203–214.

Jacobson, M.Z. 2001. Strong radiative heating due to the mixing state of black carbon in atmospheric aerosols. *Nature*, **409**, 695–697.

Jacobson, M.Z. 2004. Climate response of fossil fuel and biofuel soot, accounting for soot's feedback to snow and sea ice albedo and emissivity. *Journal of geophysical research*, **109**, D21201, doi:10.1029/2004JD004945.

Jaedicke, C. 2001. *Drifting snow and snow accumulation in complex Arctic terrain*. PhD thesis, Geophyscial Institute, University of Bergen.

Jaedicke, C. 2002. Snow drift losses from an Arctic catchment on Spitsbergen: An additional process in the water balance. *Cold regions science and technology*, **34 (1)**, 1–10.

Jaedicke, C., & Sandvik, A.D. 2001. The influence of drifting snow on the location of glaciers on Western Spitsbergen. *In: European geophysical society general assembly*.

Jones, H.G., Pomeroy, J.W., Walker, D.A., & Hoham, R.W. 2001. *Snow ecology an interdisciplinary examination of snow-covered ecosystems*. Cambridge, United Kingdom: Cambridge University Press.

Jones, T.P., Chaloner, W.G., & Kuhlbusch, T.A.J. 1997. Proposed bio-geological and chemical based terminology for fire-altered plant matter. *Sediment records of biomass burning and global change*, **1**, 9–21.

Kallenborn, R., Økstad, E., & Vestreng, V. 2009. *Historical, present and future inventories for climate influencing emissions at Svalbard*. The Norwegian Pollution Control Authorities (SFT).

Keenlyside, N.S., Latif, M., Jungclaus, J., Kornblueh, L., & Roeckner, E. 2008. Advancing decadal-scale climate prediction in the North Atlantic sector. *Nature*, **453**, doi:10.1038/nature06921.

Klonecki, A., Hess, P., Emmons, L., Smith, L., Orlando, J., & Blake, D. 2003. Seasonal changes in the transport of pollutants into the Arctic troposphere - model study. *Journal of geophysical research*, **108 (D4)**, 8367, doi:10.1029/2002JD002199.

Koch, D., Bond, T.C., Streets, D., Unger, N., & van der Werf, G.R. 2007. Global impacts of aerosols from particular source regions and sectors. *Journal of geophysical research*, **112**, D02205, doi:10.1029/2005JD007024.

Koerner, R.M. 1997. Some comments on climatic reconstructions from ice cores drilled in areas of high melt. *Journal of glaciology*, **43 (143)**, 90–97.

Landvik, J.Y. 1998. Seasonal deflation and wind transport in an Arctic watershed, Svalbard, Norway. *Page (viii) & 168pp of: 28th international arctic workskop, arctic and alpine environments, past and present, program with abstracts*.

Law, K.S., & Stohl, A. 2007. Arctic air pollution: Origins and impacts. *Science*, **315**, 1537–1540.

Legates, D.R., & Willmott, C.J. 1990. Mean seasonal and spatial variability in gauge-corrected, global precipitation. *International journal of climatology*, **10**, 111–127.

Lemke, P., Ren, J., Alley, R.B., Allison, I., Carrasco, J., Flato, G., Fujii, Y., Kaser, G., Mote, P., Thomas, R.H., & Zhang, T. 2007. Observations: Changes in snow, ice and frozen ground. *In: The physical science basis. contribution of working group 1 to the fourth assessment report of the intergovernmental panel on climate change*. Cambridge University Press.

Liou, K.N. 2002. *An introduction to atmospheric radiation*. Second edition edn. San Diego: Academic Press.

Lund, M. T. 2008. *A study of transport and deposition of black carbon using the Oslo CTM2 chemical transport model; a comparison of two aerosol parameterizations*. Master Thesis, Department of Geosciences, University of Oslo.

Male, D.H. 1980. The seasonal snowcover. *Pages 305–395 of: Dynamics of snow and ice masses*. Academic Press.

McConnell, J.R., Edwards, R., Kok, G.L., Flanner, M.G., Zender, C.S., Saltzman, E.S., Banta, J.R., Pasteris, D.R., Carter, M.M., & Kahl, J.D.W. 2007. 20th-Century industrial black carbon emissions altered Arctic climate forcing. *Sciencexpress*, **science.1144856**, 10.1126.

Morgner, E. 2009. *The effect of vegetation type and snow depth on annual co_2 efflux in a High Arctic tundra region*. Master Thesis, Department of Biology, Faculty of Science, The University of Bergen & The University Centre in Svalbard.

Myhr, K. A. 2003. *Støv i arbeidsmiljø og ytre miljø i Svea*. Diploma Thesis, Faculty of Engineering and Technology, Norwegian University of Science and Technology.

Myhre, G., Stordal, F., Restad, K., & Isaksen, I.S. 1998. Estimation of the direct radiative forcing due to sulfate and soot aerosols. *Tellus*, **B50**, 463–477.

Novakov, T., Ramanathan, V., Hansen, J.E., Kirchstetter, T.W., Sato, M., Sinton, J.E., & Sathaye, J.A. 2003. Large historical changes of fossil-fuel black carbon aerosols. *Geophysical research letters*, **30 (6)**, 1324, doi:10.1029/2002GL016345.

Ogren, J.A., & Charlson, R.J. 1983. Elemental carbon in the atmosphere: Cycle and lifetime. *Tellus*, **35B**, 241–254.

Ogren, J.A., Charlson, R.J., & Groblicki, P.J. 1983. Determination of elemental carbon in rainwater. *Analytical chemistry*, **55 (9)**, 1569–1572.

Ørbæk, J.B., Hisdal, V., & Svaasand, L.E. 1999. Radiation climate variability in Svalbard: Surface and satellite observations. *Polar research*, **18 (2)**, 127–134.

Owens, P.N., & Slaymaker, O. 1997. Contemporary and post-glacial rates of Aeolian deposition in the coast mountains of British Columbia, Canada. *Geografiska annaler*, **79A (4)**, 267–276.

Pohjola, V.A., Moore, J.C., Isaksson, E., Jauhiainen, T., van de Wal, R.S.W., Martma, T.A., Meijer, H.A.J., & Vaikmäe, R. 2002. Effect of periodic melting on geochemical and isotopic signals in an ice core from Lomonosovfonna, Svalbard. *Journal of geophysical research*, **107 (D4)**, 4036, doi:10.1029/2000JD000149.

Pomeroy, J.W., & Gray, D.M. 1995. *Snowcover accumulation, relocation and management*. Saskatoon, Saskatchewan: Hydrological Sciences Division, NHRI, Division of Hydrology, University of Saskatchewan.

Quinn, P.K., Bates, T.S., Baum, E., Doubleday, N., Fiore, A.M., Flanner, M., Fridlind, A., Garrett, T.J., Koch, D., Menon, S., Shindell, D., Stohl, A., & Warren, S.G. 2008. Short-lived pollutants in the Arctic: Their climate impact and possible mitigation strategies. *Atmospheric chemistry and physics*, **8**, 1723–1735.

Raes, F., Van Dingenen, R., Vignati, E., Wilson, J., Putaud, J.-P., Seinfeld, J.H., & Adams, P. 2000. Formation and cycling of aerosols in the global troposphere. *Atmospheric environment*, **34**, 4215–4240.

Randall, D.A., Cess, R.D., Blanchet, J.P., Chalita, S., Colman, R., Dazlich, D.A., Del Genio, A.D., Keup, E., Lacis, A., Le Treut, H., Liang, X.-Z., McAvaney, B.J., Mahfouf, J.F., Meleshko, V.P., Morcrette, J.-J., Norris, P.M., Potter, G.L., Rikus, L., Roeckner, E., Royer, J.F., Schlese, U., Sheinin, D.A., Sokolov, A.P., Taylor, K.E., Wetherald, R.T., Yagai, I., & Zhang, M.-H. 1994. Analysis of snow feedbacks in 14 general circulation models. *Journal of geophysical research*, **99 (D10)**, 20757–20771.

Randerson, J.T., van der Werf, G.R., Giglio, L., Collatz, G.J., & Kasibhatla, P.S. 2007. *Global Fire Emissions Database, Version 2 (GFEDv2.1). data set. available on-line [http://daac.ornl.gov/]*. Oak Ridge National Laboratory Distributed Active Archive Center, Oak Ridge, Tennessee, USA. doi:10.3334/ORNLDAAC/849.

Reddy, M.S., & Boucher, O. 2007. Climate impact of black carbon emitted from energy consumption in the world's regions. *Geophysical research letters*, **34**, L11802, doi:10.1029/2006GL028904.

Reeh, N. 1991. Parameterization of melt rate and surface temperature on the Greenland Ice Sheet. *Polarforschung*, **59 (3)**, 113–128.

Reimann, S., Kallenbron, R., & Schmidbauer, N. Submitted. Severe aromatic hydrocarbon pollution in the Arctic town of Longyearbyen (Svalbard) due to snowmobile emissions.

Rosenthal, W., Saleta, J., & Dozier, J. 2007. Scanning electron microscopy of impurity structures in snow. *Cold regions science and technology*, **47**, 80–89.

Rypdal, K., Rive, N., Berntsen, T., Klimont, Z., Mideksa, T.K., Myhre, G., & Skeie, R.B. Submitted. Costs and global impacts of black carbon abatement strategies. *Tellus b*.

Samuelsson, C. 1921. Till frågan om vinderosion i arktiska trakter med särskild haänsyn till de å Spetsbergen rådande förhållandena. *Ymer. årg.*, H.2.

Sato, M., Hansen, J., Koch, D., Lacis, A., Ruedy, R., Dubovik, O., Holben, B., Chin, M., & Novakov, T. 2003. Global atmospheric black carbon inferred from AERONET. *Pnas*, **100 (11)**, 6319–6324.

Schulz, M., Textor, C., Kinne, S., Balkanski, Y., Bauer, S., Berntsen, T., Berglen, T., Boucher, O., Dentener, F., Guibert, S., Isaksen, I.S.A., Iversen, T., Koch, D., Kirkevåg, A., Liu, X., Montanaro, V., Myhre, G., Penner, J.E., Pitari, G., Reddy, S., Seland, Ø. Stier, P., & Takemura, T. 2006. Radiative forcing by aerosols as derived from the AeroCom present-day and pre-industrial simulations. *Atmospheric chemistry and physics*, **6**, 5225–5246.

Semb, A., Brækkan, R., & Joranger, E. 1984. Major ions in Spitsbergen snow samples. *Geophysical research letters*, **11 (5)**, 445–448.

Seppälä, M. 2004. *Wind as a geomorphic agent in cold climates*. Cambridge: Cambridge University Press.

Sharma, S., Lavoué, D., Cachier, H., Barrie, L.A., & Gong, S.L. 2004. Long-term trends of the black carbon concentrations in the Canadian Arctic. *Journal of geophysical research*, **109**, D15203, doi:10.1029/2003JD004331.

Sharma, S., Andrews, E., Barrie, L.A., Ogren, J.A., & Lavoué, D. 2006. Variations and sources of the equivalent black carbon in the high Arctic revealed by long-term observations at Alert and Barrow: 1989-2003. *Journal of geophysical research*, **111**, D14208, doi:10.1029/2005JD006581.

Shaw, G.E. 1995. The Arctic haze phenomenon. *Bulletin american meteorological society*, **76**, 2403–2413.

Shindell, D.T., Chin, M., Dentener, F., Doherty, R.M., Faluvegi, G., Fiore, A.M., Hess, P., Koch, D.M., MacKenzie, I.A., Sanderson, M.G., Schultz, M.G., Schulz, M., Stevenson, D.S., Teich, H., Textor, C., Wild, O., Bergmann, D.J., Bey, I., Bian, H., Cuvelier, C., Duncan, B.N., Folberth, G., Horowitz, L.W., Jonson, J., Kaminski, J.W., Marmer, E., Park, R., Pringle, K.J., Schroeder, S., Szopa, S., Takemura, T., Zeng, G., Keating, T.J., & Zuber, A. 2008. A multi-model assessment of pollution transport to the Arctic. *Atmospheric chemistry and physics*, **8**, 5353–5372.

Simonsen, S.B. 2007. *Measurement of black carbon in Arctic snow*. Centre for Ice and Climate, Niels Bohr Institute, University of Copenhagen.

Stohl, A. 2006. Characteristics of atmospheric transport into the Arctic troposphere. *Journal of geophysical research*, **111**, D11306, doi:10.1029/2005JD006888.

Stohl, A., Andrews, E., Burkhart, J.F., Forster, C., Herber, A., Hoch, W., Kowal, D., Lunder, C., Mefford, T., Ogren, J.A., Sharma, S., Spichtinger, N., Stebel, K., Stone, R., Ström, J., Tørseth, K., Wehrli, C., & Yttri, K.E. 2006. Pan-Arctic enhancements of light absorbing aerosol concentrations

due to North American boreal forest fires during summer 2004. *Journal of geophysical research*, **111**, D22214, doi:10.1029/2006JD007216.

Stohl, A., Berg, T., Burkhart, J.F., Fjæraa, A.M., Forster, C., Herber, A., Hov, Ø., Lunder, C., McMillan, W.W., Oltmans, S., Shiobara, M., Simpson, D., Solberg, S., Stebel, K., Ström, J., Tørseth, K., Treffeisen, R., Virkkunen, K., & Yttri, K.E. 2007. Arctic smoke - record high air pollution levels in the European Arctic due to agricultural fires in Eastern Europe in spring 2006. *Atmospheric chemistry and physics*, **7**, 511–534.

Stokkan, T. 2007. *Pollution from Svea Nord in both the inner and the outer environment, concentrated mainly on the dust issue*. Master Thesis, Faculty of Engineering and Technology, Norwegian University of Science and Technology.

Ström, J., Umegård, J., Tørseth, K., Tunved, P., Hansson, H.-C., Holmén, K., Wismann, V., Herber, A., & König-Langlo, G. 2003. One year of particle size distribution and aerosol chemical composition measurments at the Zeppelin Station, Svalbard, March 2000 - March 2001. *Physics and chemistry of the earth*, **28**, 1181–1190.

Suzuki, T., Nakayama, N., Igarashi, M., Kamiyama, K., & Watanabe, O. 1996. Concentrations of ^{210}pb and ^{210}po in the atmosphere of Ny-Ålesund, Svalbard. *Memoirs of national institute of polar research. special issue*, **51**, 233–237.

Svendsen, H., Beszcynska-Møller, A., Hagen, J.O., Lefauconnier, B., Tverberg, V., Gerland, S., Ørbæk, J.B., Bischof, K., Papucci, C., Zajaczkowaki, M., Azzolini, R., Bruland, O., Wiencke, C., Winther, J.-G., & Dallmann, W. 2002. The physical environment of Kongsfjorden-Krossfjorden, an Arctic fjord system in Svalbard. *Polar research*, **21 (1)**, 133–166.

Takeuchi, Y., Kodama, Y., & Nakabayashi, H. 1995. Characteristics of evaporation from snow and tundra surface in Spitsbergen in the snowmelt season 1993. *Proc. nipr symp. polar meteorol. glacio.*, **9**, 54–65.

Ungersböck, M., Rubel, F., Fuchs, T., & Rudolf, B. 2000. Bias correction of global daily rain gauge measurements. *Physics and chemistry of the earth*, **26**, 411–414.

Vignati, E., & Wilson, J. 2004. M7: An efficient size-resolved aerosol microphysics module for large-scale aerosol transport models. *Journal of geophysical research*, **109**, D22202, doi:10.1029/2003JD004485.

Visted, K., & Stigum, H. 1971. *Vår gamle bondekultur 1*. Third edn. Oslo: Cappelen.

Wallace, J.M., & Hobbs, P.V. 2006. *Atmospheric science. an introductory survey*. Second edn. New York: Academic Press.

Warren, S.G. 1982. Optical properties. *Reviews of geophysics and space physics*, **20 (1)**, 67–89.

Warren, S.G. 1984. Impurities in snow: Effects on albedo and snowmelt. *Annals of glaciology*, **5**, 177–179.

Warren, S.G., & Clarke, A.D. 1990. Soot in the atmosphere and snow surface of Antarctica. *Journal of geophysical research*, **95 (D2)**, 1811–1816.

Warren, S.G., & Wiscombe, W.J. 1980. A model for the spectral albedo of snow. 2: Snow containing atmospheric aerosols. *Journal of atmospheric aerosols*, **37**, 2734–2745.

Warren, S.G., & Wiscombe, W.J. 1985. Dirty snow after nuclear war. *Nature*, **313 (6002)**, 467–470.

Watson, J.G., Chow, J.C., & Chen, L.-W.A. 2005. Summary of organic and elemental carbon/black carbon analysis methods and intercomparisons. *Aerosol and air quality research*, **5 (1)**, 65–102.

Winther, J.-G., Bruland, O., Sand, K., Killingtveit, Å., & Marechal, D. 1998. Snow accumulation distribution on Spitsbergen, Svalbard, in 1997. *Polar research*, **17 (2)**, 155–164.

Winther, J.-G., Godtliebsen, F., Gerland, S., & Isachsen, P.E. 2002. Surface albedo in Ny-Ålesund, Svalbard: Variability and trends during 1981-1997. *Global and planetary change*, **32**, 127–139.

Wiscombe, W.J., & Warren, S.G. 1980. A model for the spectral albedo of snow. 1: Pure snow. *Journal of the atmospheric sciences*, **37**, 2712–2733.

Index

Appendix A

EC measurements

Table A.1: A list of all EC measurements. Most sample IDs contain some letters that state the area, a number that lists what snow pit number, and a final number for the which snow layer. The top layer is here 1, while the bottom layer is 5.

ID	OC concentration $[\mu g/l]$	EC concentration $[\mu g/l]$	TC concentration $[\mu g/l]$	Latitute $[^\circ N]$	Longitude $[^\circ E]$
0-1	1258.34	316.21	1574.55	78.23689	015.52303
Test 1	656.31	849.48	1505.79	78.21959	015.64096
Test 1B	328.41	2103.81	2432.22	78.21959	015.64096
Test 2	332.97	195.85	528.82	78.21959	015.64096
Test 3	100.10	0.00	100.05	78.21959	015.64096
1-1	478.28	95.91	574.20	78.16756	016.03941
1-2	1309.63	206.04	1515.66	78.16756	016.03941
1-3	696.06	143.89	839.94	78.16756	016.03941
1-4	655.41	36.80	692.22	78.16756	016.03941
1-5	969.03	6.68	1003.51	78.16756	016.03941
2-1	211.05	42.51	253.55	78.17232	016.14302
2-2	996.83	6.68	1003.51	78.17232	016.14302
3A1	243.84	41.48	285.32	78.17232	016.27229
3A2	193.58	44.40	237.97	78.17232	016.27229
3A3	1404.09	12.00	1416.08	78.17232	016.27229
3A4	326.52	60.32	386.84	78.17232	016.27229
3A5	493.63	97.09	590.72	78.17232	016.27229
3B1	185.48	44.29	229.77	78.17232	016.27229
3B2	160.55	33.45	193.99	78.17232	016.27229
3B3	285.83	58.83	344.66	78.17232	016.27229

ID	OC concentration $[\mu g/l]$	EC concentration $[\mu g/l]$	TC concentration $[\mu g/l]$	Latitute $[^\circ N]$	Longitude $[^\circ E]$
3B4	313.06	63.49	376.55	78.17232	016.27229
3B5	568.72	94.49	663.20	78.17232	016.27229
3C1	196.01	53.18	249.19	78.17232	016.27229
3C2	253.38	39.71	293.09	78.17232	016.27229
3C3	262.88	71.14	334.03	78.17232	016.27229
3C4	159.30	44.43	203.74	78.17232	016.27229
3C5	260.28	60.76	321.04	78.17232	016.27229
3D1	352.77	64.29	417.06	78.17232	016.27229
3D2	278.62	46.77	325.39	78.17232	016.27229
3D3	84.72	43.44	128.16	78.17232	016.27229
3D4	140.15	58.00	198.15	78.17232	016.27229
3D5	235.97	68.47	304.44	78.17232	016.27229
NW5-1	90.82	3.66	94.48	78.96307	011.32489
NW5-2	86.37	0.13	86.50	78.96307	011.32489
NW5-3	50.86	1.77	52.63	78.96307	011.32489
NW5-4	80.03	4.41	84.44	78.96307	011.32489
NW5-5	384.05	11.15	395.20	78.96307	011.32489
NW4-1	104.86	3.54	108.40	78.95690	011.47341
NW4-2	49.12	2.20	51.32	78.95690	011.47341
NW4-3	112.03	0.05	112.08	78.95690	011.47341
NW4-4	68.50	9.57	78.07	78.95690	011.47341
NW4-5	108.94	12.19	121.13	78.95690	011.47341
NW3-1	97.53	0.00	97.50	78.96227	011.62805
NW3-2	90.09	4.02	94.11	78.96227	011.62805
NW3-3	97.89	4.15	102.04	78.96227	011.62805
NW3-4	72.93	13.64	86.57	78.96227	011.62805
NW3-5	313.19	3.96	317.15	78.96227	011.62805
NW2-1	60.01	0.00	59.96	78.95086	011.72992
NW2-2	69.75	0.00	69.71	78.95086	011.72992
NW2-3	52.57	10.99	63.57	78.95086	011.72992
NW2-4	186.70	5.68	192.38	78.95086	011.72992
NW2-5	131.05	6.36	137.40	78.95086	011.72992
NW1-1	95.99	14.44	110.43	78.93840	011.80746
NW1-2	46.07	2.27	48.34	78.93840	011.80746
NW1-3	43.70	7.12	50.82	78.93840	011.80746
NW1-4	97.34	9.16	106.52	78.93840	011.80746

ID	OC concentration $[\mu g/l]$	EC concentration $[\mu g/l]$	TC concentration $[\mu g/l]$	Latitute $[^\circ N]$	Longitude $[^\circ E]$
NW1-5	286.31	12.39	298.69	78.93840	011.80746
NE1-1	129.96	0.00	129.92	78.91561	011.96630
NE1-2	75.83	5.48	81.30	78.91561	011.96630
NE1-3	137.62	7.25	144.87	78.91561	011.96630
NE1-4	403.71	11.49	415.20	78.91561	011.96630
NE1-5	338.87	8.79	347.66	78.91561	011.96630
NE2-1	119.81	9.50	129.32	78.91228	012.01231
NE2-2	212.21	6.83	219.05	78.91228	012.01231
NE2-3	211.60	0.00	211.57	78.91228	012.01231
NE2-4	183.46	13.23	196.69	78.91228	012.01231
NE2-5	260.46	7.51	267.97	78.91228	012.01231
NE3-1	298.15	0.00	298.11	78.89732	012.14692
NE3-2	173.46	5.17	178.63	78.89732	012.14692
NE3-3	195.91	4.64	200.55	78.89732	012.14692
NE3-4	248.27	9.51	257.78	78.89732	012.14692
NE3-5	477.03	8.17	485.19	78.89732	012.14692
NE4-1	108.63	11.04	119.67	78.84450	012.60636
NE4-2	126.88	12.74	139.62	78.84450	012.60636
NE4-3	99.52	8.40	107.93	78.84450	012.60636
NE4-4	166.66	6.45	173.11	78.84450	012.60636
NE4-5	388.95	7.99	396.94	78.84450	012.60636
NE5-1	128.38	9.29	137.67	78.86380	012.51760
NE5-2	65.82	0.00	65.79	78.86380	012.51760
NE5-3	158.97	10.37	169.35	78.86380	012.51760
NE5-4	179.15	5.92	185.07	78.86380	012.51760
NE5-5	119.87	5.43	125.30	78.86380	012.51760
B3-1	317.08	55.46	333.30	78.23547	015.33334
B3-2	878.54	53.87	907.08	78.23547	015.33334
B3-3	345.75	67.83	391.34	78.23547	015.33334
B3-4	465.31	39.83	480.85	78.23547	015.33334
B3-5	446.25	125.74	542.88	78.23547	015.33334
A18-2	21739.44	791.54	22467.63	78.25018	015.43842
A18-3	24839.39	1156.18	25892.63	78.25018	015.43842
A18-4	18998.82	1919.51	20838.52	78.25018	015.43842
A18-5	8138.89	1606.21	9648.34	78.25018	015.43842
A15-1	1310.79	285.14	1559.14	78.22014	015.72662

ID	OC concentration $[\mu g/l]$	EC concentration $[\mu g/l]$	TC concentration $[\mu g/l]$	Latitute $[^\circ N]$	Longitude $[^\circ E]$
A15-2	14152.47	968.18	15085.45	78.22014	015.72662
A11-1	471.94	88.36	527.63	78.21197	015.81134
A11-2	373.36	82.64	433.31	78.21197	015.81134
A11-3	110.30	16.16	89.67	78.21197	015.81134
A11-4	150.67	33.27	153.95	78.21197	015.81134
A11-5	517.19	103.76	594.15	78.21197	015.81134
A7-1	343.54	53.47	369.06	78.20440	015.90691
A7-2	220.25	19.67	210.68	78.20440	015.90691
A7-3	360.59	46.96	375.26	78.20440	015.90691
A7-4	265.23	46.56	287.15	78.20440	015.90691
A2-1	287.66	39.70	290.73	78.19327	016.01134
A2-2	290.70	15.77	281.61	78.19327	016.01134
A2-3	519.87	92.54	581.78	78.19327	016.01134
A2-4	287.83	35.34	296.13	78.19327	016.01134
A2-5	239.71	30.50	234.53	78.19327	016.01134
SA13-1	393.62	67.76	427.18	78.19600	016.34688
SA13-2	140.51	17.49	126.04	78.19600	016.34688
SA13-3	115.12	15.24	98.89	78.19600	016.34688
SA13-4	423.55	72.00	468.16	78.19600	016.34688
SA13-5	299.53	45.31	306.47	78.19600	016.34688
SA11-1	148.92	3.63	123.72	78.19583	016.65177
SA11-2	140.15	16.73	121.11	78.19583	016.65177
SA11-3	261.02	30.80	263.61	78.19583	016.65177
SA11-4	535.11	60.91	553.27	78.19583	016.65177
SA11-5	363.64	14.55	349.88	78.19583	016.65177
SA8-1	95.67	9.51	72.50	78.22450	016.97071
SA8-2	96.99	3.86	63.11	78.22450	016.97071
SA8-3	476.98	20.42	469.45	78.22450	016.97071
SA8-4	349.41	12.18	333.59	78.22450	016.97071
SA8-5	174.20	6.90	147.11	78.22450	016.97071
SA5-1	146.67	6.04	120.09	78.25480	017.18516
SA5-2	88.07	6.35	72.54	78.25480	017.18516
SA5-3	275.57	14.17	273.00	78.25480	017.18516
SA5-5	153.71	7.97	141.57	78.25480	017.18516
SA2-1	213.12	9.72	195.91	78.25573	017.59194
SA2-2	404.82	7.56	383.43	78.25573	017.59194

ID	OC concentration $[\mu g/l]$	EC concentration $[\mu g/l]$	TC concentration $[\mu g/l]$	Latitute $[^\circ N]$	Longitude $[^\circ E]$
SA2-3	314.25	8.62	300.79	78.25573	017.59194
SA2-4	247.33	3.95	230.21	78.25573	017.59194
SA2-5	347.92	4.49	331.87	78.25573	017.59194
L4-1	547.73	73.12	574.21	78.19766	015.56605
L4-2	175.47	10.41	153.97	78.19766	015.56605
L4-3	108.81	1.44	81.95	78.19766	015.56605
L4-4	252.71	64.29	289.68	78.19766	015.56605
L4-5	326.50	15.86	309.53	78.19766	015.56605
L3-1	326.94	40.54	335.94	78.19176	015.52973
L3-2	174.23	10.98	154.11	78.19176	015.52973
L3-3	225.45	30.33	229.07	78.19176	015.52973
L3-4	365.81	42.96	381.43	78.19176	015.52973
L3-5	107.16	2.15	79.75	78.19176	015.52973
L2-1	225.93	37.87	227.41	78.17884	015.48394
L2-2	142.14	5.28	116.32	78.17884	015.48394
L2-3	139.42	18.47	130.80	78.17884	015.48394
L2-4	186.78	5.01	166.40	78.17884	015.48394
L2-5	61.89	6.85	44.97	78.17884	015.48394
L1-1	338.56	43.20	345.13	78.16815	015.46535
L1-2	177.50	10.10	158.39	78.16815	015.46535
L1-3	105.15	9.15	89.05	78.16815	015.46535
L1-4	214.04	10.97	199.98	78.16815	015.46535
L1-5	232.39	15.31	217.81	78.16815	015.46535
F1-1	287.13	15.55	263.88	78.15310	015.48661
E1	5897.94	338.33	6211.17	78.17884	015.48394
E2	2052.02	141.02	2172.52	78.17884	015.48394
E3	9040.65	276.14	9293.42	78.17884	015.48394
SU1	1325.29	327.13	1621.10	78.16756	015.45921
SU2	1091.32	70.63	1144.46	78.16756	015.45921
S9-1	77.91	13.38	55.60	77.86375	015.55953
S13-1	580.28	158.08	710.15	77.84113	016.03000
S16-1	709.39	38.79	721.56	77.86626	016.49620
S8-1	240.84	50.30	249.29	77.91029	016.81205
S5-1	117.44	11.40	100.60	77.94656	017.13530
S1-1	257.76	9.19	228.79	77.98193	017.62721